THE PROCEEDINGS OF
THE PHYSICAL SOCIETY

Section B

VOL. 63, PART 4 1 April 1950 No. 364 B

Experimental Studies in Thermal Convection

BY A. O. RANKINE*

33rd Guthrie Lecture, delivered 21st March 1949

Mr. President, Ladies and Gentlemen,

I feel that I ought to begin this lecture with a confession. When it was proposed last year that we should celebrate the seventy-fifth anniversary of our Society I discouraged the idea. This was partly because the number 75 did not seem to me round enough to make a fuss about, but even more because I knew from experience how much work the arrangement of the event might involve. My recollections of the Society's Jubilee in 1924 were still vivid. At that time I had recently been appointed Business Secretary, and thus had to shoulder much of the responsibility of organizing the proceedings, which lasted several days and included a series of elaborate functions, the most notable of which was the Jubilee Dinner at which our present King was the principal guest of honour. So now, out of sympathy for the present Officers, whose routine duties are so much more onerous than in my day, I wanted to save them from the additional labour of another celebration, which I judged to be premature.

I thought that my views would be shared by most of the members of the Society, but it appears quite definitely that I was wrong, and, anyhow, I have been overruled. For modesty forbids me from flattering myself that this large gathering is assembled here today merely to hear me discourse, and I know that several hundred Fellows and their friends intend to participate in the Soireé later on this evening. I suppose the truth is that the younger members of our Society particularly, for whom this celebration is the first, welcome the opportunities it affords for social intercourse which has been missed so much during the dark days of the war and its aftermath. And even those of us who are older must agree with them in believing that today's functions, limited in scope though they be for reasons of economy, will help us to get to know one another better, and foster our united efforts to make our Society flourish still more in the years that lie ahead.

Now, as a sort of penance for my former reluctance, it falls to my lot to open the proceedings by giving the thirty-third Guthrie Lecture on this day exactly seventy-five years after our Society was founded through Guthrie's influence on 21st March 1874. We have therefore a double reason for remembering him afresh and paying tribute to the energy and foresight he exercised in our interests during the formative years. We do so now sincerely in the presence of several members of his family and other relatives, whom we welcome as on many former occasions, but with a note of deep regret that his daughter, Miss Hilda Guthrie, who has attended these lectures with great regularity and was present last year, has since died. We are especially pleased to be honoured again by the presence of another daughter, Miss Elfrida Guthrie, who has made a long journey to join us, in spite of her advancing age.

---

* This article will also appear in the May issue of *Proc. Phys. Soc.* A.

This would seem also to be an appropriate occasion for reviewing our Society's development from its foundation until now, with special emphasis on the last twenty-five years—indeed to make this the subject of my lecture. But this would be what the theologians would call a work of supererogation. For such a review has been done comparatively recently, and by one whose ability to tell the story effectively and elegantly is far superior to my own. I refer to our former President, Professor Andrade, whose presidential address in 1945 on "The History and Future of the Physical Society" I have found so refreshing to read again that I recommend all of you to do likewise.

The subject which I have chosen instead is one which, on account of its largely experimental character, would, I think, have had Guthrie's approval. Yet I have some doubts as to whether it will be worthy of its place in the Guthrie Lecture series. I have attended most of these lectures since they were instituted, and I recognize both the eminence of my predecessors and the scientific importance of the matters they dealt with. I have indeed a suspicion that I have been chosen as the lecturer this year more in recognition of my long official connection with the Society than for my contributions to physics. If that be so, I appreciate all the more the honour conferred on me, and the opportunity it may provide for putting on record in the *Proceedings* of our Society some of the results of the most arduous piece of work I ever did in my life, and in which I myself feel a certain pride in having performed. It was done during the war in collaboration with several colleagues, of whom I desire to mention particularly Mr. C. R. Young and Mr. C. Bird, in connection with the operation of dissipating fog over airfields. The results comprise comprehensive data relating to certain aspects of thermal convection in the air, and are at present accessible only in the documents of the now defunct Petroleum Warfare Department. Some at least of them I think may be found to be of more general interest and applicability, and it will be for the Editing Committee to say how much of the contents of my final report might properly be published by the Society.

It is not my intention to deal now with the question of fog clearance, except incidentally. My main purpose is to direct attention to some experimental facts that emerged concerning the behaviour of air heated artificially, and to the means whereby the facts were discovered. But to provide a suitable background for describing the work, and to explain how these experiments came to be undertaken, I must first recall the way in which the problem of dissipating fog by artificial means presented itself for solution as a war-time operation.

Towards the end of 1942 Mr. Churchill charged the Petroleum Warfare Department with the duty of providing means of dissipating fog over airfields. The method chosen was to heat the air by burning petrol close to the ground. Such a scheme had already been contemplated before the war, and experiments had been carried out by the Royal Aircraft Establishment under the direction of the Meteorological Committee of the Air Ministry. The results then obtained provided useful guidance, and there were available also the important calculations made by Professor Brunt indicating the minimum fuel requirements, having regard to the fact that fog drifting across an airfield needs to be dissipated continually as it encroaches thereon.

The first step taken was to construct in the large unfinished reservoir at Staines a petrol-burning installation approximately on the required airfield scale. A similar installation with coke as the fuel was also laid out. Both these were used when atmospheric conditions were suitable to obtain data regarding the distribution of convective heat in the air, employing ordinary meteorological thermometers and anemometers for the purpose. But useful information was slow in accumulating, and it was decided to institute model experiments in which conditions would be under control. I was put in charge of this work and submitted my final report early in 1945.

What follows is mainly extracted from this report. As before indicated I have selected what appears to me likely to be of some general interest, not particularly in relation to the original problem. It being possible, however, that a few readers of this lecture may desire access to the whole report, I have deposited several copies of it in the Society's library where they will be available for perusal.

EXPERIMENTS IN THE EMPRESS HALL, EARL'S COURT, LONDON, ON THE DISTRIBUTION OF HEAT FROM LINE BURNERS, IN RELATION TO THE PROBLEM OF FOG CLEARANCE ON AIRFIELDS

Introduction

The process of clearing fog consists in establishing in the required regions conditions which lead to the re-evaporation of the water droplets constituting the fog. If the method employed is the thermal one the practical requirement is the delivery of heat in sufficient quantity to all those parts of the atmosphere from which the fog is to be removed by evaporation. In respect of airfields *rapid* fog clearance is also requisite, and this has in practice to be brought about by providing in general much more heat than is necessary merely to vaporize the water, so that, by sufficient drying of the atmosphere as well, the fog droplets vaporize quickly enough. Given the constitution of a particular fog—its temperature, its water content and the speed with which it is moving—the heat requirements for its rapid dissipation are easy to calculate.

A question obviously of fundamental importance is the manner in which the heat provided becomes distributed in the atmosphere. It has been held necessary to adhere strictly to certain conditions laid down by the air authorities, namely, that the sources of heat used—in practice lines of burning fuel—must be very close to the ground, and not nearer than 50 yards from the edge of the runway over which it is desired to clear fog. A further desideratum is that clearance should extend to a height of at least 100 feet above the centre of the runway. The problem thus became one of investigating the behaviour of the thermal convective jets originating in lines of burning fuel, under the influence of winds of various strengths and directions, including, of course, the special case of no natural wind at all.

In theory this problem could be solved by carrying out a large number of experiments in the open air on the actual scale of the proposed airfield installation. In practice, however, this would be a very lengthy and difficult process, as no control could be had over the atmospheric conditions, and observations would be restricted on the occasions when those conditions happened to be favourable. It appeared, therefore, that experiments might with advantage be carried out on a much diminished linear scale, under artificial conditions fully under control and capable of reproduction whenever required. There were, in fact, good reasons for believing that, with proper adjustments of the rate of heat emission from the burning line, and of the speed of the imposed wind, a pattern of heat flow, resembling the full-scale pattern, could be produced and investigated with a model installation, the linear dimensions of which were, say, one-thirtieth or one-sixtieth of that used in the field. The sequel will show that this belief has been fully justified.

A further word of explanation is necessary before proceeding to describe the model experiments. Strictly speaking, the measurements of heat flow, whether in the model or in the field, ought to be made under atmospheric conditions involving actually precipitated fog. But the results obtained are nearly enough correct in a clear atmosphere, and, if necessary, an appropriate allowance can be made. Consequently, in the model experiments the observations throughout have been made without the inconvenience of having to create and maintain artificial fogs.

Wind Tunnel for Model Experiments

The model work has been carried out in the Empress Hall during the period from April 1943 to December 1944. For the purpose of most of the experiments a wind tunnel was constructed within the hall, which is a very spacious enclosure about 200 ft. long, 150 ft. broad and 70 ft. high. The tunnel itself was constructed with the advice and collaboration of the National Physical Laboratory, especially of Mr. L. F. G. Simmons, of that laboratory. It was built on the concrete floor of what had been a skating rink, and the main part was 100 ft. long, 30 ft. wide and 12 ft. high, the sides and roof being composed of wooden boards. At one end the rectangular cross section was flared down in a distance of 30 ft. to a square cross section of 12 ft. side, and thereafter to a circular channel 10 ft. in diameter which housed a 27 H.P. electric fan lent by the London Passenger Transport Board. At 30 feet inside the tunnel from the open end a wire mesh partition (30 meshes to the inch) was inserted for the purpose of rendering regular the air flow created by the suction of the fan. Doors in the sides gave access to the tunnel between the wire screen and the fan. Photographs of the exterior and interior of the tunnel are shown in Figures 1 and 2 (see Plates).

Investigation of Wind Structure in Tunnel

The range of air speeds required was from zero to a few feet per second, so as to correspond, with due allowance for scaling, with the winds likely to be operative in fogs on airfields. Running at its normal speed the fan made the air in the tunnel move much too fast. It was necessary, therefore, to reduce this by appropriate resistance adjustments on the fan motor. Further reduction was secured, as necessary, by shutting a pair of perforated doors housed in the square part of the tunnel just in front of the fan. In this way a range of air-speeds from 0·5 to 5 feet per second could be produced and reproduced as required. On a 1/60 linear scale, on which a large part of the work was done, this range corresponds to full scale values from 2·65 to 26·5 miles per hour.

Preliminary tests with a meteorological cup anemometer showed that the general air movement was fairly uniform in the tunnel except near the floor, roof and walls. Such anemometers were, however, not accurate enough for

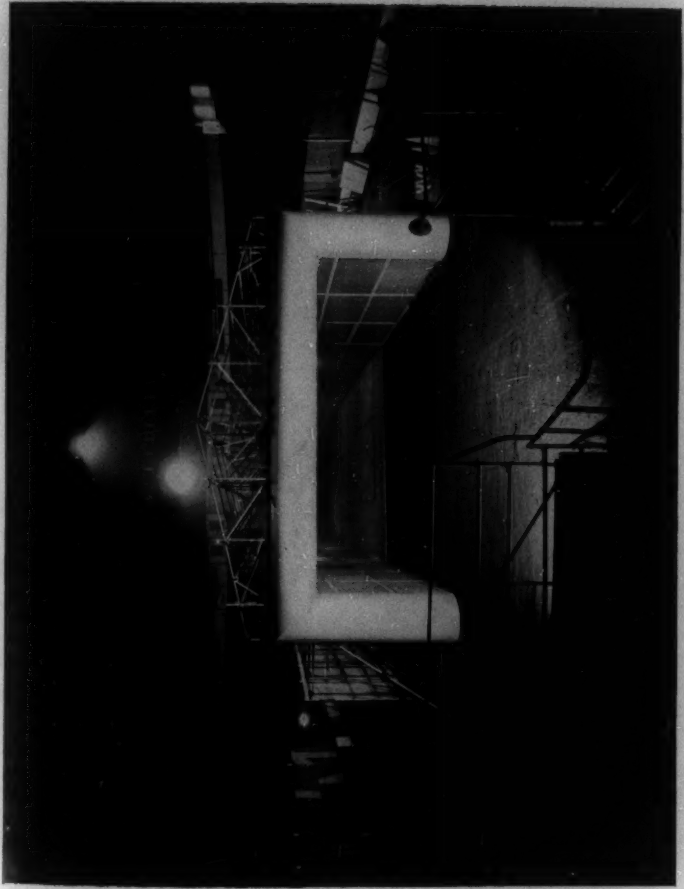

Figure 1. Exterior view of wind tunnel.

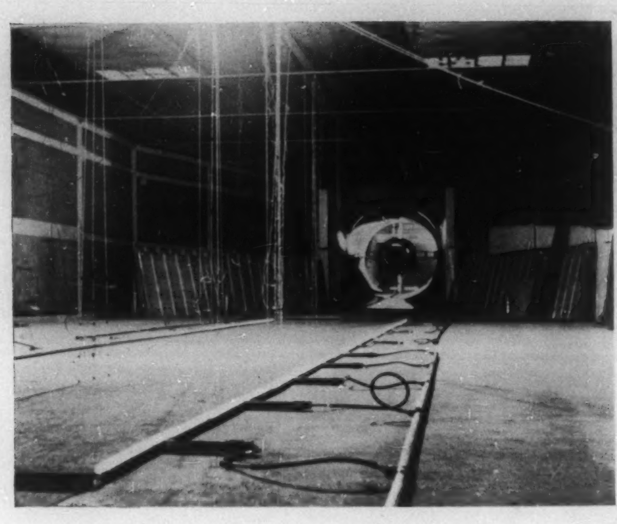

Figure 2. Interior view of wind tunnel showing fan and one arrangement of apparatus.

the purpose of measuring low wind speeds. Moreover, on the scale of the work they were too large, thereby interfering unduly with the air flow they would purport to measure. Recourse was had again to Mr. Simmons, who produced and made available about a dozen small electrical anemometers of a form which would not disturb appreciably the air currents under investigation. These anemometers will be described fully elsewhere. Here it must suffice to indicate that they depend on the principle that a thin wire electrically heated is cooled by air flowing past it to an extent which increases with the air speed, and that the cooling is measured electrically by thermocouple elements held close to the hot wires. These anemometers, besides being small and of suitable sensitivity, had the additional advantage of providing remote observation, so that the measuring operations could be performed outside the tunnel by means of instruments connected by thin wires to the anemometers disposed at suitable points inside.

Before being employed to investigate the wind structure in the tunnel under the various conditions of the experiments the anemometers had to be calibrated, so that the corresponding air speed could be derived from the measured electric potential of the thermocouple. In their original form the anemometers were calibrated at the National Physical Laboratory, but evidence soon accumulated that they changed sometimes in behaviour, so as to necessitate recalibration rather frequently. In order to do this without having to disconnect the anemometers and remove them from the tunnel—a somewhat laborious procedure also liable in itself to produce changes in them—a method was devised to re-calibrate them *in situ*. It consisted of establishing the air speeds along the centre of the tunnel, for various settings of the electric controls of the fan motor, by observing the times of passage between two fixed planes of almost weightless flakes of suitable material carried along by the air stream. The material used was the solid fuel known by the trade name of 'Meta', which is provided in small sticks. On touching a stick with a hot rod such as a soldering iron the material volatilizes and condenses again almost immediately in a form like snow flakes, but relatively much lighter. These fall very slowly, and in a horizontal air stream moving even as slowly as 0·5 foot per second, travel nearly horizontally. By releasing them in the tunnel and determining the average times of passage of many individual flakes between fixed planes 10, 20 or 30 feet apart, it proved possible to obtain reliable values of the air speed in the parts of the tunnel unaffected by the proximity of the floor, roof and sides. This was done for a range of air speeds from about 0·5 to 5 feet per second, and provided a convenient means of checking periodically the performance of the anemometers. Eventually Mr. Simmons modified the instruments into a form which was much more stable and reliable, but it was not until the later stages of the experiments that confidence could be placed on the results. The patterns of the wind structure were, in fact, re-determined in most cases by means of the anemometers in their final reliable form, the accuracy of measurement attained being a few per cent.

Measurement of Air Temperatures

Besides air speeds it was necessary to know the degree of heating of the air in order to define the complete pattern of the heat flow originating in the line burners. For this purpose electrical thermocouples were used so as to have again the advantage of remote observation outside the tunnel. Moreover, this kind of thermometer, consisting as it does of thin wires, could be disposed in the air stream without modifying appreciably its structure. The installation of these thermocouples was facilitated greatly in the early stages of the experiments by the cooperation of the General Electric Company, and in particular of Mr. Lait, who spent many days on the work. The thermocouples consisted of soldered junctions of 30 S.W.G. copper wire and 32 S.W.G. Eureka wire, and they were calibrated so that the temperatures of air passing them could be deduced from the electrical potentials measured on a Tinsley potentiometer. As in the case of the anemometers, suitable switchboards enabled measurements to be made in turn on the various thermocouples mounted on slender frames at the points of investigation in the tunnel. At first measurements of the actual temperatures (above 0° C.) were made in the heated air and at a point outside the influence of the burning lines, the temperature rise being deduced by subtraction. Later the more convenient method was adopted of disposing the two elements of the thermocouple, one in the heated air and the other where there was no heat flow, so that the temperature rise could be obtained from a single measurement of potential. The accuracy of temperature measurement attainable was about 0·1° C. or 0·2° F. Investigation showed that radiation from the burner lines did not affect the thermocouples appreciably, and that they in fact assumed quickly enough the actual temperature of the air surrounding them.

The Burning Lines, and Method of controlling Heat Emission

The fuel used for the burning lines was butane, provided in iron bottles supplied from Petroleum Warfare Research Station, Langhurst. This fuel is especially convenient for small scale work because, the normal boiling point being about 0° C., it usually develops in the bottles a vapour pressure somewhat above atmospheric, so that it is delivered as gas to the burners. Except occasionally on very cold days (when artificial warming of the bottles had to be resorted to) sufficient gas could be delivered to the burners at convenient pressures to provide the quantities of heat required, which, for the purpose in hand, had to range from zero up to a total value of about 5 therms per hour. The design and construction of suitable burners presented something of a problem. It was desired to burn the gas so that combustion was as complete as possible, for it was known that convective or sensible heat, as distinct from thermal radiation, was in fact the means whereby fog could be surely dissipated. Consequently, so-called non-luminous burning, such as occurs normally in a bunsen burner using coal gas, was aimed at. But ordinary bunsen burner nozzles and air inlets were not suitable, on account of the much greater (six times) calorific value of butane as compared with coal gas. New burners had to be made to meet the case, and, in the first instance, two pipes each 30 ft. long were provided from P.W.R.S., Langhurst, which through numerous orifices in the top about ½ in. apart gave lines of non-luminous flames reasonably uniform in size over the whole length, although the butane entered the pipe through a suitable nozzle, and past a variable air inlet at one end only. These burners were used extensively in the earlier part of the investigation, but their dimensions were too great for all purposes. When laid on the floor, for example, the flames originated about 4 in. high, which, on the basis of model work on 1/60 field scale, would correspond to 20 ft. high in the field, whereas in airfield installations they start a foot or even less from the ground. To avoid this dimensional discrepancy, which would have vitiated the application of scaling in the manner hereinafter described, the tunnel floor was in effect raised to the level of the flame orifices by boards mounted on blocks.

Later on a large number of smaller burners were made at the P.W.D. Experimental Station at Staines, some 10 ft. long and some 4 ft. long and all of 1 in. diameter, served by suitable nozzles obtained from the Physics Department of the Imperial College of Science and Technology. These burners proved to have a more uniform and quite satisfactory flame distribution, and, being relatively short, gave greater flexibility in constructing the various patterns of installation which had to be investigated. Moreover, on account of their small diameter, adjustment of floor level was not considered to be necessary. Another useful feature, as will appear presently, was that they could be altered, by means of the adjustable air inlet, so that the butane burnt luminously.

The various nozzles belonging to the burners were calibrated in relation to pressure above atmospheric and passage of butane. The pressure was measured by U-tube gauges, usually containing mercury, but occasionally water, and the rate of flow of butane was observed by a gas meter. With the nozzles thus calibrated serving any particular layout of burners, and the butane pressure being held constant by a control valve, any desired rate of delivery of butane per yard of burning line could be maintained. With the butane ignited, the calorific value being known, the corresponding gross heat emission rate per unit length could be deduced. The range in fact covered in the experiments was from 0·03 to 0·48 therms/yard.hour.

With the multiple burners sometimes used it was, of course, necessary to provide a system of service pipes connected with the bottles of butane and provided with sufficient taps to deliver gas to the individual burners. This was constructed as required out of 1 in. piping, and the connections to the burner nozzles were made with flexible rubber tubing. There was, however, no appreciable loss of pressure in the service system, the burner nozzles being so relatively small as to ensure that practically the whole pressure drop occurred across their orifices. Thus, with equal nozzles in burners of equal length, uniform heat output could be secured at a single pressure in all parts of the system.

Observational Procedure in Wind and Temperature Measurements

The procedure at first visualized was to lay out the particular type of burner system to be investigated, to instal the electrical anemometers and thermometers at suitable points, and then to make a few observations simultaneously of the air speeds and temperatures at these points both without and with the burners in operation. In practice this procedure had to be much modified in several respects. It was soon found that, owing to the turbulence of the air movement, the velocity and the temperature at a fixed point varied, sometimes very greatly, from moment to moment, and that, in order to be able to assign to the point reliable average values, a much larger number of readings would be necessary. Instead of a few readings usually fifty were taken, and the time occupied in thus dealing with every anemometer and thermocouple became much longer than had been anticipated. In all, several hundred thousand observations were made, each involving the manipulation of the appropriate potentiometer; and on some days more than two thousand data were added to the records. All these had to be corrected as necessary, classified and analysed before the final results emerged.

For reasons already mentioned, namely, the relative unreliability of the anemometers in their original form, it was not possible to carry out consistently the idea of simultaneous measurement of temperatures and air speeds. In some of the experiments for this reason no velocity measurements were made. In others, where a knowledge of velocities was more essential, they were re-determined during the latter stages of the investigation, when the improved anemometers became available. For example, what would naturally have been done first —the examination of variation of flow of the unheated air in the tunnel near the floor and sides—had to be thus postponed. Some of these vertical profiles of horizontal velocity are shown in Figure 3.

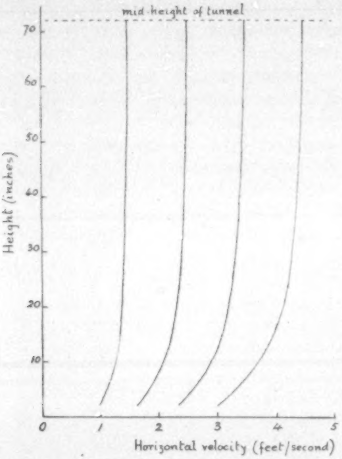

Figure 3. Vertical profiles of horizontal velocities of the air (unheated) in tunnel.

Detailed Investigation of Convective Heat Flow produced by Winds across Burner Lines

The principal feature of the work in the tunnel was the systematic investigation of the pattern of heat flow downwind of a burning line across which imposed winds of various strengths were operating. This particular case, in its full scale realization, is probably the most important in relation to fog clearance over runways, for it may be expected to provide answers to the questions—how much heat should be provided in a burning line, and where should the line be placed relative to the axis of the runway in order that fog clearance may be achieved to adequate heights over the middle of the runway, even when the wind originally blowing across both line and runway attains so high a value as, perhaps, 25 miles per hour?

Previous field experience has shown that in such circumstances the convective heat from a burning line is very easily deflected from the nearly vertical flow which occurs in air originally stagnant. Quite a low wind—a few miles per hour—

causes the heated jet to engage the ground on the downwind side of the line, while the upper edge makes an angle with the ground which diminishes rapidly as the imposed wind increases. Above this edge no appreciable amount of heat is imparted to the air, so that no fog dissipation can be expected there. Near the ground the required heat supply is more than adequate for the purpose; it is higher up that deficiency is liable to occur, and the aim is to ensure that at the minimum specified height for fog clearance the heat supply is at least enough. In other words the heat flow pattern under the influence of naturally occurring winds is not ideal. Such winds help in transporting the heat in the right direction from the burning line, but they give rise to a distribution of the heat which compels considerable waste at low levels in order to have at least enough at, say, 100 feet high over the middle of the runway.

This was the problem now tackled with the model. A burner line was laid across the full width of the tunnel, usually about midway between the wire screen and the plane where the cross section began to flare down to the fan. Anemometers and thermo-elements were installed at suitable heights above the floor in the axial vertical plane of the tunnel at distances of 3 ft. 9 in., 7 ft. 6 in. and 15 ft. downwind of the burner line, and, as required, in the unheated upwind air as well. Systematic measurements of the temperatures and velocities of the moving air were carried out for a range of heat emissions from 0·03 to 0·48 therms/yard.hour, and of imposed winds from 1 to 5 feet per second at the mid-height (6 ft.) of the tunnel. Auxiliary measurements defined the vertical profiles of the various imposed winds when the air was unheated, as indicated in Figure 3, so that the changes caused by the burning operations could be determined. Also, traverses with anemometers and thermo-elements across the tunnel showed no appreciable variations except near the walls. Thus the results given for the axial vertical plane apply also to any parallel plane not too near the ends of the burning line.

These results have been analysed, interpolated and smoothed to remove evident errors in the customary manner, and are given in tabular form in the Appendix, with intervals small enough for it to be permissible to interpolate by proportional parts. A graphical method of representation which, *prima facie*, might have been deemed preferable, has been found too elaborate, on account of the multiplicity of the variations, since it would involve drawing some 380 graphs.

Discussion of Results for Winds across Burner Lines

It is, however, instructive to represent a few of the cases graphically, and the chief points are thus illustrated in Figures 4, 5, 6, 7 and 8. Figure 4(*a*) shows the vertical profile of temperature rise of the air 7 ft. 6 in. downwind of the burning line when the gross heat emission is 0·24 therms/yard.hour, under the influence of an imposed wind of the magnitude 2 feet per second at the mid-height (72 in.) of the tunnel. This value implies a vertical profile of velocity of the type shown in Figure 3 for unheated air, and the particular profile in the present case appears in the dotted line in Figure 4(*b*), which exhibits also, by the full line, the profile modified by the heating of the air. Figure 5 represents a similar case, except that the imposed wind here is higher, namely 3·5 feet per second, with corresponding different profiles both heated and unheated. It will be noticed by comparison of Figures 4(*a*) and 5(*a*) that increase of wind speed reduces the temperature rise at the higher levels and increases it at the lower levels. Also, inspection of Figures 4(*b*) and 5(*b*) shows, under burning conditions, that the original air-speed is enhanced considerably except at the higher levels, where there is little change. Figure 4(*b*) in fact demonstrates that, for low speeds of the imposed wind, the enhancement due to heating may cause the speed at low levels to exceed that at points higher up. This phenomenon of wind enhancement has been found to be generally true, and to be emphasized both by a reduction of imposed wind speed and an increase in the degree of heating.

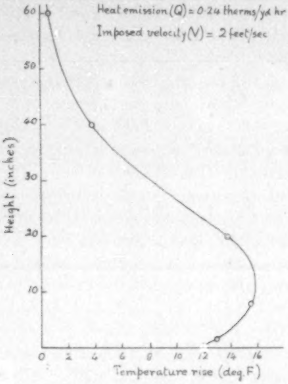

(*a*)

Figure 4(*a*). Temperature pattern 7′ 6″ downwind of burner.

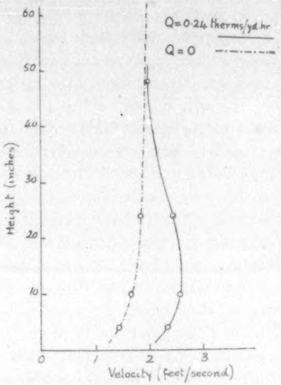

(*b*)

Figure 4(*b*). Velocity pattern 7′ 6″ downwind of burner.

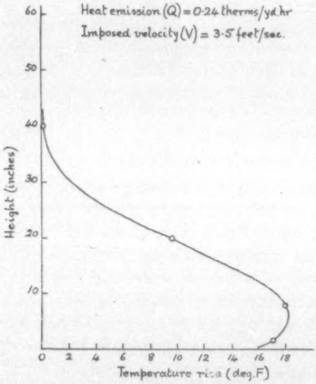

(*a*)

Figure 5(*a*). Temperature pattern 7′ 6″ downwind of burner.

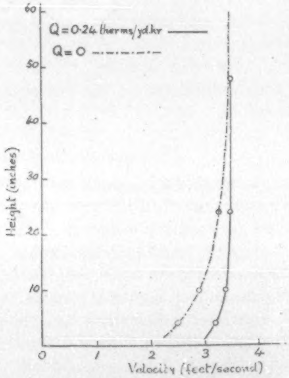

(*b*)

Figure 5(*b*). Velocity pattern ·7′ 6″ downwind of burner.

The effect on the temperature rise of increasing the heat emission from the burning line is shown in Figure 6. Under the same imposed wind the temperature rise becomes greater at all heights, although not in a proportional manner, the ratio increasing rapidly with height. The heat emission in fact exercises control over the shape of the temperature profile as well as its dimensions. Another set of curves (Figure 7) illustrates the way in which the temperature

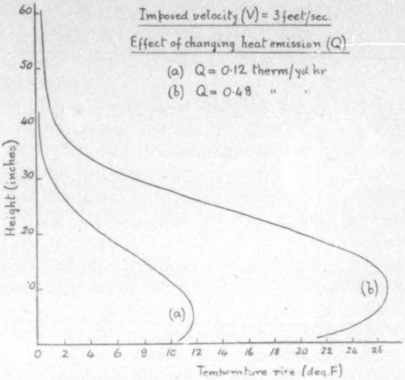

Figure 6. Temperature pattern 7′6″ downwind of burner.

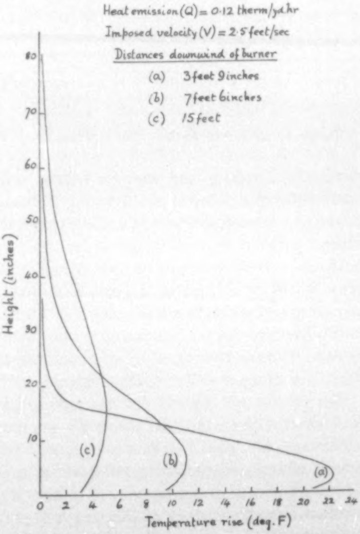

Figure 7. Temperature pattern downwind of burner.

profiles vary with distance downwind of the burning line, heat emission and imposed wind being constant. The most striking feature is the way in which the 'nose' of the curve (to which reference is made later) becomes blunted and elevated as the distance from the burning line increases.

Integration of Convective Heat Flow. Losses by Radiation and Ground Absorption

An important check can be made on the accuracy of the results by calculating the total quantity of convective heat passing downwind. This can be done when, as in most cases, the temperature rise is zero, or nearly so, at the maximum height of observation. The density and specific heat of air are known; the remaining factor involved in the determination is the product at all heights of the temperature rise and the wind speed, which is effectively horizontal. Figure 8 shows these products, plotted against height, for the data contained in Figures 4 and 5, and each of the two curves, for the same heat emission but different wind speeds, provide the means of graphical integration of the total convective heat flux, which is proportional to the area enclosed by the curve. The areas enclosed by the two curves are found to be nearly equal, implying that the convective heat flux is the same in the two cases. It is, however, considerably less than the gross thermal energy developed by combustion in the burning line. This is true, not merely for the two cases here considered, but quite generally. On the average only about 80 per cent of combustion heat has been found to cross any of the downwind planes of observation, in the form of convective heat, which alone could be effective in clearing fog.

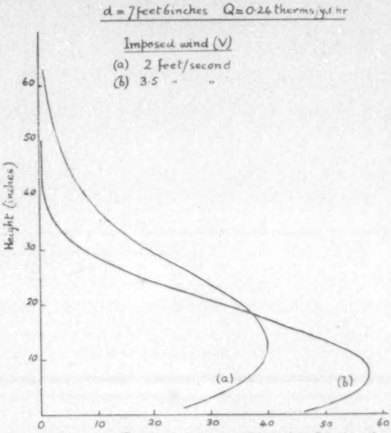

Figure 8. Heat flux downwind of burning line.

This loss of about 20 per cent is accounted for in two ways. Some is lost to the floor, as is evident from the shapes of the temperature profiles. Always the temperature of the air close to the floor is lower than that somewhat higher up, giving rise to the 'nose' of the profile. Moreover, the floor itself is always colder still, and this temperature gradient implies that the air does lose heat to the floor. The amount is not great; a fair estimate is about 5 per cent of the total thermal emission from the burning line, and most of this loss occurs closer to the burner line than 3 ft. 9 in., since there is no consistent evidence of variation of convective heat flux between this and greater distances downwind. It is probable that the ground of an airfield behaves in much the same way as the concrete floor of the tunnel with regard to transfer of heat from the air, so that the heat loss to the ground may also be taken as 5 per cent. It is fortunate that it is so small, and that most of the sensible heat remains in the air, where it is wanted for fog dissipation.

The remaining 15 per cent or so of the gross thermal energy of combustion, which does not appear as convective heat, is without doubt in the form of thermal radiation, including, of course, the small fraction of this which is luminous (even for so-called non-luminous flames). This is not appreciably absorbed by the air in the short distances (up to 15 ft.) over which measurements were made, and therefore does not become converted into sensible heat which would be registered by the thermometers. As regards full scale installations it may be reasonably assumed that the hydrocarbons constituting the petrol there used do not differ appreciably from the particular hydrocarbon butane in respect of radiation from flames. So that here also, unless the radiation is converted by absorption into heat capable of evaporating fog, it must be written off as a loss. The degree of this absorption is not known, but it may be said that conditions are somewhat more favourable in the full scale installation than in the model, owing mainly to the greater distances involved, and also to the fact that the constituents of a fog-laden atmosphere have a greater absorbing power than the clear unsaturated atmosphere in the tunnel, in respect of the specific radiation emitted by hydrocarbons burning non-luminously.

Radiation from Luminous and Non-luminous Flames—Experimental Comparison

This question of radiation was under constant discussion during the course of the model work at Empress Hall, and is the basis of the additional experiments now to be described. In the airfield installations the petrol has not been burnt non-luminously, but with less than the requisite supply of air for complete combustion, so that the flames have been highly luminous, and often near to being smoky. In this respect the burning lines have been different from the non-luminous (blue) flames of the butane ordinarily used in the model work. As mentioned earlier, however, it was possible, by restricting the air supply, to make the butane burn with luminous yellow flames more nearly similar to the petrol flames in the field. With this arrangement many measurements were made of the convective heat flux, for comparison with the corresponding flux for non-luminous burning. The results were of considerable significance. Generally, with equal rates of supply of butane to the burning line, the convective heat derived from luminous burning was found to be only about 80 per cent of that derived from non-luminous burning, i.e. 64 per cent of the gross amount calculated from the calorific value of the fuel. It appeared, therefore, that the loss by radiation was increased by a further 16 per cent if luminous burning was employed, making a total of about twice that for non-luminous burning.

This result was confirmed subsequently by direct comparisons made between the amount of radiation emitted by luminous and non-luminous flames consuming equal quantities of butane, the same fraction of the total radiation from a line burner being received on a thermopile suitably disposed. With a butane consumption rate per yard equal to that in the former measurements of heat flux, the ratio of the total radiation from the flames when luminous to that for non-luminous combustion was found in a long series of observations to be 1·8, compared with the ratio 2 estimated indirectly as indicated in the previous paragraph. It was observed also that this radiation ratio depended upon the size of the flames, increasing as the flames were made larger by raising the fuel consumption rate. At the highest rate employed, when the flames were still only about 3 inches long, the radiation ratio was 2·4. This would imply, allowing also for the 5 per cent loss of heat to the ground, that the available convective heat is rather less than 60 per cent of the gross thermal emission. Compare this with the 80 per cent that can be obtained with non-luminous burning.

As regards the implications in full-scale petrol burning installations much the same conditions are likely to apply, or they may be even worse. The flames are much larger, perhaps two feet long, with a tendency to be smoky, consequently the degree of radiation from them will be even larger than in the model. Moreover, the additional radiation associated with their luminosity, occurring as it does in the near infra-red spectral region, is absorbed very little by any of the constituents of foggy air. Its transformation in the regions required to the only form of heat capable of dissipating fog, namely, convective or sensible heat, cannot, therefore, be relied upon to a useful extent. In fact, it is most unlikely that, with the petrol burners usually employed, the useful heat for purposes of fog clearance exceeds 60 per cent of the total calorific value of the petrol; it is probably considerably less when the burners are on the point of smoking.

The implication is clear. The petrol should be burnt non-luminously, in which case somewhat more than 80 per cent of the gross heat supply will be available for fog dissipation. An economic saving of 25 per cent of the petrol consumption could be achieved in this way.

Comparison of Model with full-scale Installation. Application of Principles of Dimensional Scaling

The measurements embodied in the tables of the Appendix provided the means of carrying out the crucial test as to whether, by the proper application of the principles of scaling (or dynamical similarity), the model results could be used to predict the behaviour of full-size installations, and thereby to specify the field requirements for the successful dissipation of fog. For this test some full-scale observations were necessary, and certain data of this character were available from field work at Staines.

Without going into the reasons thereof, the principles of scaling believed to be applicable may be simply stated as follows. Denote by L_m any particular length in the model (such as the distance of an observation point from the burning line) and by L_f the corresponding full-scale length. Similarly, V_m denotes the air speed at any point in the model, and V_f that at the corresponding point in the full-size installation. If also θ_m and θ_f are in like manner the corresponding temperature rises of the air, then

$$\frac{V_m^2}{L_m\theta_m} = \frac{V_f^2}{L_f\theta_f}$$

for all points. It is to be noted that this relation approximates to the truth only when θ_m and θ_f are small compared with the absolute temperature of the air, and this limitation must therefore be observed in applying it. The special application of the equation to the present argument deals with the case when

$$\frac{V_m^2}{L_m} = \frac{V_f^2}{L_f} \quad \text{or} \quad \frac{V_f^2}{V_m^2} = \frac{L_f}{L_m},$$

in which case $\theta_m = \theta_f$ or the temperature rises at corresponding points in the full-size installation and its linearly scaled model are the same. To realize this, having chosen the linear scale ratio L_m/L_f to be r, say, it is necessary to arrange that $V_m^2/V_f^2 = r$, or $V_m/V_f = \sqrt{r}$. We have control over the air velocities in the model in two respects, namely, the speed of the artificially produced wind across the burner, and the convective velocity of the thermal jet originating in the burner itself. As regards the latter, theoretical considerations * have shown that the velocities produced in the air by convective action are proportional to the cube root of the heat per unit length, H, of a long line source, which issues in convective form. Thus, to make the convective emission tally as between the full-scale installation and the model, the condition

$$H_m/H_f = V_m^3/V_f^3 = r\sqrt{r}$$

must be fulfilled in making comparisons.

The question then is this. If we take a series of measurements on full scale at Staines when a natural wind was blowing across a burning line, and select by the above rules corresponding observation points, imposed wind speeds and convective heat flux in the tables of the Appendix, do we in fact find in the model temperature rises equal to those of similarly placed points at Staines? This has been answered affirmatively by several comparisons carried out in the manner indicated, using data from Staines which appeared to be self-consistent and reliable. Figure 9, for example, relates to a petrol burning at Staines in which observations of temperature rise were made at several heights 75 yards downwind opposite the middle of a burning line 600 yards long. The scope of the model measurements was great enough to permit predictions by scaling for three different values of r, namely 1/60, 1/30, and 1/15. It will be observed that these predictions are reasonably consistent among themselves, indicating that internal scaling, i.e. within the range covered by the model investigation, is applicable. The curve represents the mean predicted temperature profile, and the closeness of the Staines observations to it is striking evidence of the validity of the scaling principles employed, even up to full scale.

Another result of the same kind is shown in Figure 10, which relates to a coke burning at Staines under like conditions as regard the relative positions of the observation points and the burning line. Here only two predictions from the model are possible, but they are fairly consistent, and the mean profile is again close to the actual Staines observations. It will be noticed that in both cases the temperature rises are small, the maximum value being 13·5° F., which is less than 3 per cent of the absolute temperature, so that the condition for the constancy of $V^2/L\theta$ is not violated. The difference between the predicted and actual values of the temperature rises nowhere exceeds 0·8° F., and this is well within the accuracy of measurement, having regard to the errors to which both field and tunnel observations were liable.

---

* Sir Geoffrey Taylor drew attention in 1943 to the work of W. Schmidt published in November 1941 in the *Zeitschrift für angewandte Mathematik u. Mechanik*, and himself contributed valuable notes on the subject of thermal and forced jets.

On the basis of these and other similar satisfactory comparisons it seems reasonable to conclude that the principles of comparison described are of general validity even for linear ratios as great as 60 : 1. In particular, the data contained in the Appendix may be confidently used in this way to discover the nature of the convective heat flow from a field burning line for all the higher cross-wind speeds likely in fog-clearing practice to be encountered, and for all heat emissions within reasonable practical attainment. Conversely, the requirements as to the position and heat emission of the burning line can be specified so as to ensure fog clearance over a runway to any requisite height.

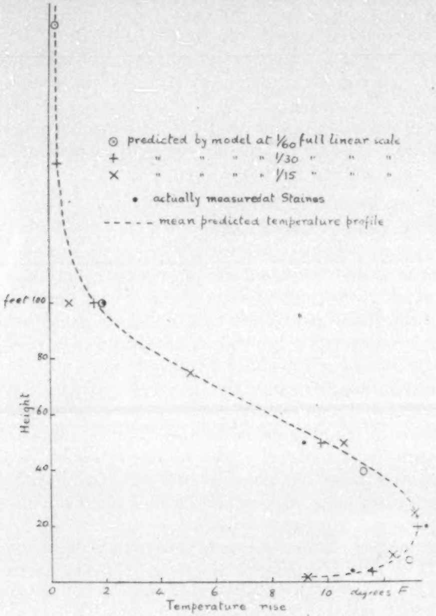

Figure 9.

Petrol burning, Staines, 14.12.42. Wind speed normal to burning line 8½ m.p.h.; convective heat flux 22·4 therms/yd.hr.

Comparison of predictions from model observations with field results, using principles of dynamical similarity.

Limitation of Use of Tunnel in respect of Low Wind Speeds

Soon after the tunnel had been constructed early in 1943 Sir Geoffrey Taylor pointed out that its utility would be restricted, possibly seriously, by the existence of the roof, which would have no counterpart in the open atmosphere. He suggested modifications to transform the tunnel into what may be called a channel by removing the roof, and, by reversing the fan motion, to create the artificial wind by blowing instead of sucking. His proposals also contained other ancillary measures to render the velocity profiles suitable.

It turned out to be impracticable to implement these modifications, although, later, a separate channel was constructed and used, as described presently. The restrictions on the use of the tunnel had, therefore, to be examined and assessed.

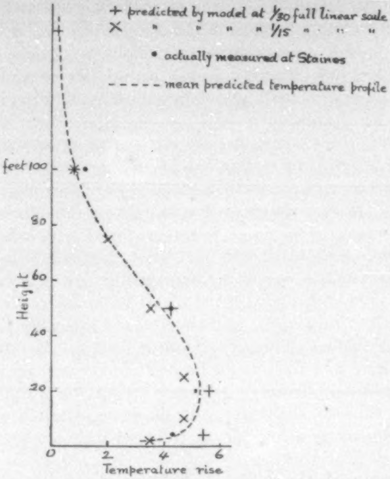

Figure 10.

Coke burning, Staines, 18.1.43. Wind speed normal to burning line 5 m.p.h.; convective heat flux 5·9 therms/yd. hr.
Comparison of predictions from model observations with field results, using principles of dynamical similarity.

Clearly, it would not permit the simulation of full-scale burning lines in calm atmospheres; for the heated air jet, rising vertically and reaching the roof, would be forced to spread out in *both* directions along the tunnel, in a manner which would not occur in the open atmosphere. The same would be true when the jet became deflected from the vertical by low-speed imposed winds; there would still be reversed air flow near the roof which would vitiate simulation of full-scale operations. The question to be decided was at what imposed wind speed this reversal, or re-circulation, ceased, owing to the thermal jet being depressed sufficiently not to engage the roof. This occurrence of re-circulation was tested both by observing visually the flight of meta flakes, and by observations with anemometers suitably disposed between roof and floor. If there is re-circulation the reversal near the roof is accompanied by increased velocity in the original direction near the floor, with a zero speed somewhere in between.

The result of these tests was to show that re-circulation was more liable to occur with the higher values of the heat emissions employed, as would be expected. Even with these heat ratings, however, it ceased to be noticeable for imposed wind speeds somewhat in excess of 1 foot per second. Consequently, the application of the tunnel experiments to predict open-air results has been limited in this sense, and the tables in the Appendix have been deliberately restricted at the lower limits of V. To be on the safe side the lowest value of V included for the range up to $Q=0{\cdot}20$ therms/yard.hour is 1·5 feet per second, and for the range of Q from 0·24 to 0·48 therms/yard.hour to 2 feet per second.

This completes the description of the part of the work at Earl's Court which I deem to be suitable for publication in the *Proceedings*. For the rest, reference must be made to the full report, copies of which, as already stated, have been deposited in the Society's library. But I would like to indicate briefly here two aspects of this additional work which may find application in other directions in the future.

The first relates to the channel already mentioned as having been constructed with no roof in an attempt to realize conditions comparable with the open air. The difficulty here was to produce a reasonably uniform horizontal flow of air along the channel. Motor blowers directed along the channel proved to be abortive. Consideration was given to other possible methods, in particular that of using across one end of the channel a thermal line jet which, by its sideways entrainment of air, might be expected to create a horizontal wind of good uniformity. Theoretically, according to Schmidt, the entrainment speed would be independent of height, and, over a considerable distance along the channel, would vary little. This promising system could not be used because it required much more fuel than could be provided, but it remains one I should like to see implemented. Instead, a somewhat similar system was employed. Motor blowers of cold air directed upwards were installed at one end of the channel so as to constitute a line jet, thereby creating a horizontal drift of the air eventually entrained in this jet.

The other aspect of the work to which I wish finally to refer is the use of a device proposed and demonstrated early in 1944 by the General Electric Company's staff (Mr. Ryde in particular) to study visually the behaviour of thermal jets. This device, which has been called the 'Shadowgraph', consists of projecting through the jet a beam of light, originating in a small but very brilliant source, on to a white screen suitably situated beyond the jet. The result is that a pattern of fluctuating lights and shades appears on the screen, due to the point to point changes of the refractivity of the heated air. This pattern is very instructive, for, while not a complete substitute for the systematic investigation of the temperature and velocity structure of the jet, it does provide a quick means of getting a general picture of the movements of the heated air associated with various arrangements of burning lines. Through the courtesy of the General Electric Company the shadowgraph was used extensively during the later stages of the investigation. Had it been available earlier the planning of the work would have been greatly facilitated.

It proved to be possible to make some motion picture films of the patterns appearing on the shadowgraph screen in the tunnel. These, although by no means so brilliant as the originals, are reasonably good. By the nature of things, they cannot be included in this publication, and I am therefore glad to have been able to exhibit them, during the course of this lecture, through the courtesy of the Ministry of Supply.

REFERENCES

ANDRADE, E. N. DA C., 1945, *Proc. Phys. Soc.*, **57**, xxi.
BRUNT, D., 1936, *Trans. Faraday Soc.*, **32**, 1264; 1939, *J. Sci. Instrum.*, **16**, 137.
SIMMONS, L. F. G. 1949, *J. Sci. Instrum.*, **26**, 407.

APPENDIX

EXPERIMENTS IN THE WIND TUNNEL AT EMPRESS HALL

Structure of convective air jets, originating in a burning line of non-luminous butane flames, under the influence of winds blowing normally across the line, as derived from observations of velocities and temperatures of the flowing air.

V denotes the air speed at the mid-height of the tunnel (72 in.) when no heat is being injected. This defines the structure of the air current imposed on the thermal jet emerging from the burning line.

Q denotes the thermal emission rate per unit length of the burning line, calculated from the calorific value of the butane.

h denotes the height of the point of observation above the floor.

d denotes the horizontal distance downwind of the burning line.

θ denotes the excess of temperature of the air in the thermal jet at the point indicated over that of the air upwind of the burning line.

v denotes the local horizontal air speed. The values of v in relation to those of h for $Q=0$ show the initial vertical velocity profile of the unheated air current. The heat-modified velocity profiles are derived similarly for the corresponding Q values.

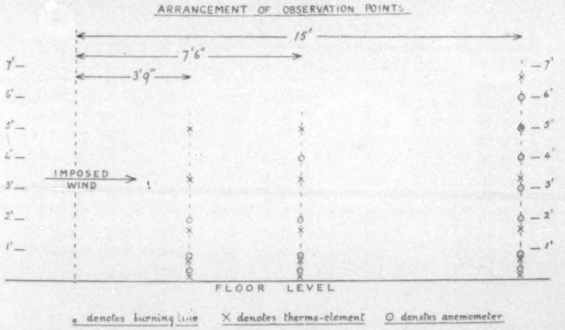

The data given are derived from the averages of multiple observations, of which there were at least 50 for each experimental point. The temperature rises recorded are believed to be accurate to within 0·5° F., or 5 per cent, whichever is the greater. The errors of the velocities shown are estimated not to exceed ±5 per cent.

The chief purpose of the tabulated data of these model experiments is to provide means of predicting the conditions applicable to installations on other scales, by use of the accepted principles of dynamical similarity, namely, the constancy of the dimensional ratio $[V^2/L\theta]$, when θ is small, with the further relation that the fraction H of Q which is in the form of convective heat is proportional to V^3. For these tables $H=0{\cdot}8Q$, for the reasons given in the text relating to losses by radiation and ground absorption.

An apology is perhaps due for the units employed; the C.G.S. system would probably be preferred in some aspects of possible future use of the tables. The choice was determined by the fact that the data were required primarily for comparison with results obtained in the field, where British units had already been adopted for the full-scale work.

Tables of θ (in °F.) for various values of d

(Q in therms/yard.hour)

$d=3$ ft. 9 in.

$h=60$ inches

Q	V in feet per second							
	1·5	2·0	2·5	3·0	3·5	4·0	4·5	5·0
0·00	0·0							
0·04	0·0							
0·08	0·1	0·0						
0·12	0·2	0·1	0·0					
0·16	0·4	0·2	0·0					
0·20	0·6	0·3	0·1	0·0				
0·24		0·5	0·2	0·1	0·0			
0·28		0·6	0·3	0·2	0·1			
0·32		0·7	0·4	0·3	0·2	0·0		
0·36		0·8	0·5	0·4	0·3	0·1	0·0	
0·40		1·0	0·7	0·5	0·4	0·2	0·1	0·0

$h=40$ inches

Q	V in feet per second							
	1·5	2·0	2·5	3·0	3·5	4·0	4·5	5·0
0·00	0·0	0·0						
0·04	0·1	0·0						
0·08	0·3	0·1	0·0					
0·12	0·5	0·2	0·1					
0·16	0·8	0·4	0·2	0·0				
0·20	1·1	0·6	0·3	0·1	0·0			
0·24		0·8	0·5	0·2	0·1	0·0	0·0	
0·28		1·0	0·7	0·4	0·2	0·1	0·1	0·0
0·32		1·3	0·9	0·6	0·4	0·3	0·2	0·1
0·36		1·6	1·2	0·8	0·6	0·5	0·4	0·3
0·40		2·0	1·5	1·1	0·9	0·7	0·6	0·5

$h=20$ inches

Q	V in feet per second							
	1·5	2·0	2·5	3·0	3·5	4·0	4·5	5·0
0·00	0·0	0·0	0·0	0·0				
0·04	1·1	0·8	0·4	0·0				
0·08	3·0	1·8	0·7	0·1				
0·12	4·9	2·9	1·1	0·2	0·0			
0·16	6·9	3·9	1·6	0·5	0·2	0·0	0·0	
0·20	8·9	5·0	2·2	1·0	0·5	0·2	0·1	0·0
0·24		6·1	3·0	1·5	0·8	0·4	0·3	0·2
0·28		7·3	3·9	2·0	1·1	0·6	0·5	0·3
0·32		8·7	5·0	2·6	1·3	0·9	0·7	0·5
0·36		10·4	6·2	3·1	1·5	1·1	0·8	0·6
0·40		13·0	7·7	3·6	1·8	1·3	0·9	0·7

Tables of θ (in °F.) for various values of d (*cont.*)

(Q in therms/yard.hour)

d=3 ft. 9 in.

h=8 inches

Q	V in feet per second 1·5	2·0	2·5	3·0	3·5	4·0	4·5	5·0
0·00	0·0	0·0	0·0	0·0				
0·04	8·4	7·0	5·6	4·1				
0·08	14·1	13·1	11·6	9·6	7·5			
0·12	18·8	18·1	16·6	15·0	13·9			
0·16	23·0	21·8	20·3	18·4	16·9			
0·20	26·7	25·5	24·1	22·0	20·0			
0·24		29·4	28·0	25·7	23·2			
0·28		33·4	32·0	29·3	26·5	24·6	23·0	21·6
0·32		37·5	35·8	32·8	30·0	28·0	26·3	25·0
0·36		41·7	39·5	36·3	33·6	31·4	29·6	28·4
0·40		45·9	43·1	39·7	37·2	34·8	32·9	31·8

h=1·6 inches

Q	V in feet per second 1·5	2·0	2·5	3·0	3·5	4·0	4·5	5·0
0·00	0·0	0·0	0·0	0·0				
0·04	9·8	10·2	10·6	11·0				
0·08	15·0	16·3	17·5	18·8	20·0			
0·12	19·5	20·8	21·9	22·9	23·7			
0·16	23·1	24·2	25·4	26·3	27·1			
0·20	26·3	27·6	28·9	29·8	30·6			
0·24		31·1	32·4	33·2	34·0			
0·28		34·7	36·0	36·7	37·5	38·3	39·1	39·9
0·32		38·1	39·6	40·3	41·1	41·9	42·7	43·6
0·36		41·3	43·1	43·8	44·6	45·4	46·3	47·3
0·40		44·5	46·3	47·3	48·1	49·0	49·9	50·6

d=7 ft. 6 in.

h=60 inches

Q	V in feet per second 1·5	2·0	2·5	3·0	3·5	4·0	4·5	5·0
0·00	0·0	0·0						
0·04	0·2	0·1						
0·08	0·4	0·2	0·0					
0·12	0·6	0·3	0·1	0·0				
0·16	1·0	0·4	0·2	0·1				
0·20	1·4	0·5	0·3	0·2	0·0			
0·24		0·6	0·4	0·2	0·1			
0·28		0·7	0·5	0·3	0·1			
0·32		0·8	0·6	0·3	0·1			
0·36		1·0	0·7	0·4	0·2	0·0		
0·40		1·1	0·8	0·4	0·2	0·1		
0·44		1·2	0·8	0·5	0·3	0·1	0·0	
0·48		1·4	0·9	0·5	0·3	0·2	0·1	0·0

Tables of θ (in °F.) for various values of d (*cont.*)

(Q in therms/yard.hour)

d=7 ft. 6 in.

h=40 inches

Q	*V* in feet per second							
	1·5	2·0	2·5	3·0	3·5	4·0	4·5	5·0
0·00	0·0	0·0	0·0	0·0				
0·04	0·6	0·3	0·1	0·1				
0·08	1·4	0·7	0·4	0·2				
0·12	2·4	1·1	0·8	0·2				
0·16	3·6	1·7	1·0	0·3	0·0			
0·20	5·5	2·8	1·2	0·3	0·1			
0·24		3·8	1·5	0·4	0·1	0·0		
0·28		4·8	1·9	0·5	0·2	0·1	0·0	
0·32		5·7	2·3	0·7	0·4	0·2	0·1	0·0
0·36		6·6	2·8	0·9	0·6	0·3	0·2	0·1
0·40		7·6	3·3	1·1	0·8	0·5	0·4	0·3
0·44		8·6	3·8	1·4	1·0	0·7	0·6	0·5
0·48		9·6	4·3	1·8	1·2	0·9	0·8	0·7

h=20 inches

Q	*V* in feet per second							
	1·5	2·0	2·5	3·0	3·5	4·0	4·5	5·0
0·00	0·0	0·0	0·0	0·0				
0·04	3·5	2·6	1·7	0·8				
0·08	6·5	5·2	4·1	2·9	1·7			
0·12	8·4	7·9	6·5	5·0	3·6			
0·16	10·3	9·9	8·4	7·0	5·8			
0·20	12·0	11·9	10·2	9·0	7·8	6·3	4·9	3·5
0·24		13·8	12·0	10·6	9·6	8·1	6·6	5·0
0·28		15·5	13·9	12·5	11·3	10·0	8·4	6·5
0·32		17·5	15·5	14·2	12·8	11·5	9·9	8·0
0·36		19·0	17·3	15·9	14·3	12·9	11·1	9·4
0·40		20·7	18·9	17·4	15·6	14·1	12·5	10·9
0·44		22·3	20·5	18·8	17·0	15·4	13·7	12·2
0·48		23·9	22·0	20·0	18·1	16·5	14·9	13·5

h=8 inches

Q	*V* in feet per second							
	1·5	2·0	2·5	3·0	3·5	4·0	4·5	5·0
0·00	0·0	0·0	0·0	0·0				
0·04	5·1	4·9	4·6	4·2				
0·08	8·0	7·5	7·9	8·3	8·5			
0·12	10·4	9·8	10·9	11·4	11·5			
0·16	12·0	11·8	13·0	13·5	13·7			
0·20	13·4	13·6	15·0	15·5	16·0			
0·24		15·5	17·0	17·5	18·0			
0·28		17·4	18·7	19·4	20·0	20·0	19·8	19·6
0·32		19·0	20·4	21·0	21·5	21·4	21·2	21·0
0·36		20·5	21·9	22·5	23·0	23·2	23·3	23·1
0·40		22·0	23·1	24·0	24·5	24·7	24·8	24·6
0·44		23·4	24·5	25·3	25·7	25·9	26·0	25·8
0·48		24·6	25·7	26·5	27·0	27·2	27·2	26·9

Tables of θ (in °F.) for various values of d (*cont.*)

(Q in therms/yard.hour)

d=7 ft. 6 in.

h=1·6 inches

Q	V in feet per second							
	1·5	2·0	2·5	3·0	3·5	4·0	4·5	5·0
0·00	0·0	0·0	0·0	0·0				
0·04	4·9	4·4	5·1	6·2				
0·08	7·0	6·7	8·4	9·1	10·8			
0·12	8·5	8·4	10·0	11·1	11·9			
0·16	9·9	10·0	11·6	13·0	13·7			
0·20	11·0	11·5	13·4	14·8	15·5			
0·24		13·0	14·9	16·4	17·1			
0·28		14·5	16·1	17·7	18·7	19·5	20·0	20·5
0·32		15·6	17·3	19·0	20·0	20·8	21·4	22·9
0·36		16·8	18·3	20·0	21·1	21·9	22·5	23·1
0·40		17·6	19·1	20·9	22·0	22·8	23·5	24·0
0·44		18·5	20·0	21·5	22·7	23·6	24·3	24·9
0·48		19·1	20·5	22·1	23·4	24·2	24·9	25·4

d=15 ft.

h=80 inches

Q	V in feet per second							
	1·5	2·0	2·5	3·0	3·5	4·0	4·5	5·0
0·00	0·0	0·0	0·0					
0·04	0·3	0·1	0·0					
0·08	0·7	0·3	0·1	0·0				
0·12	1·3	0·5	0·2	0·1	0·0			
0·16	2·0	1·0	0·4	0·2	0·0			
0·20	3·0	1·5	0·6	0·3	0·1	0·0		
0·24		2·0	0·8	0·4	0·2	0·0		
0·28		2·5	1·1	0·5	0·2	0·0		
0·32		2·9	1·5	0·6	0·3	0·1	0·0	
0·36		3·4	1·9	0·7	0·3	0·1	0·0	
0·40		3·9	2·3	0·8	0·4	0·1	0·0	
0·44		4·4	2·7	1·0	0·4	0·2	0·0	
0·48		5·0	3·1	1·1	0·5	0·2	0·0	

h=60 inches

Q	V in feet per second							
	1·5	2·0	2·5	3·0	3·5	4·0	4·5	5·0
0·00	0·0	0·0	0·0					
0·04	0·7	0·3	0·1	0·0				
0·08	1·7	0·7	0·3	0·1	0·0			
0·12	2·7	1·5	0·7	0·3	0·1	0·0		
0·16	3·8	2·5	1·2	0·5	0·3	0·1		
0·20	4·8	3·5	1·9	0·9	0·5	0·2	0·0	
0·24		4·5	2·5	1·4	0·7	0·4	0·1	0·0
0·28		5·5	3·4	1·9	1·0	0·6	0·2	0·1
0·32		6·2	4·1	2·4	1·4	0·9	0·4	0·2
0·36		6·8	4·9	3·1	1·9	1·2	0·6	0·3
0·40		7·5	5·8	3·9	2·4	1·6	0·9	0·4
0·44		8·2	6·7	4·6	3·0	2·0	1·2	0·5
0·48		8·9	7·7	5·6	3·8	2·6	1·6	0·7

Tables of θ (in °F.) for various values of d (*cont.*)

(Q in therms/yard.hour)

$d=15$ ft.

$h=40$ inches

Q	V in feet per second							
	1·5	2·0	2·5	3·0	3·5	4·0	4·5	5·0
0·00	0·0	0·0	0·0	0·0				
0·04	1·6	1·2	0·8	0·4				
0·08	2·9	2·3	1·7	1·1				
0·12	4·0	3·1	2·4	1·7	0·9			
0·16	5·0	4·2	3·3	2·6	1·6			
0·20	5·9	5·1	4·2	3·5	2·6			
0·24		6·1	5·1	4·5	3·7			
0·28		6·9	6·1	5·5	4·6	3·9	3·1	2·3
0·32		7·5	7·1	6·5	5·6	4·8	4·0	3·1
0·36		8·2	8·1	7·6	6·5	5·6	4·9	4·1
0·40		8·9	9·1	8·7	7·5	6·5	5·7	4·9
0·44		9·6	10·0	9·9	8·4	7·2	6·5	5·6
0·48		10·2	11·0	11·2	9·3	8·0	7·1	6·4

$h=20$ inches

Q	V in feet per second							
	1·5	2·0	2·5	3·0	3·5	4·0	4·5	5·0
0·00	0·0	0·0	0·0	0·0				
0·04	2·5	2·5	2·5	2·4				
0·08	4·0	3·8	3·9	3·9				
0·12	4·9	4·4	4·8	4·9	5·0			
0·16	5·6	5·1	5·5	5·7	5·8			
0·20	6·3	5·9	6·4	6·6	6·6			
0·24		6·7	7·1	7·5	7·5			
0·28		7·5	8·0	8·4	8·5	8·5	8·5	8·5
0·32		8·3	8·9	9·3	9·5	9·5	9·5	9·5
0·36		8·9	9·6	10·1	10·4	10·4	10·4	10·4
0·40		9·5	10·4	11·0	11·2	11·2	11·2	11·2
0·44		10·2	11·1	11·9	12·0	12·0	12·0	12·0
0·48		10·9	12·0	12·7	12·7	12·7	12·7	12·7

$h=8$ inches

Q	V in feet per second							
	1·5	2·0	2·5	3·0	3·5	4·0	4·5	5·0
0·00	0·0	0·0	0·0	0·0				
0·04	2·6	2·3	2·4	2·6				
0·08	4·0	3·5	3·7	4·0				
0·12	4·9	4·4	4·6	5·0	5·4			
0·16	5·4	5·1	5·5	5·8	6·1			
0·20	5·6	5·9	6·2	6·5	7·0			
0·24		6·5	6·9	7·2	7·8			
0·28		7·0	7·5	7·9	8·5	9·1	9·7	10·3
0·32		7·5	8·0	8·6	9·3	9·9	10·5	11·1
0·36		8·1	8·6	9·4	10·0	10·5	11·2	11·9
0·40		8·6	9·2	10·0	10·6	11·2	12·0	12·5
0·44		9·1	9·9	10·7	11·4	12·0	12·7	13·4
0·48		9·9	10·9	11·7	12·4	13·2	13·9	14·5

Tables of θ (in °F.) for various values of d (*cont.*)

(Q in therms/yard.hour)

d=15 ft.

h=1·6 inches

Q	V in feet per second							
	1·5	2·0	2·5	3·0	3·5	4·0	4·5	5·0
0·00	0·0	0·0	0·0	0·0				
0·04	2·0	1·7	1·8	2·0				
0·08	3·0	2·6	2·8	3·1				
0·12	3·4	3·3	3·5	4·0	4·3			
0·16	3·7	4·0	4·1	4·5	5·0			
0·20	4·0	4·5	4·6	5·0	5·5			
0·24		4·9	5·1	5·6	6·1			
0·28		5·3	5·5	6·1	6·7	7·2	7·6	7·9
0·32		5·6	6·0	6·6	7·2	7·8	8·2	8·6
0·36		6·0	6·5	7·1	7·8	8·3	8·7	9·1
0·40		6·5	7·0	7·6	8·4	8·9	9·4	9·9
0·44		6·9	7·5	8·2	8·9	9·5	10·0	10·5
0·48		7·3	8·0	8·8	9·5	10·1	10·7	11·2

Tables of v (in ft/sec.) for various values of d

(Q in therms/yard.hour)

d=3 ft. 9 in.

h=24 inches

Q	V in feet per second							
	1·5	2·0	2·5	3·0	3·5	4·0	4·5	5·0
0·00	1·40	1·87	2·35	2·80	3·27	3·74	4·20	4·66
0·04	1·45	1·90	2·38	2·84	3·31	3·80	4·26	4·73
0·08	1·49	1·94	2·42	2·87	3·35	3·85	4·32	4·79
0·12	1·54	1·98	2·45	2·90	3·39	3·89	4·36	4·83
0·16	1·59	2·02	2·49	2·93	3·43	3·91	4·39	4·86
0·20	1·63	2·07	2·52	2·96	3·45	3·90	4·37	4·83
0·24		2·12	2·56	2·99	3·45	3·89	4·33	4·79
0·28		2·19	2·59	3·02	3·45	3·88	4·30	4·73
0·32		2·26	2·63	3·05	3·45	3·87	4·27	4·67
0·36		2·34	2·66	3·08	3·45	3·89	4·24	4·60

h=10 inches

Q	V in feet per second							
	1·5	2·0	2·5	3·0	3·5	4·0	4·5	5·0
0·00	1·25	1·68	2·08	2·50	2·89	3·28	3·68	4·08
0·04	1·49	1·83	2·22	2·66	3·06	3·45	3·85	4·23
0·08	1·72	1·98	2·36	2·81	3·22	3·59	3·98	4·36
0·12	1·90	2·14	2·50	2·95	3·37	3·72	4·10	4·48
0·16	2·06	2·29	2·64	3·08	3·50	3·84	4·21	4·57
0·20	2·17	2·44	2·78	3·20	3·61	3·94	4·30	4·63
0·24		2·59	2·92	3·31	3·70	4·02	4·36	4·68
0·28		2·74	3·06	3·41	3·77	4·08	4·40	4·71
0·32		2·89	3·20	3·50	3·82	4·12	4·43	4·73
0·36		3·04	3·34	3·58	3·85	4·14	4·45	4·74

Tables of v (in ft/sec.) for various values of d (*cont.*)

(Q in therms/yard.hour)

$d=3$ ft. 9 in.

$h=4$ inches

Q	V in feet per second							
	1·5	2·0	2·5	3·0	3·5	4·0	4·5	5·0
0·00	1·07	1·43	1·78	2·14	2·49	2·86	3·20	3·55
0·04	1·41	1·73	2·05	2·37	2·71	3·05	3·39	3·71
0·08	1·64	1·93	2·24	2·54	2·87	3·18	3·51	3·80
0·12	1·84	2·04	2·36	2·65	2·97	3·26	3·57	3·86
0·16	2·01	2·12	2·42	2·71	3·02	3·30	3·59	3·88
0·20	2·12	2·19	2·47	2·75	3·03	3·31	3·60	3·87
0·24		2·26	2·51	2·77	3·03	3·30	3·56	3·81
0·28		2·33	2·54	2·79	3·02	3·27	3·51	3·76
0·32		2·40	2·57	2·80	3·00	3·22	3·46	3·70
0·36		2·46	2·59	2·80	2·98	3·17	3·39	3·63

$d=7$ ft. 6 in.

$h=48$ inches

Q	V in feet per second							
	1·5	2·0	2·5	3·0	3·5	4·0	4·5	5·0
0·00	1·46	1·96	2·46	2·96	3·44	3·93	4·42	4·90
0·04	1·48	1·96	2·47	2·97	3·46	3·95	4·45	4·95
0·08	1·49	1·97	2·48	2·98	3·48	3·97	4·47	4·98
0·12	1·50	1·98	2·49	2·99	3·49	3·99	4·49	4·99
0·16	1·51	1·99	2·50	3·00	3·50	4·00	4·50	5·00
0·20	1·52	2·00	2·49	2·99	3·49	3·99	4·49	4·99
0·24		2·01	2·48	2·98	3·48	3·97	4·48	4·98
0·28		2·02	2·47	2·97	3·47	3·95	4·46	4·96
0·32		2·03	2·46	2·96	3·45	3·93	4·44	4·94
0·36		2·04	2·45	2·95	3·43	3·91	4·42	4·92

$h=24$ inches

Q	V in feet per second							
	1·5	2·0	2·5	3·0	3·5	4·0	4·5	5·0
0·00	1·40	1·87	2·35	2·80	3·27	3·74	4·20	4·66
0·04	1·58	1·97	2·43	2·86	3·32	3·77	4·21	4·66
0·08	1·75	2·07	2·51	2·92	3·36	3·80	4·22	4·66
0·12	1·90	2·17	2·59	2·98	3·40	3·83	4·24	4·66
0·16	2·03	2·27	2·67	3·04	3·44	3·86	4·26	4·65
0·20	2·15	2·37	2·74	3·10	3·48	3·88	4·27	4·64
0·24		2·46	2·81	3·16	3·52	3·90	4·27	4·63
0·28		2·55	2·88	3·22	3·55	3·92	4·27	4·61
0·32		2·63	2·95	3·27	3·58	3·93	4·27	4·59
0·36		2·71	3·02	3·33	3·61	3·94	4·26	4·57

Tables of *v* (in ft/sec.) for various values of *d* (*cont.*)

(*Q* in therms/yard.hour)

d=7 ft. 6 in.

h=10 inches

Q	*V* in feet per second							
	1·5	2·0	2·5	3·0	3·5	4·0	4·5	5·0
0·00	1·25	1·68	2·08	2·50	2·89	3·28	3·68	4·08
0·04	1·52	1·91	2·24	2·63	3·00	3·40	3·76	4·15
0·08	1·73	2·09	2·38	2·74	3·09	3·48	3·82	4·19
0·12	1·92	2·23	2·51	2·84	3·17	3·54	3·88	4·23
0·16	2·07	2·35	2·62	2·93	3·25	3·60	3·94	4·27
0·20	2·20	2·46	2·72	3·01	3·32	3·65	3·98	4·30
0·24		2·57	2·81	3·08	3·38	3·70	4·02	4·32
0·28		2·67	2·89	3·14	3·43	3·75	4·05	4·34
0·32		2·77	2·96	3·20	3·48	3·79	4·08	4·36
0·36		2·87	3·02	3·25	3·52	3·83	4·10	4·38

h=4 inches

Q	*V* in feet per second							
	1·5	2·0	2·5	3·0	3·5	4·0	4·5	5·0
0·00	1·07	1·43	1·78	2·14	2·49	2·86	3·20	3·55
0·04	1·39	1·76	2·10	2·45	2·79	3·13	3·49	3·82
0·08	1·63	1·97	2·30	2·62	2·96	3·29	3·61	3·95
0·12	1·80	2·10	2·43	2·74	3·06	3·39	3·70	4·02
0·16	1·94	2·19	2·52	2·81	3·12	3·43	3·75	4·06
0·20	2·04	2·26	2·59	2·86	3·16	3·45	3·78	4·06
0·24		2·32	2·64	2·90	3·19	3·47	3·77	4·04
0·28		2·38	2·67	2·93	3·21	3·48	3·76	4·02
0·32		2·43	2·69	2·95	3·23	3·48	3·75	4·01
0·36		2·48	2·71	2·96	3·24	3·48	3·74	4·00

d=15 ft.

h=72 inches

Q	*V* in feet per second			
	2·0	2·5	3·0	3·5
0·00	2·00	2·50	3·00	3·50
0·12	2·00	2·49	2·99	3·50

h=60 inches

Q	*V* in feet per second			
	2·0	2·5	3·0	3·5
0·00	1·98	2·48	2·98	3·47
0·12	2·08	2·51	2·99	3·47

h=48 inches

Q	*V* in feet per second			
	2·0	2·5	3·0	3·5
0·00	1·96	2·46	2·96	3·44
0·12	2·16	2·56	3·01	3·49

h=36 inches

Q	*V* in feet per second			
	2·0	2·5	3·0	3·5
0·00	1·92	2·42	2·90	3·39
0·12	2·23	2·60	3·00	3·46

h=24 inches

Q	*V* in feet per second			
	2·0	2·5	3·0	3·5
0·00	1·87	2·35	2·80	3·27
0·12	2·27	2·60	2·97	3·42

h=10 inches

Q	*V* in feet per second			
	2·0	2·5	3·0	3·5
0·00	1·68	2·08	2·50	2·89
0·12	2·14	2·49	2·91	3·35

h=4 inches

Q	*V* in feet per second			
	2·0	2·5	3·0	3·5
0·00	1·43	1·78	2·14	2·49
0·12	1·99	2·39	2·84	3·31

Physics and the Atmosphere

By G. M. B. DOBSON
Oxford

5th Charles Chree Address, delivered 4th November 1949; *MS. received 28th November* 1949

I feel it a very great honour that you should have asked me to give this year's Charles Chree address. I remember, when he was President of the Royal Meteorological Society, Dr. Chree introducing a speaker with the remark that, for him, all meteorologists were divided into two groups, viz. those who had worked at Kew Observatory and those who had not, and that the speaker, fortunately, belonged to the first group. I am personally doubly fortunate, in that, not only did I work at Kew Observatory for some 18 months immediately after leaving Cambridge, but I worked there while Chree was the Superintendent.

A mathematician of the first rank, Chree also did much for the study of the Earth's magnetic field in organizing accurate measurements and in discussing the results. When the magnetic observatory at Eskdalemuir was started he had much to do with the selection of the site and the organization of the observations. I remember him telling me how, after he had carefully tested the rock around the proposed site for magnetic effect, the Office of Works managed to find just the small amount of magnetic rock which had escaped him with which to build the walls, and they had all to be pulled down again when a few feet high and rebuilt with non-magnetic stone!

He was much interested in the various long period and cyclic changes in the Earth's magnetic or electric field, and when a series of measurements had been running for a long time he was most insistent that nothing should be changed in the method of observing lest it might introduce some discontinuity into the series. To some of his juniors this was sometimes rather irksome when they thought they had detected errors in the method of observation which they could easily put right. Perhaps the right thing to have done would have been to have run the old and improved measurements together for some time for intercomparison. A remarkable characteristic of Chree was his great preference for results to be expressed by tables or figures rather than by a series of curves, and I remember how, when an assistant brought him a foolscap sheet covered with figures—say the hourly values of the Earth's horizontal magnetic force for a month—he would glance through it and almost immediately pick out any irregularity or some interesting point.

He avoided speculation about causes until he thought that sufficient facts were known by which to test such speculation, and if he thought that the observations indicated a definite connection between two phenomena he would test the reality of such a connection in every way possible before he would be satisfied that the connection was real. One of the last papers which Chree wrote (in 1925) was on the results of his investigation of a possible connection between the amount of ozone in the atmosphere and the disturbance of the Earth's magnetic field. The ozone measurements had only been running for about a year, but after analysing them in many different ways, Chree concluded that there was an apparent connection between the two phenomena. He ended his paper with the words :

> "It is never prudent to accept the results of a single year as final. Events analogous to the breaking of the bank of Monte Carlo do occur occasionally even in Nature. But it seems abundantly clear that the systematic continuation of ozone observations for some time to come is desirable in the interests of terrestrial magnetism" (Chree 1926).

On the more personal side I would stress his kindness to all around, and I well remember how he and his sister used to invite me, though much their junior, to their house. Chree was, of course, an ardent Scotsman, and it was a familar picture to see him every day, after a frugal meal in his room at the Observatory, walking round the Observatory enclosure with a golf-club and ball until two o'clock. I have heard it said that there were few beggars who knocked at his house and had the astuteness to say that they came from north of the Border, and went away empty!

§ 1

The Charles Chree prize is associated with Geophysics, and it has been suggested to me by the Officers that I should give some account of geophysical work with which I have been associated. This I gladly do, for I feel that it is an opportunity to bring before physicists something of the fascinating work that still remains to be done in studying the Physics of the Atmosphere and to suggest that more of them might think of turning their attention to this subject. Experimental geophysical research differs somewhat from the more usual experimental physics in that, while there is much work to done in the laboratory, a great deal of the work is observing the actual conditions in the Earth or Atmosphere. An American publication recently suggested that one of the great attractions of research on Cosmic Radiation was that it could be made to take you to all sorts of interesting parts of the Earth. I may say that Geophysics is just as helpful in this matter! (While mentioning Cosmic Radiation, let me remind the atomic physicists that it was workers in Geophysics who presented them with this powerful tool, as evidenced by the older German name of 'Hesssche Strahlung,' which might perhaps with advantage be retained today.) But to return to experimental geophysics : this has both its peculiar difficulties and peculiar attractions—difficulties due to the fact that, as in the case of Astrophysics, one must observe Nature as it presents itself, and one cannot, in general, control the conditions of an experiment as one can in laboratory physics, while one of its great attractions is that much of the work is done out of doors under the open sky. It is recorded of Rutherford that, at a time when experiments were going particularly well, he remarked to a colleague: "I do pity those people who haven't got laboratories to work in". The geophysicist, after a good day's observations in the upper Alps, or even on our little hill above Oxford, feels like remarking: "I do pity those poor physicists who have to work cooped up in their stuffy laboratories".

As I see it today, the great need in Geophysics is for much more experimental work. Theorists we want and, indeed, we already have many of high standing, but they seem to me to be seriously hampered by the absence of facts based on experimental work on which to found, and by which to test, their work. May I give two instances of what I mean and to which I shall refer again. In the theoretical study of the temperature of the stratosphere, the amount of water vapour was, until a few years ago, entirely unknown, and it was generally assumed that the air would be saturated. On this assumption the absorption and emission of long-wave radiation by water vapour would outweigh that of any other gases which might take part in the radiative equilibrium. When, during the war, it became necessary to measure the humidity of the stratosphere on account of the operational importance of aircraft condensation trails, it was at once found that, far from being saturated with water vapour, the air in the stratosphere was, in fact, very dry. Again, at the present time most theoretical work on the stratosphere assumes that the air there is in radiative equilibrium, but no measurements to find out whether this is so have yet been made, though this should be quite possible and some work on the subject is now in hand.

I believe that there is a growing tendency for some physicists to dislike what I may call 'factory methods' in research, where the work can only be carried out by a large team of workers with elaborate and expensive apparatus and where the individual worker—particularly if he be a junior—may feel that he is merely a cog in the machine and his individuality is to some extent submerged, with consequent loss of interest. While this applies to one important branch of Geophysics just opening up, viz. the exploration of the highest atmosphere by rockets, much work of value can be carried out by individuals without elaborate apparatus. The first pioneer work of Aitken and, later, of C. T. R. Wilson on the condensation of water vapour and the importance of condensation nuclei was carried out with the simplest of apparatus (Aitken 1880, 1887, Wilson 1895, 1900). When W. H. Dines started to measure the temperature of the upper atmosphere by instruments carried on free balloons, the available funds were very small, but by very skilful design he was able to make instruments which were so simple that they could easily be made in quantity in his workshop, and so light that they needed only small, and therefore cheap, balloons to lift them. With one instrument maker and a very small grant from the Meteorological Office he was largely responsible for first obtaining most of our knowledge of the temperature and pressure of the upper atmosphere and the correlations between them (Dines 1909 to 1919). When in the early years of this century Mr. C. J. P. Cave began to study the wind at various heights above the Earth's surface, much of the work was carried out with the sole help of his gardener for launching the balloons (Cave 1912).

There are still many problems in Geophysics waiting to be solved which can well be tackled by individual workers with relatively simple apparatus. Any physicist who is prepared to be his own instrument maker will find a wide field open to him.

§ 2. ATMOSPHERIC OZONE

Turning now to describe some of the geophysical work that has been carried out at Oxford, I will first take the measurements of the amount of atmospheric ozone. The total amount of ozone in the air is less than a millionth of the oxygen and nitrogen, and this small amount is very largely situated high up in the atmosphere, chiefly between 10 and 30 km. Anyone might therefore well ask why it should be of much interest to study the variations of such a rare constituent of the atmosphere. There are several things which make this small amount of ozone very interesting. As you will know, ozone very strongly absorbs ultra-violet radiation of wavelength shorter than 3200 A. and cuts off all the solar radiation in shorter wavelengths so that, until the advent of high flying rockets, the solar spectrum was entirely unknown for wavelengths shorter than 2900 A. Secondly, as Dr. Gowan has shown (Gowan 1936), the upper part of the ozone region absorbs enough solar radiation to cause the temperature at heights of 40 to 60 km. to rise to values above that at the surface of the Earth at the Equator. (Incidentally, the presence of this warm region is responsible for a number of other interesting effects which I have not time to discuss here.) Thirdly, there is some evidence that the energy of the outgoing terrestrial radiation of wavelengths around 9 μ, which is absorbed by ozone, is sufficient to have a marked effect on the temperature of the stratosphere. Finally, it is an observed fact that the amount of ozone in the upper atmosphere is closely correlated with the general meteorological conditions and particularly with the conditions at great heights. It may well be that when our knowledge of the subject is more complete we shall find such measurements of practical importance.

The method used to measure the ozone content of the atmosphere follows closely that employed by Fabry and Buisson (1913, 1921), who were the first to make any accurate measurements of atmospheric ozone. Utilizing the strong ultra-violet absorption band of ozone, which increases in intensity from about 3300 A. to a maximum at about 2500 A., measurements of the relative intensity of the solar spectrum at two wavelengths on the long-wave edge of this absorption band are used to deduce the amount of ozone through which the light has passed and hence the ozone content of the atmosphere above the place of observation. In designing the apparatus for such measurements great care must be taken to avoid errors due to light scattered within the spectrograph since the intensity of the Sun's radiation at these short wavelengths after absorption by ozone is extremely small compared with that in the visible region.

Simple Feré spectrographs built in my laboratory were used up to about 1930 and gave excellent results when direct sunlight was available, but they suffered from the great disadvantage that the photographic plates had to be sent back for development and measurement, so that the ozone values were not known until several days after the spectra were taken, while no measurements were possible on completely cloudy days. Largely for this reason, a much more elaborate photoelectric spectrophotometer was built which allowed the ozone content to be measured by the absorption of ultra-violet light in the same way as with the photographic instruments. The latter instrument is both more sensitive and also allows the ozone value to be calculated immediately after the observation, observation and calculation taking about ten minutes. The first instrument was built in my laboratory, but when a large number were required they had to be manufactured by an optical firm. Some nineteen of those photoelectric instruments had been made at the beginning of the war and some fourteen more instruments are now under construction.

While the pre-war instruments used sodium photoelectric cells, the present instruments use photo-multipliers. Photo-multipliers have the great advantage of low 'signal/noise ratio' and hence allow measurements to be made with much weaker light than was possible before. This is particularly important where the vertical distribution of the ozone in the atmosphere is to be measured by observations using the light from the zenith sky when the Sun is very low. We can also now make measurements at night using the light of the full moon with fairly good accuracy, and such measurements should be valuable in very high latitudes in winter.

It is possible to estimate the vertical distribution of the atmospheric ozone by measurements of the zenith sky-light and also, more directly, by sending up spectrographs on free balloons or rockets to photograph the solar ultra-violet spectrum at great heights. Both these methods agree in showing that most of the ozone is situated between 10 km. and 30 km. Figure 1 shows the vertical distribution of ozone deduced from observations of the zenith sky-light, while Figure 2 shows spectra obtained at various heights from a rocket in America.

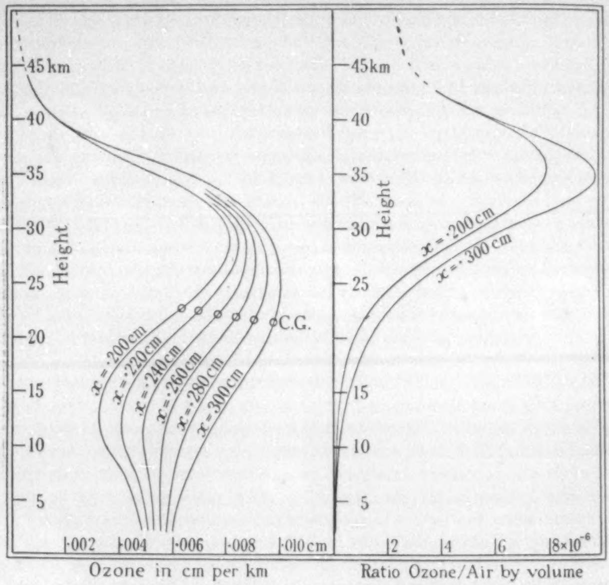

Figure 1. Vertical distribution of ozone as measured at Arosa by observations of the zenith skylight. (*Proc. Roy. Soc.* A, 1943, **145,** 440, Figure 8.)

These spectra show, for the first time, the spectrum of the Sun in the region beyond 2900 A. Spectra obtained from rockets or even high altitude balloons can only be obtained occasionally but, given good weather, the vertical distribution can be deduced from zenith sky-light observations every day and can be used for comparisons with the weather conditions. Contrary to what I said in the early part of this address, in this particular case, while the experimental geophysicist can make the necessary observations with good accuracy, he is at present somewhat held up by lack of theoretical work which would help him to deduce the vertical distribution from those observations.

Figure 3 shows the annual variation of ozone content at eleven places widely distributed over the globe and refers to the years 1926 to 1929. The chief points of interest in this figure are firstly the peculiar annual variation in the ozone content with a maximum in the local spring and minimum in the local autumn for both hemispheres, with little annual variation in low latitudes. Secondly, it is of interest to note the general increase in ozone content from low to high latitudes, this increase being much more marked in the spring than in the autumn.

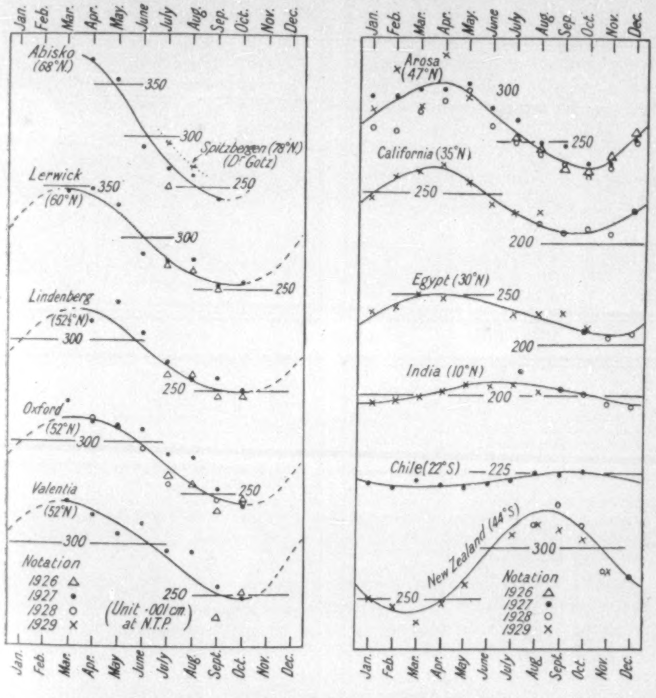

Figure 3. Annual variation of the amount of ozone in the atmosphere in different parts of the world. (*Proc. Roy. Soc.* A, 1930, **129,** 417, Figures 1 (*a*) and 1 (*b*).)

As an illustration of the way in which the amount of ozone varies from day to day with weather conditions, Figure 4 shows the distribution of ozone over N.W. Europe on 4th, 6th, 7th and 8th April 1927, when a depression, with an associated secondary, passed across the British Isles. I would particularly draw your attention to the large increase in atmospheric ozone in S.W. Ireland (0·306 cm. to 0·420 cm.) as the secondary passed over. On the other hand, Figure 5 shows the large fall in ozone content, first at S.W. Ireland and later in Great Britain, as a warm front approached from the west.

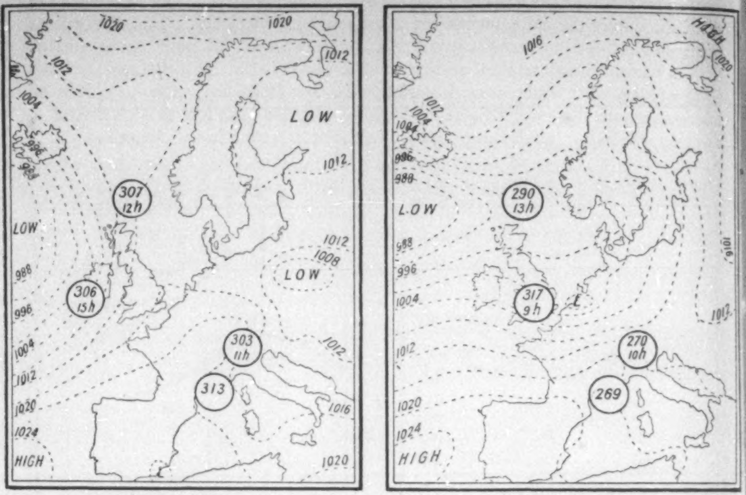
1020
1020
1012
1012
1004
996
988
LOW
307
12h
306
15h
988
996
1004
1012
1020
1024
HIGH
LOW
1012
1012
1008
LOW
303
11h
313
1012
1016
1020
1016
HIGH
1020
1012
1004
996
988
LOW
290
13h
988
996
1004
317
9h
L
1012
270
10h
269
1020
1024
HIGH
1016
1012

April 4, 1927. 7 A.M.

April 6, 1927. 7 A.M.

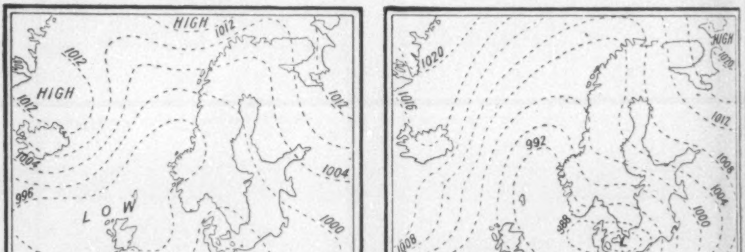
HIGH
1012
1012
HIGH
1012
1012
1004
996
LOW
1004
1000
352
9h
359
16h
1004
1004
1012
272
11h
268
1008
1012
1020
HIGH
1020
HIGH
1020
1016
1012
992
1008
1004
988
L
1000
1008
1000
L
420
13h
378
9h
1004
1000
1016
1020
HIGH
279
LOW
1004
L

April 7, 1927. 7 A.M.

April 8, 1927. 7 A.M.

Figure 4. Figures within the circles show the amount of ozone (unit 0·001 cm.) at various places in N.W. Europe. Note the large increase in the amount of ozone in the secondary depression on 8th April. (*Proc. Roy. Soc.* A, 1929, **122,** 473, Figure 5.)

As a further example of my previous point, that much work in Geophysics can be done with very simple apparatus, I would say that the marked connection between the ozone content and the weather, shown more fully in Figures 4 and 5, was first indicated by the results given by a simple Feré spectrograph built in my small laboratory for a total cost of under £25, while the observations at the various stations shown in Figures 3 and 4 were made by similar instruments also built in my small laboratory, though with a grant from the Royal Society for the optical parts.

The changes in atmospheric ozone which occur between one day and the next in temperate latitudes are almost certainly due, in part, to large-scale transport of air from higher or from lower latitudes, but whether this is the whole cause is by no means certain at the present time. A co-operative scheme is now being organized by Sir Charles Normand, under the auspices of the International Meteorological Association and with the generous support of the Royal Society, to study synoptically the changes in the ozone content at a dozen or more stations distributed over N.W. Europe, and to relate these changes to the meteorological conditions. This involves very careful inter-comparison at Oxford of all the instruments before they are distributed, so that the ozone values obtained from them shall be comparable. Several other instruments destined for more distant parts of the world are also being calibrated at Oxford.

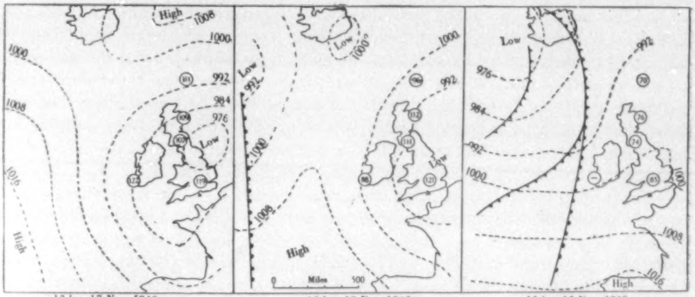

13 hr., 17 Nov. 1940 13 hr., 18 Nov. 1940 13 hr., 19 Nov. 1940

Figure 5. Figures within the circle give the amount of ozone at five places in the British Isles expressed as percentages of the mean value for the season. Note the large fall in the west of Ireland on 18th November and in Great Britain on 19th November, when the warm front, which caused the fall, was still several hundred miles to the west.

(*Proc. Roy. Soc.* A, 1946, **185,** 160, Figure 8.)

The earlier synoptic studies from which Figures 4 and 5 are taken suffered from a paucity of ozone observing stations, but quite as much from a paucity of observations of the meteorological conditions in the upper atmosphere. At the present time the number of daily meteorological balloon ascents has been greatly increased and should be adequate for such a study, though we may perhaps wish for meteorological observations at even greater heights than those now available since the correlation between the zone changes and other meteorological conditions appears to become closer with increasing height up to the limit reached by meteorological balloons.

§3. THE HUMIDITY OF THE UPPER ATMOSPHERE

For many years measurements of the humidity of the upper air have been made by wet and dry bulb psychrometers on aircraft and by small instruments carried up by balloons. In this country the instruments carried by balloons used the expansion of hairs or gold-beater's skin to measure the relative humidity, while in America the changes of electrical resistance of a thin film containing a hygroscopic salt was employed. Unfortunately all these methods become impracticable at very low temperatures where the amount of water vapour is very small. After a thorough examination of all the possible methods of measuring humidity, we concluded in 1941 that the dew-point (or rather frost-point) method was the most hopeful for use at very low temperatures. The first problem to solve was how to measure the very small amount of deposit of dew or hoar-frost on the thimble of the hygrometer. The driest air which has so far been found in the atmosphere contains only about 300 micrograms of water vapour per cubic metre. Since only a few litres of air can be passed over the hygrometer thimble in a minute, and since only a very small fraction of the water vapour can be removed from the air, it will be seen that we have to measure an amount of water vapour of the order of a few micrograms. If this were spread uniformly over the thimble it would be quite invisible. Fortunately, with the exception to be noted later, dew and hoar-frost tend to be deposited as droplets or particles of a size very suitable for scattering light, and if the clean thimble surface scatters very little light, it is possible to see extremely small amounts of deposit. The amount of deposit may be judged by eye observation or may be measured more accurately by the aid of a photocell. In the first case the air stream is made to impinge on to the thimble as a narrow jet so that the deposit tends to form as a streak across the otherwise clean thimble surface. The eye is thus helped by the contrast between the clean thimble and the deposit. In the second case the thimble is illuminated by a strong beam or light inclined at about 45° to the surface, while the photocell receives only light scattered normally from the surface. If the polishing of the thimble surface is always done in the plane of the beam of light, very little light is scattered by the clean thimble. Using a single valve amplification, it is easy to detect extremely small deposits of hoar-frost on the thimble. When using the eye-observation method it is necessary to find two temperatures of the thimble (as close together as possible) at which the deposit is firstly slowly growing and secondly equally slowly evaporating. The photoelectric method is so much more sensitive that one has only to cool the thimble until a small deposit has formed on it and then raise the temperature until the indicator shows that the amount of deposit is remaining constant.

Using such methods one can measure the frost-point of air down to temperatures of about 190° K. (−83° C.), where the water-vapour content of saturated air is only about 300 micrograms per cubic metre. Unfortunately at still lower temperatures ice tends to be deposited as a glassy layer which does not scatter light. It is possible, in principle, to measure changes in the thickness of the layer of glassy ice by optical interference methods, but as the layer would only change in thickness by one-tenth to one-hundredth of a wavelength per minute, one could not expect to measure air with frost-points much below those which have been measured with existing instruments.

In this work ceaseless watch must be kept for possible errors, one of the chief being contamination of the air on its way to the hygrometer by water vapour given off from the walls of the piping. To avoid errors of this kind, a clean metal tube, at least ½ inch in diameter, is led from outside the aircraft to the hygrometer and out again to the outside air. As the entrance of the tube faces forward, a strong blast of air passes through the tube continually when the aircraft is in flight. A very small fraction of this air stream is led by a very short branch tube to the thimble of the hygrometer. A cap covers the external entrance to the tube when the aircraft is flying through cloud.

There had been much speculation among meteorologists about the humidity of the air in the stratosphere, and it was therefore with great interest that the first results were awaited. The first accurate measurements were made by Mr. Brewer in a Fortress aircraft. On the 26th August and the 7th September 1943 the aircraft just entered the stratosphere and the measurements at the top of the climb indicated a great reduction in humidity. On the 22nd December 1943 the aircraft reached heights well within the stratosphere and the measurements left no doubt that the stratosphere air was very dry (see Figure 6). This conclusion has been confirmed by some hundred or more ascents which have since been made by the Meteorological Research Flight of the Air Ministry. The early measurements were made in aircraft without pressure cabins, and success was as much due to physical endurance as to observational skill. Even now no measurements have been made of the stratosphere when the tropopause is very high.

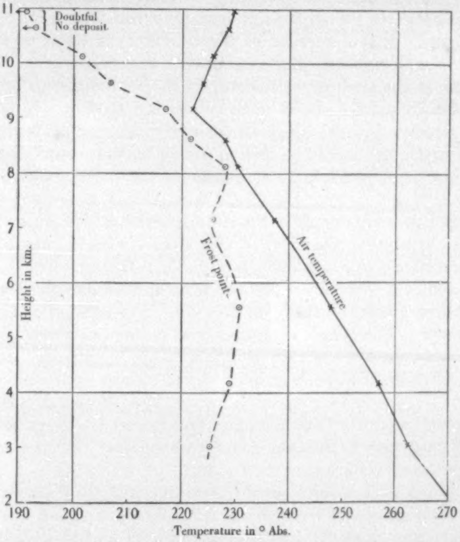

Figure 6. Frost-points and temperatures of the upper air on 22nd December 1943, this being the first case of a successful measurement of the humidity in the stratosphere. Note the very dry air in the stratosphere, indicated by the large difference between frost-point and air temperature.

(*Proc. Roy. Soc.* A, 1946, **185**, 154, Figure 4.)

In Figure 6 it will be noted that the rapid fall in frost-point with height begins about one kilometre below the tropopause and continues up to the maximum height attained. In Figure 7 the troposphere was nearly saturated throughout and there was a marked increase in the rate of fall of the frost-point immediately the stratosphere was entered. In some cases the rapid fall in the frost-point seems to begin a little above the tropopause and in others a little below it. Figure 8 shows results given by Mr. Shellard (Shellard 1949) for the average rate of change of both temperature and frost-point in the neighbourhood of the tropopause, in summer, in winter and for the year. In this diagram all heights are reckoned upwards and downwards from the tropopause. It will be seen that there is an increase in the rate of fall of the frost-point immediately above the tropopause, but that the rate of fall decreases again near the maximum height reached, though there is no evidence of the frost-point becoming constant or increasing again at greater heights. It is a question of much interest to know whether the air becomes still drier above the highest aircraft observations.

In addition to the very dry air found in the stratosphere, the frost-point hygrometer also frequently shows most interesting shallow dry layers in the troposphere associated with temperature inversions. It is remarkable that these shallow dry layers should be able to persist between much damper layers above and below them, and it is by no means clear at present where the dry air came from.

The origin of the very dry air in the stratosphere has also given rise to much speculation. The only obvious way in which the air could have been dried is by having been cooled to a low temperature, when the water vapour would be condensed and fall out of the air. The lowest natural temperature ever measured in the atmosphere is a little below 190° K. (−83° C.) in the air at about 20 km. over the Equator. The lowest measured frost-points are almost down to this figure, and one can therefore just explain them by the hypothesis that the air was dried over the Equator and has not since picked up any appreciable amount of water vapour. It should be noticed, however, that the wind currents in the stratosphere may come from any direction and the air is always very dry. In many cases it must have been many days or weeks since the air was last in the region of the low temperature over the Equator.

Very interesting work is going on at Cambridge with the object of measuring the intensity of sunlight in the region of the 6·3 μ absorption band of water vapour at great heights from aircraft. Such measurements should indicate the total amount of water vapour above the height of the aircraft, and from them it should be possible to deduce something about the humidity of the air at heights where at present we cannot operate frost-point hygrometers. It is also hoped that it may be possible shortly to develop frost-point hygrometers suitable for use on free balloons. Not only will the balloons reach greater heights than can be attained by aircraft, but it should be possible to send up several instruments daily and so study the distribution of humidity synoptically.

§ 4. ICE-FORMING NUCLEI IN THE ATMOSPHERE

A short time ago I witnessed the following phenomenon: a bank of alto-cumulus cloud, consisting of rather large dense cloudlets, was moving eastwards across the sky and, when each cloudlet reached a given position, snow began to fall from it and the cloudlet vanished in a few minutes, only a faint trail

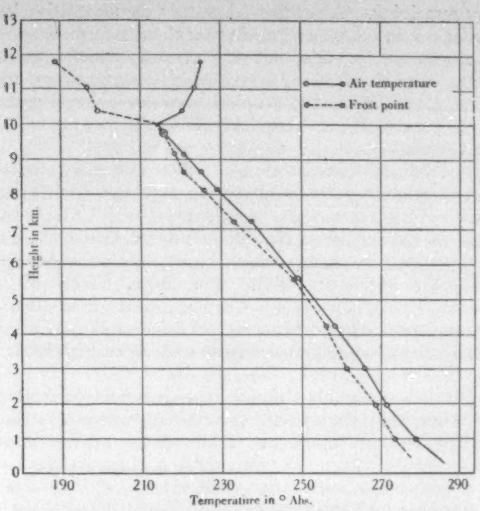

Figure 7. Frost-points and temperature of the upper air on 30th May 1945. Note that in this ascent the air throughout the troposphere is nearly saturated but there is a sharp increase in the rate of fall of the frost-point on entering the stratosphere.

(*Proc. Roy. Soc.* A, 1946, **185,** 156, Figure 5 (*a*).)

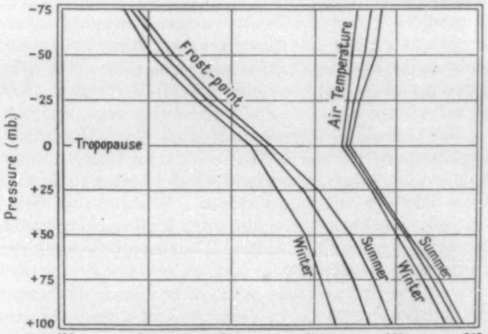

Figure 8. Average change of frost-point and air temperature with height in the neighbourhood of the tropopause.

(*Reproduced from Meteorological Research Paper 486 by H. C. Shellard, by permission of the Director of the Meteorological Office.*)

of falling snow remaining. A striking laboratory demonstration is easily made showing a similar result. A supercooled water cloud is formed by breathing into a refrigerated chamber at, say, 260° K. (−13° C.) and then, if a piece of solid CO_2 be passed through the cloud, it will leave behind many minute crystals of ice. Within a few seconds the water droplets have evaporated and the vapour condensed on the ice crystals, which quickly fall out if they are not too numerous and, therefore, too small.

The history of the alto-cumulus cloud droplets and the water fog formed in the cold vessel illustrate a problem about which I now wish to speak briefly. The formation of ice crystals in clouds is also of much interest since Professor Bergeron has suggested that all raindrops, except those in a drizzle, first start their existence as ice crystals, which, because of their lower vapour pressure compared with water drops, are able to grow large. Work of great interest has recently been done at Oxford by Cwilong, Fournier d'Albe, Palmer and Brewer on ice-forming nuclei, while similar work has been carried on independently in Germany by Findeisen and by Weickmann and in America by Langmuir and his associates.

Until recently it was thought that ice crystals would be formed on special 'sublimation nuclei' when the air was saturated with respect to ice in the same way as water droplets are formed on 'condensation nuclei' when the air is saturated with respect to water. The first result of the work was to show that if 'sublimation nuclei' existed at all they were exceedingly rare, and we are now able to show that true 'sublimation nuclei' probably do not exist at all in the atmosphere. The work at Oxford has shown that while there are no 'sublimation nuclei' there are many 'ice-forming nuclei,' and that each nucleus has a definite threshold temperature below which it begins to act as an 'ice-forming nucleus'. While the number of nuclei which are active at any particular temperature increases as the temperature is lowered, there are two special threshold temperatures at which large numbers of particles become active as ice-forming nuclei. The nuclei can therefore be divided into three groups. The first group consists of very few nuclei (though they may be very important meteorologically) which are active at temperatures above 241° K. (−32° C.). The number which are active at temperatures as high as 258° K. (−15° C.) is probably negligible, but as the temperature falls to 241° K. (−32° C.) the number of active nuclei gradually increases.

When the temperature reaches 241° K. (−32° C.) a large number of particles are normally found in the lower air over land which become active as 'ice-forming nuclei', and these belong to the second group. When the temperature falls to 232° K. (−41° C.) all particles of whatever kind which may be floating in the air seem to become active ice-forming nuclei. This threshold temperature is very sharp indeed. Particles, as different as sodium chloride or the dust produced by sparks between metal electrodes, all act exactly alike in this way. Moreover they all have ice formed on them only when the humidity of the air reaches (or very closely approaches) saturation over *water*. It now seems (in contradiction to some earlier experiments) that in perfectly clean air no water droplets or ice particles are formed at any temperature unless the air is very highly supersaturated.

It is now easy to explain the formation of the water fog in the cold chamber and its subsequent transformation into an ice fog. There being no 'ice-forming nuclei' which are active at 260° K. (−13° C.), a water fog is formed and, since there are very many condensation nuclei present in surface air, a very large number of small droplets will be formed which will settle very slowly, and the cloud will be stable. When we draw a piece of solid CO_2 through the water fog the air in immediate contact with the CO_2 will be cooled to a temperature below 232° K. (−41° C.), so that many particles will be active as ice-forming nuclei and a trail of ice crystals will be left in its track. These will be in air supersaturated with respect to ice so that they will grow rapidly and fall out, so that the fog will disappear. (If a very large number of ice particles are formed they may remain small and a stable ice fog will be formed.)

We can also offer a reasonable explanation of why the alto-cumulus clouds persisted for a long time as water clouds and then were quickly transformed into large snowflakes. At the height of the alto-cumulus there would probably be very few, if any, particles which were active ice-forming nuclei at the temperature of the cloud. Hence the cloud formed and continued as a water cloud. I presume that at the later stage the cloudlets drifted into a region where ice crystals were falling from some higher cloud—probably too thin to be seen—there being probably a change of wind with height above the alto-cumulus cloud. The water-drops evaporated in the presence of the ice particles, just as in the experiment in the cold chamber, owing to the higher vapour pressure over water than over ice, and the ice particles grew rapidly for the same reason.

Cwilong made measurements at the Jungfraujoch and over the oceans and showed that in these conditions ice-forming nuclei which were active at temperatures above 232° K. (−41° C.) were generally absent or very rare. Palmer has used the same apparatus in aircraft and has shown that these nuclei are also absent (or very rare) above the level of the first temperature inversion or a low cloud layer, though there are, of course, many condensation nuclei present which will also act as 'ice-forming nuclei' at temperatures below 232° K. (−41° C.). Whether there are *any* of the ice-forming nuclei active at temperatures above 232° K. in the upper atmosphere is not known, and it is extremely difficult to detect the presence of very rare nuclei.

Findeisen observed that the actual freezing of water or sublimation of water vapour seemed to throw off nuclei on which ice can form (possibly they are actual spicules of ice). The production of 'ice-forming nuclei' by these processes has been confirmed at Oxford, and the matter is still under investigation. If the formation of these new nuclei is rapid enough, it is possible that a very few ice crystals, formed by some means in the upper part of a supercooled water cloud, could throw off more nuclei as they grow, and on these nuclei other ice particles would be formed. In this way a very few ice-forming nuclei might lead to the whole cloud of small water droplets evaporating and the vapour condensing on ice particles which would grow very large and fall rapidly. As mentioned before, very little is at present known about this process and it may or may not be important in the formation of rain and snow in the atmosphere.

I have been able to describe only three out of many problems in Geophysics which are awaiting investigation, but I hope that I have shown both that there is much to do which is of great interest and also that elaborate and expensive apparatus is not required. Many of the problems are, as I have said, suitable for individual workers, or a small group, in one of the smaller physical laboratories where such things as cyclotrons and million-volt generators are out of the question. There have never been more than three persons at any one time actively engaged on any one of the questions that I have discussed.

Finally I would thank you again as Members of the Physical Society for doing me the great honour of allowing my name to be associated in this way with that of Charles Chree.

ACKNOWLEDGMENTS

Figures 1, 3, 4, 5, 6 and 7 are reproduced from the *Proceedings of the Royal Society* by permission of the Council. Figure 8 is reproduced by permission of the Director of the Meteorological Office. Figure 2 is reproduced from *Sky and Telecope.*

REFERENCES

AITKEN, J., 1880, *Trans. Roy. Soc. Edin.*, **30**; 1887, *Ibid.*, **33**.

BREWER, A. W., and PALMER, H. P., 1949, *Nature, Lond.*, **164**, 312.

CAVE, C. J. P., 1912, *The Structure of the Atmosphere in Clear Weather* (Cambridge: University Press).

CHREE, C., 1926, *Proc. Roy. Soc.* A, **110**, 693.

CWILONG, B. M., 1947, *Proc. Roy. Soc.* A, **190**, 137.

DINES, W. H., 1909, *Met. Office Publication* No. 202; 1911, *Phil. Trans. Roy. Soc.* A, **211**; 1912, *Met. Office, Geophys. Memoir* No. 2; 1919, *Ibid.*, No. 13.

FABRY, CH., and BUISSON, H., 1913, *J. Phys. Radium*, ser. 5, **3**, 196; 1921, *Ibid.*, ser. 6 **2**, 197.

FOURNIER D'ALBE, E. M., 1949, *Quart. J. R. Met. Soc.*, **75**, 1.

GOWAN, E. H., 1936, *Quart. J. R. Met. Soc.*, **62**, 34.

PALMER, H. P., 1949, *Quart. J. R. Met. Soc.*, **75**, 15.

SHELLARD, H. C., 1949, *Meteorological Research Paper No.* 486 (London: Air Ministry).

WILSON, C. T. R., 1895–1900, *Proc. Camb. Phil. Soc.* and *Proc. Roy. Soc.* A, sundry papers.

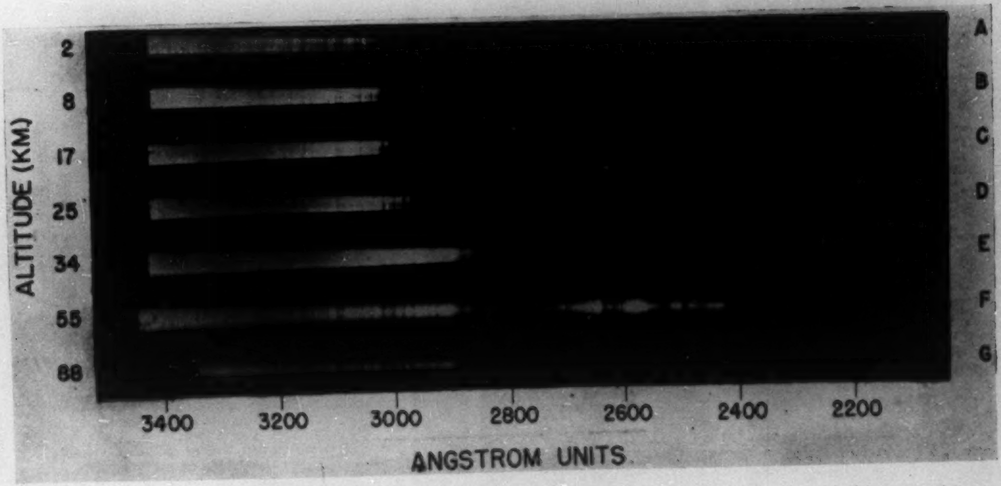

Figure 2. Spectra of solar radiation obtained at different heights by a V.2 rocket sent up in America. Note that in the last two spectra the rocket had rolled over and the spectrograph was not properly exposed.

(From *Sky and Telescope*.)

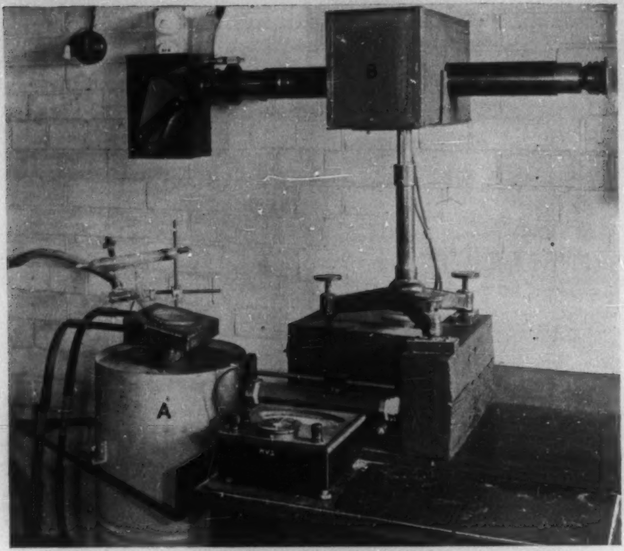

Figure 2. The assembled dilatometer.

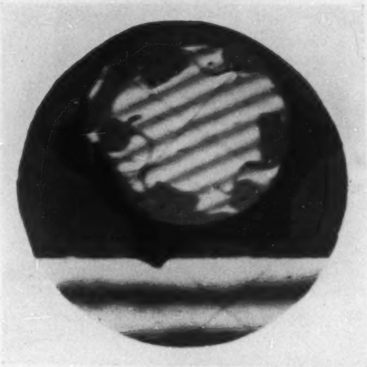

Figure 4. Fringes from expansion interferometer (above) and interference thermometer (below).

The Measurement of the Thermal Expansion of Single Crystals of Tin by an Interferometric Method

By B. G. CHILDS and S. WEINTROUB
University College, Southampton

MS. received 27*th September* 1949, *and in amended form* 14*th November* 1949

ABSTRACT. Single crystals of tin have been grown by the Kapitza method, their orientations measured, and the crystals converted into sets of three spacers for use in an interferometric dilatometer. The dilatometer consisted of a vacuum furnace for heating the spacers and interferometer, and an auto-collimating monochromator. The movement of the fringes with change of temperature was observed visually. The apparatus, its assembly, and method of use are described in detail.

The linear expansion coefficients, α_θ, of six crystals of different orientations, θ, have been measured over the range of temperature 30–220° c., and α_θ for a given temperature was found to vary linearly with $\cos^2\theta$ in accordance with Voigt's relation. The two principal coefficients, $\alpha_\parallel$ and $\alpha_\perp$, corresponding to $\theta=0$ and $\theta=90°$ were found by extrapolation. $\alpha_\parallel$ and $\alpha_\perp$ increase with temperature from 32·0 and $16{\cdot}2\times10^{-6}$/deg. c. at 30° c. to 41·5 and $20{\cdot}3\times10^{-6}$/deg. c. at 230° c. respectively. The accuracy of the determination is estimated to be within 1%. The results are exhibited in graphical and tabular form.

---

§1. INTRODUCTION

For metals with tetragonal structure, such as tin above its transition temperature, the linear thermal expansion coefficient, α, is not independent of the direction in the lattice as is the case for isotropic metals. The expansion of the lattice in any specified direction can however be calculated from a knowledge of two independent coefficients $\alpha_\parallel$ and $\alpha_\perp$ which refer respectively to the directions parallel and perpendicular to the principal tetragonal axis. Thus, for a direction making angle θ with the axis, the corresponding expansion coefficient α_θ is, in accordance with the relation stated by Voigt (1910),

$$\alpha_\theta=\alpha_\parallel\cos^2\theta+\alpha_\perp\sin^2\theta.$$

Since the coefficients vary considerably with temperature, a complete description of the thermal expansion of tetragonal tin must consist of values of $\alpha_\parallel$ and $\alpha_\perp$ for all temperatures between the transition point (13° c.) and the melting point (232° c.).

In the present paper a description is given of measurements, by an interferometric method, of the expansion of tin single crystals, of various orientations, over the range from room temperature up to the melting point. It is believed that this is the first time that such an investigation has been made. The results, which are discussed in detail in §7, show that Voigt's relation is obeyed, that $\alpha_\parallel$ is approximately twice $\alpha_\perp$, and that both $\alpha_\parallel$ and $\alpha_\perp$ steadily increase with temperature over the whole range of temperature.

§2. METHOD OF MEASUREMENT

Of the several methods which have been used for the measurement of the linear expansion of small crystal specimens, that which is capable of the greatest accuracy is the Fizeau (1869) interferometric method. The specimen in this case is converted into a form suitable for the three point support of an optically flat, glass or quartz, plate vertically above another similar plate, the whole assembly forming an optical interferometer. If the three pieces of the specimen, or 'spacers', are nearly equal in length, so that the wedge angle between the inner plate surfaces is not greater than some four seconds of arc, a fringe system is produced by interference of the reflections, at the interior surfaces of the plates, of a parallel beam of monochromatic light of wavelength λ, incident normally on the plates. The fringe system, which is located in the 'film', the space between the plates, consists of contour lines of equal film thickness at intervals of $\lambda/2$.

When the temperature of the interferometer is raised, thus causing the spacers to expand, the fringes move laterally, and their movement past a fixed point serves to measure the expansion of the film at that point. Under the most favourable conditions using automatic recording it may be possible to observe the fringe passage to 1/50 fringe or $\lambda/100$. For Hg green light ($\lambda = 5{\cdot}46 \times 10^{-5}$ cm.) and spacers of length 1 cm. and expansion coefficient $\alpha = 25 \times 10^{-6}$/deg. c. a temperature difference of only 2° c. would be required in order to measure the coefficient with an accuracy within 1%. This would enable the expansion coefficients to be measured to the same order of accuracy within a degree or two of the melting point or transition point, provided that the temperature of the spacers was suitably measured. The apparatus used in this investigation was merely a preliminary form of an accurate automatically recording dilatometer and was not capable of the above high order of accuracy.

The interferometric method, despite its obvious advantages, has been little used for expansion measurements on metal crystals. This is partly due to the necessity for continuous observation of the fringe movement over long periods of time, but, principally, because of the difficulty of construction of the three spacers. These must have the same expansion coefficient, and hence orientation, which, in practice, means that they must be cut from one single crystal.

A successful technique (Childs 1950) was developed for the preparation of such spacers from tin single crystals, and the distortion of the crystal lattice introduced during the process of construction of the spacers was kept sufficiently low to be of negligible effect on the thermal expansion.

§ 3. THE SINGLE-CRYSTAL SPACERS

(i) *Growth of the Tin Single Crystals*

The crystals were produced from 'Chempur' tin, in the form of rods 6 cm. long and 3 mm. diameter using a horizontal gradient furnace of the Kapitza (1928) type. This consisted of a rectangular copper bar of dimensions 30 cm. × 4 cm. × 0·7 cm., supported on asbestos knife edges in a draught-proof enclosure. An exponential temperature gradient of some 1·7–2·7° c/cm. was maintained along its length by an electrical heater of resistance 77·5 ohm wound round one end of the bar. The rods of tin which were to be crystallized were laid on the surface of the bar with their axes in the direction of the maximum temperature gradient. Some of the rods were sealed into evacuated, and previously outgassed, glass tubes of slightly greater diameter than that of the rods. Others were placed directly on a clean Pyrex glass plate lying on the bar, the combined action of surface tension forces and the thick oxide coating serving to retain the shape of the rods even when molten.

The heater current was slowly reduced from a value at which the cool end of the rod was just molten to one at which the hot end became solid. This reduction was accomplished, using a manually operated rheostat, in steps of 0·005 amp. every 2–3 min., from 1·25 to 1·00 amp., corresponding to a minimum rate of growth of 1·8 mm/min. The thermal inertia of the bar was sufficient to cause a steady movement of the liquid–solid interface in the growing crystal. The percentage of crystals successfully grown in this way was rather low—35%—but was adequate for the investigation. No attempt was made, by seeding, to grow crystals of pre-determined orientations of 0 and 90°.

(ii) *Measurement of Orientation*

The orientations, ranging from 30 to 90°, of sixteen tin crystals were measured to within 1° by an optical method based on that of Chalmers (1936).

(iii) *Conversion into Spacers*

The distance of separation of the interferometer plates, chosen as a compromise between good definition of the fringes and large expansion of the crystal spacers, was 8·5 mm. Each crystal was cut into pieces of approximately this length, using a fine saw the set of which had been removed. Care was taken to avoid excessive pressure and impulsive stress during the cutting. The ends of the cut pieces were prevented from bending by a wooden backing strip to which the crystal had been glued.

After removal of the backing, the ends were sharpened separately using a fine flexible metal file, the pieces being held in the rubber-padded jaws of a lathe chuck. The lengths were measured with a travelling microscope and the pieces made equal in length to within 10^{-1} mm. by further filing.

At this stage the pieces of crystal, while substantially monocrystalline in form, were badly deformed at the ends. Much of the strained portion was then removed by etching each piece in concentrated hydrochloric acid until its length had been reduced by 0·2 mm. Finally, the lengths of all the pieces were made equal, to within 5 microns, by further periods of controlled etching and measuring.

By this technique crystal spacers were obtained with nearly all (more than 98%) of their volume apparently unaffected by the mechanical working. Some strain was still present, but once this had been released by annealing no differential expansion of the spacers, indicating changes in orientation, could be detected.

§ 4. THE INTERFEROMETER

The interferometer consisted of the two plates, P_1 and P_2 in Figure 1, separated by three spacers mounted in a holder. This holder was a brass ring 11 mm. internal diameter, and 2·5 mm. high. The spacers were located in grooves cut on the inside of the ring parallel to its axis, and were kept in position by individual leaf springs. Attached to the outside of the ring were three vertical guides of equal length. These served to locate the position of the upper plate without impedance to its motion caused by the expansion of the spacers.

The holder was inverted, and supported by the three guides on a flat glass surface. Each spring, in turn, was extended and a crystal spacer allowed to slide down the groove until it rested on the surface of a second piece of glass lying on the first. In this way the normal to the plane defined by the points of the three spacers was made approximately parallel to the axis of the holder. The parallelism of the spacers was checked by using a coordinate travelling microscope and traversing, first along the length of a spacer, and then, at right angles along the holder. An angular deviation of a spacer from the axis of the holder of less than $\frac{1}{2}°$ could thus be determined. After adjustment, the assembled spacer unit was stored in an inverted position until it was required for use.

The plates P_1 and P_2 were of optical glass 0·5 cm. thick. The upper plate P_1 was 1·3 cm. in diameter and its two optically flat surfaces were inclined at such an angle that light reflected at its top surface is thrown to one side. The lower plate P_2, 3·8 cm. in diameter, was divided into two portions. One half supported the spacer unit and formed part of the expansion interferometer. The bottom surface of this half was blackened to prevent reflection. The other half, the surfaces of which were inclined at an angle of 10 seconds, formed an interference thermometer of the type described by Luckeisch *et al.* (1922). This thermometer, though useful, was not of primary importance in the investigation.

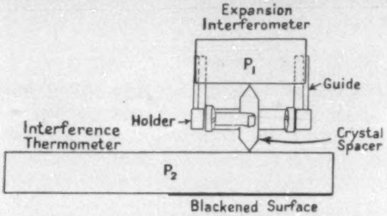

Figure 1. The assembled interferometer.

The lateral movements of the fringes in the expansion interferometer and in the interference thermometer were observed relative to two sets of nylon cross hairs. These were attached under tension across the plates. Although not coinciding precisely with the location of the fringe systems no undesirable parallax was observed.

§ 5. APPARATUS

The dilatometer used for the measurement of the expansion of the single tin crystals is shown in Figure 2 (Plate). It consisted of a vacuum furnace A, shown diagrammatically in Figure 3, for heating the specimens and interferometer, and an autocollimating monochromator B, for producing a parallel beam of monochromatic light with which to illuminate the interferometer, and for viewing the passage of the fringe systems.

The inner furnace tube was made massive in order to ensure a slow, uniform rise in temperature for a given heater current, and the upper end was closed by an inclined circular plate-glass window which was sealed with Apiezon Q to the furnace tube and water-cooled. A rotary oil pump maintained a pressure of 10^{-2} to 10^{-3} mm. Hg.

The interferometer was mounted on a three-point support inside a thick copper bucket which, in its lowest position, rested on a metal cylinder standing on the base plate of the furnace tube. Through a central tube, one of two which protruded from the lower end of the furnace tube, there was a rod which served to raise and lower the bucket, and a Wilson (1941) sliding seal at the end of this tube allowed free movement of the rod without the vacuum being broken. Through the other tube there was a copper–constantan thermocouple, the hot junction of which passed through a slot in the interferometer bucket and was at the same level as the crystal spacers. It was not possible to bring this junction into close contact with the spacers, and it was found, from a series of subsidiary tests, that the temperature of the spacers at 200° c. was approximately 3° c. higher than that recorded by the thermocouple. This is considered to be due to the upper interferometer plate acting as a shield against radiation loss. The thermocouple readings were accordingly corrected to give the true spacer temperatures.

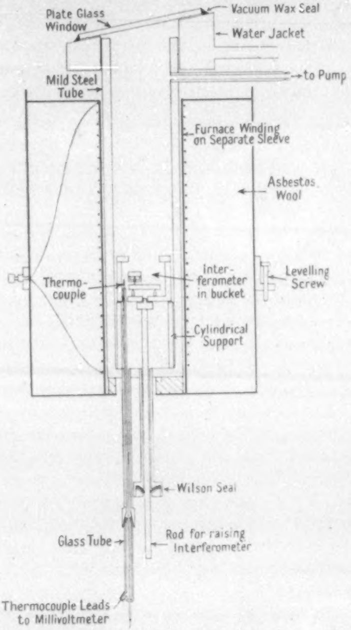
Plate Glass Window
Vacuum Wax Seal
Water Jacket
to Pump
Mild Steel Tube
Furnace Winding on Separate Sleeve
Asbestos Wool
Thermo-couple
Inter-ferometer in bucket
Levelling Screw
Cylindrical Support
Wilson Seal
Glass Tube
Rod for raising Interferometer
Thermocouple Leads to Millivoltmeter

Figure 3. The vacuum furnace.

The thermo-E.M.F. was measured to 0·01 mv. (0·2° c.) with a millivoltmeter, the thermocouple being calibrated before, during and after each set of expansion measurements.

The furnace could be tilted without translation by three levelling screws mounted at the level of the interferometer.

The monochromator and viewing apparatus was a modified form of that described by Saunders (1945). The light from a mercury discharge tube which was situated perpendicular to, and slightly above, the horizontal axis of an aplanatic lens combination, was reflected by a 45° front silvered mirror which formed a virtual image of the lamp just above the lens axis. A horizontal adjustable slit placed in the focal plane of the lens combination and in front of the lamp image limited the light and formed the true source, the length of which could be varied by means of a wedge diaphragm placed in front of it.

Emerging from the lens combination as a parallel beam, the light passed through a Pellin–Broca constant-deviation prism where it was dispersed and deviated downwards on to the horizontal plate surfaces of the interferometer. The paths of the reflected beams, which were slightly inclined to one another, were approximately coincident with the direction of the incident beam. These reflected beams passed through the prism, where they were further dispersed, and focused by the lens combination to pass through an aperture just below the slit source. Due to the dispersion of the prism, of the several overlapping images of the source formed at this point, only those of one particular wavelength (the mercury green $\lambda = 5460$ A.) continued through to an adjustable eyepiece, where an image of the interferometer crossed by the two sets of interference fringes was formed (Figure 4, see Plate).

§ 6. EXPERIMENTAL PROCEDURE

(i) *Production of Fringes*

The following procedure was adopted in arranging the interferometer and spacers in position inside the furnace. The lower interferometer plate P_2 was placed on the three-point support in the copper bucket, and the bucket lowered by the rod to the bottom of the furnace. The bucket and plate were arranged so that the slot in the base of the bucket was vertically above the thermocouple tube, and the dividing line on the plate was parallel to the slit source. The furnace was then levelled by means of the levelling screws until the pair of images of the source formed by reflection at the plate appeared at the top of the aperture below the source. The field of view as seen through the eyepiece was bisected, the lower half being crossed by the horizontal temperature fringes.

The bucket was raised to the top of the furnace, and the spacer unit placed on the appropriate half of P_2 with the longest spacer nearest to the temperature fringes. The upper plate P_1 was then rested gently on the three spacers, with the cross-wires uppermost and at 45° to the dividing line of the lower plate. Great care had to be exercised to avoid moving the holder on the lower plate while the spacers were in contact with the glass since the points of the spacers were easily worn away by friction.

When the interferometer was lowered to the bottom of the furnace, two pairs of images of the source, one from the expansion interferometer and the other from the interference thermometer, were visible in the entrance aperture.

By slight adjustments of the level of the furnace these pairs of images were arranged so that one pair was at the top, and the two pairs symmetrically placed about the centre, of the aperture. Refraction at the wedge-shaped upper plate P_1 of the interferometer was the cause of the separation of the two pairs of images.

In general, fringes as in Figure 4 would then be visible across the interferometer. The spacing and orientation of these fringes naturally depended upon the precise differences in length of the three spacers. Slight uneven wear on their points, caused by vibration of the bucket when being lowered into position, frequently resulted in the number of fringes being too great for accurate observation of their movement. To correct for this, first, the direction of the apex of the wedge-shaped film between the plates was found by identifying the images, due to reflection at the various surfaces, of a pin held over the interferometer. Slight vibration of the upper plate, produced by gentle tapping over the longest spacer with a pin attached to a length of thread, then sufficed to reduce the number of fringes to less than ten. After insertion of the thermocouple, the furnace window was waxed on, and the apparatus evacuated. Finally, in order to remove the last remnants of strain, the spacers were annealed above 200° C. for about five hours. Provided that the rotation and change in spacing of the fringes consequent upon the differential changes in length of the spacers during the release of strain were not such as to prevent accurate observation of the fringe passage relative to the cross-wires, the measurements of the expansion of the spacers could then be commenced.

(ii) *Method of Observation*

The movement of the interference fringes as the temperature of the furnace altered was observed visually and continuously, and the E.M.F. of the thermocouple corresponding to coincidence of each expansion fringe with the cross-wires was recorded. The alternative method of procedure, whereby the absolute length of the spacers at various steady temperatures is found using the method of fringe coincidences, could not be used since the intensities of the mercury lines, other than the green, emitted by the lamp were too low.

The rate of rise of temperature of the furnace was kept low in order to reduce the time lag in temperature between the spacers and the thermocouple. Further, by keeping the lag constant it disappeared from the calculation of the expansion coefficients. The rate used was 12° C/hr., corresponding to a lag of about 1° C., and this rate was maintained constant to within 20%, i.e. ±0·2° C. in the lag, by further small adjustments to the furnace current.

For each crystal the range of temperature from 20–225° C. was covered twice; generally, by one continuous run over the whole range, occupying some sixteen hours, and three shorter, overlapping, runs of 50–100° C. each. Observations were made for increasing temperatures only.

In calculating the expansion coefficients from the observational data the values of the thermocouple E.M.F. corresponding to coincidence of expansion fringe and cross-wires were found by interpolation from a smoothed E.M.F.–time curve.

The average expansion, at the cross-wires, of the three crystal spacers was next plotted as a function of temperature. The values of temperature corresponding to every tenth expansion fringe were read off from the smooth curve and the mean expansion coefficients over the intervals of 20, 30 and 40 fringes were calculated.

No direct use was made of the interference thermometer. It afforded much indirect practical assistance, however, since it ensured that if the thermocouple failed, an alternative temperature measuring device was available. Readings of the fractional order of the temperature fringes were taken at every coincidence of expansion fringe and cross-wires, and an independent calibration of the interference thermometer against the thermocouple was made.

Despite the careful annealing of the spacers before expansion measurements were taken, some slight further irreversible differential expansion of the spacers, amounting to one or two fringes over the whole range, often occurred. The consequent rotation and change in spacing of the fringes was observed by noting periodically the number of fringes between pairs of the spacers.

At the completion of observations on each crystal, the spacers were re-measured, etched, and examined for signs of secondary growth.

§7. EXPERIMENTAL RESULTS

Six tin crystals of orientations $\theta = 86\frac{1}{2}$, $79\frac{1}{2}$, $44\frac{1}{2}$, $43\frac{1}{2}$, $31\frac{1}{2}$, and 30° were investigated. Except for the $79\frac{1}{2}$° crystal, the temperature interval 20–225° c. was covered twice; generally by one continuous run and three shorter overlapping runs. For the $79\frac{1}{2}$° crystal, the temperature interval 20–190° c. only was covered, in five overlapping ranges, readings being taken both for increasing and decreasing temperatures. The spacers in this case were unannealed and some rotation of the fringes occurred. As a check on the influence of this rotation on the thermal expansion, the observations over the lowest temperature range were repeated, and excellent agreement was found.

The expansion coefficients of the six crystals, as functions of temperature, are shown in Figure 5. On account of their large number, it is unfortunately impossible to show the individual experimental points, but only the smooth curves through them. The maximum deviation of a point from the corresponding curve is $1{\cdot}2 \times 10^{-6}$/deg. c. in the expansion coefficient, a 3% difference. The mean deviation is $0{\cdot}3 \times 10^{-6}$/deg. c.

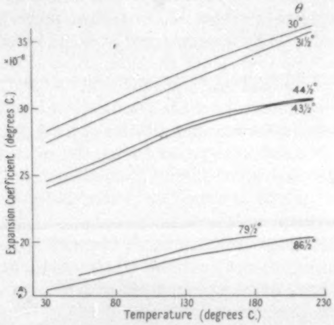

Figure 5. The variation of expansion coefficient with temperature for six tin crystals of different orientations.

It will be seen from the figure that in each case the expansion coefficient increases by about 25% between room temperature and the melting point. In addition, the coefficients increase for decrease in θ, ranging at 30° c. from $16{\cdot}4 \times 10^{-6}$/deg. c. for $\theta = 86\frac{1}{2}$° to $28{\cdot}3 \times 10^{-6}$/deg. c. for $\theta = 30°$.

The variation of the expansion coefficient with the cosine squared of the orientation is given, at 20° c. intervals, in Table 1, and shown graphically for three temperatures in Figure 6. This variation is linear, in agreement with Voigt's relation. Some idea of the accuracy of the observations may be obtained from the scatter of the experimental points which are completely independent. This scatter naturally includes errors in the orientation as well as in the expansion coefficients.

Table 1. The Expansion Coefficients of the six Tin Crystals at Various Temperatures

The values for 0° ($\alpha_{\parallel}$) and 90° ($\alpha_{\perp}$) have been obtained by extrapolation.

Temperature	Expansion coefficients ($\times 10^{-6}$/deg. c.) for tin crystals of given orientation							
(° c.)	0	30	31½	43½	44½	79½	86½	90
30	32·0	28·3	27·4	24·0	24·5	—	16·4	16·2
50	32·9	29·1	28·3	24·8	25·3	17·4	16·8	16·6
70	34·1	30·1	29·3	25·7	26·1	17·9	17·3	17·2
90	35·1	31·0	30·2	26·6	27·0	18·4	17·8	17·7
110	36·4	31·9	31·0	27·6	27·9	18·9	18·3	18·2
130	37·4	32·8	31·9	28·4	28·7	19·4	18·8	18·7
150	38·4	33·6	32·7	29·1	29·4	19·9	19·2	19·2
170	39·2	34·3	33·6	29·6	29·8	20·3	19·5	19·5
190	40·0	35·0	34·4	30·1	30·2	20·5	19·8	19·7
210	40·8	35·6	35·2	30·5	30·6	—	20·1	20·1
220	41·2	36·0	35·6	30·6	30·7	—	20·3	20·2

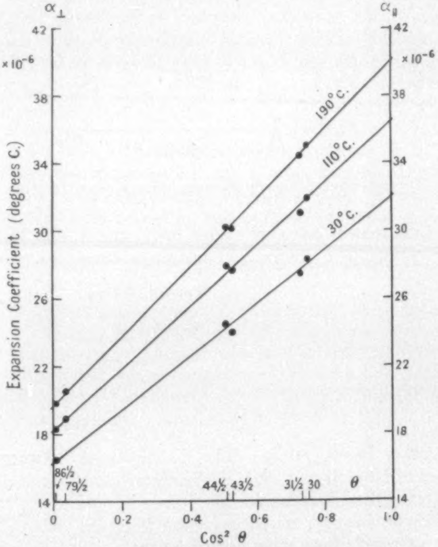

Figure 6. Variation of expansion coefficient with $\cos^2\theta$ for three temperatures.

Finally, the values at 20° c. intervals of $\alpha_{\perp}$ and $\alpha_{\parallel}$, obtained by extrapolation of curves such as those of Figure 6, are given in Table 1 and are shown as functions of temperature in Figure 7. Both coefficients increase with temperature, the increase being less marked at the higher temperatures. $\alpha_{\parallel}$ is almost exactly double $\alpha_{\perp}$; at 30° c. $\alpha_{\parallel}$ and $\alpha_{\perp}$ are 32·0 and $16{\cdot}2 \times 10^{-6}$/deg. c. respectively, and at 230° c., by extrapolation, 41·5 and $20{\cdot}3 \times 10^{-6}$/deg. c. respectively.

The absence of any discontinuity in the curves of $\alpha_\perp$ and $\alpha_\parallel$ against temperature provides additional evidence against the existence of a rhombic form of tin which was once thought probable (Homer and Plummer 1939).

In Table 2 a comparison is made between the values for $\alpha_\parallel$ and $\alpha_\perp$ obtained in this investigation and the single values for the coefficients which have been determined by other investigators. The discrepancies between the authors' values and those of Kossolapow and Trapesnikow (1936) and Shinoda (1933) are very much greater than the probable inaccuracy in the authors' values (see § 8). This may possibly be due to some effect arising from the Debye–Scherrer x-ray method which was used in both those investigations.

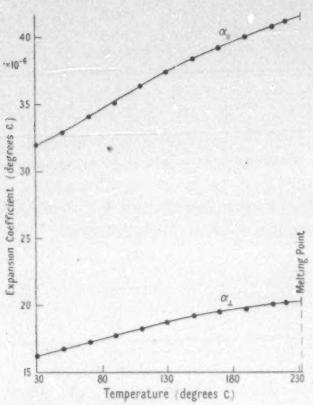

Figure 7. The principal expansion coefficients of tin as functions of temperature.

Table 2. Comparison between Values for $\alpha_\parallel$ and $\alpha_\perp$ for Tin found by various observers (O) and the authors (A).

Observer	Method	Temp. range (° c.)	Mean temp. (° c.)	$\alpha_\perp$ $\times 10^{-6}$/°c. O	$\alpha_\perp$ $\times 10^{-6}$/°c. A	$\alpha_\parallel$ $\times 10^{-6}$/°c. O	$\alpha_\parallel$ $\times 10^{-6}$/°c. A
Bridgman (1925)	Optical lever	15–25	20	15·4	15·9	30·5	31·5
Kossolapow and Trapesnikow (1936)	Debye-Scherrer x-ray	23–120	72	22·4	17·2	46·4	34·2
Shinoda (1933)	Debye-Scherrer x-ray	34–194	114	25·7	18·3	45·8	36·6

§ 8. ESTIMATION OF ACCURACY

The factors which contribute to the random experimental scatter present in the curves of Figure 6 can be divided into two groups: (i) those which involve errors of observation and calculation of the expansion coefficients of the spacers as assembled, and (ii) those which are due to the uncertainty in the crystallographic orientation corresponding to the measured coefficients of expansion.

Group (i). The total maximum error of determination of the temperature of the spacers at the moment of coincidence of an expansion fringe with the cross-wires was ±0·6° c. This figure includes errors in the thermocouple calibration (0·2° c.), in the observation of the fringe coincidence and the reading of the millivoltmeter (0·2° c.), and due to the variation in the thermal lag of the spacers behind the thermocouple (0·2° c.). In practice, the combined error was rarely found to exceed ±0·3° c. It was reduced to ±0·2° c. or less by suitable choice of the (expansion fringe, temperature) curve. Hence, when temperature differences were taken to obtain the mean coefficient over a certain range of temperature a maximum error of ±0·4° c. in the difference was possible. This corresponds, for a temperature interval of 40° c., to an error in the observed expansion coefficient of ±1%.

Group (ii). The orientations of the single crystals were measured to ±1°. Further errors due to the residual strain and recrystallization remaining in the spacers after conversion from the crystal and, on assembly of the spacers in the interferometer, due to their departure from normality to the plate surfaces ($\frac{1}{2}$°), also occurred.

If the measured orientation is assumed as correct, an additional maximum error of some ±2% must then be allowed for in the measured expansion coefficients of the individual crystals, thus making ±3% in all. By fitting the best line to the (expansion coefficient, $\cos^2\theta$) curves, the final error in $\alpha_\perp$ and $\alpha_\parallel$ was reduced to about ±1%.

§9. CONCLUSIONS

Previous to this investigation the only reliable data for the variation of the coefficients $\alpha_\perp$ and $\alpha_\parallel$ with temperature for highly anistropic metals were those for Zn and Cd. The variation of $\alpha_\perp$ and $\alpha_\parallel$ found for Sn is different from that exhibited by Zn and Cd, so that the data provide a further opportunity for the testing of the theoretical relationships such as that given by Grüneisen and Goens (1924).

ACKNOWLEDGMENTS

It is a pleasure to record our thanks to the College authorities, and to Professor A. M. Taylor, in whose department the work was carried out, for the facilities provided, also to the Department of Scientific and Industrial Research for the award of a maintenance grant to one of us (B. G. C.).

REFERENCES

Bridgman, P. W., 1925, *Proc. Amer. Acad. Arts Sci.* **60**, 305.
Chalmers, B., 1936, *Proc. Phys. Soc.*, **47**, 1.
Childs, B. G., 1950, *J. Sci. Instrum.*, in the press.
Fizeau, A. H., 1869, *C.R. Acad. Sci., Paris*, **68**, 1125.
Grüneisen, E., and Goens, E., 1924, *Z. Phys.*, **29**, 141.
Homer, C., and Plummer, H., 1939, *J. Inst. Met.*, **64**, 169.
Kapitza, P., 1928, *Proc. Roy. Soc.* A, **119**, 359.
Kossolapow, G. F., and Trapesnikow, A. K., 1936, *J. Exp. Theor. Phys. U.S.S.R.*, **6**, 577.
Luckeisch, M., Holladay, L., and Sinden, R., 1922, *J. Franklin Inst.*, **194**, 251.
Saunders, J. B., 1945, *Bur. Stand. J. Res., Wash.*, **35**, 157.
Shinoda, G., 1933, *Kyoto Imp. Univ. Proc.* A, **16**, 193.
Voigt, W., 1910, *Lehrbuch d. Kristallphysik.*
Wilson, R. R., 1941, *Rev. Sci. Instrum.*, **12**, 91.

A Toroidal Magnetron*

By O. BUNEMAN
Atomic Energy Research Establishment, Harwell, Berks.

MS. received 24th August 1949

ABSTRACT. A rearrangement of the geometry of cavity magnetron oscillators is proposed such that the magnetic field loops around the cathode, whereas waves and electrons travel along it. Application of various magnetron theories to the new geometry leads to the result that the device will oscillate under conditions similar to those for a conventional cavity magnetron. The required magnetic field can be generated by a heavy current passed axially through the cathode.

§1. INTRODUCTION

A new kind of generator of microwaves is proposed here which resembles the conventional cavity magnetron in that it uses the action of crossed constant electric and magnetic fields upon a dense cloud of electrons for the purpose of exciting oscillations. The device differs from the conventional cavity magnetron chiefly in the orientation of the field and the oscillating cavities: a typical geometry is sketched in Figures 1 (*a*) and (*b*).

There are advantages in this new type of geometry which may make the development of the device worth while. But it was not the outcome of a search for better microwave generators· it was conceived as the result of a general analysis of electron cloud behaviour under crossed fields. Possibly the only merit of the theory developed in connection with it will be a negative one, i.e. to serve as a warning as to what general oscillatory instabilities may arise in various electronic devices which employ crossed fields.

§2. PRINCIPLE OF THE TOROIDAL MAGNETRON

A sketch of the toroidal magnetron (the name 'torotron' might be proposed unless it has already been used elsewhere) is shown in Figures 1 (*a*) and (*b*), but its principles can be more readily understood from the straightened-out version shown in Figure 2. The latter will be referred to as the 'axial flow magnetron'.

The cathode surface is cylindrical, as usual, and the anode is a concentric cylinder with resonator slots. The constant electric field, **E**, is radial, but the resonators, instead of being arranged azimuthally around the anode as in the conventional cavity magnetron, are arranged in a longitudinal succession as in the corrugated guide employed in linear accelerators.

Conversely, the magnetic field, **H**, instead of being longitudinal, loops around the cathode azimuthally. In fact the θ and z directions (Figure 2) have been interchanged relative to those in the conventional cavity magnetron.

The electrons, instead of circulating around the cathode, travel along it, at right angles to both electric and magnetic fields. The wave which is excited by them follows the same direction and is of the same type as that travelling in a linear accelerator. It will be shown that instability of the electron cloud to waves of a given frequency takes place under conditions very similar to those for conventional cavity magnetrons, i.e. similar voltages and magnetic field values

---

* Published by permission of the Controller, H.M. Stationery Office.

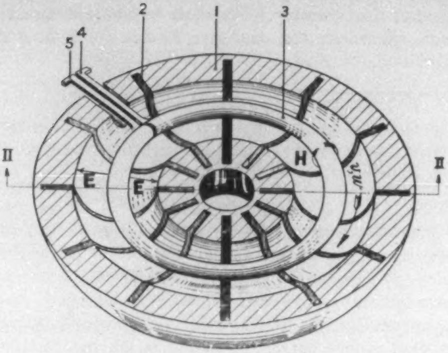

Figure 1 (*a*). Section of block and cathode.

1. Anode block.
2. Resonator slots.
3. Cathode.
4, 5. Cathode leads.

E. Electric field.
H. Magnetic field.
v. Electron velocity.
w. Wave velocity.

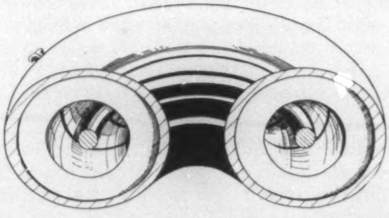

Section II-II

Figure 1 (*b*). Anode block showing resonators and cathode inside.

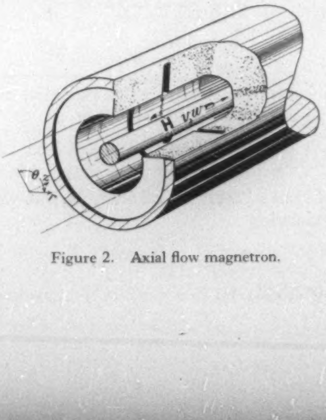

Figure 2. Axial flow magnetron.

must be employed: the interchange of the two directions in space only represents a minor distortion of the geometry. We shall derive approximate formulae for voltages, currents, efficiencies etc., and give reasons for hoping that very high power may be attained.

§ 3. ESTABLISHING THE MAGNETIC FIELD

A possible advantage of an azimuthal magnetic field is that it can be generated by a heavy current passed longitudinally through the cathode. The magnetic field due to such a current I_0 varies inversely as r:

$$H(r) = H_c r_c / r = 2I_0/r \qquad (\text{E.M.U.}) \qquad \ldots\ldots(1)$$

where suffix c refers to values at the cathode. Using as units amperes, gauss and centimetres,

$$rH(r) = r_c H_c = I_0/5.$$

Typical values required would be: $H_c = 1{,}500$ gauss, $r_c = 0{\cdot}5$ cm. Hence $I_0 = 3{,}750$ amp., current density $= 15{,}000/\pi$ amp/cm^2, giving a field of 0·01 volt/cm. along a water-cooled copper conductor placed inside the cathode ($\sigma = 450{,}000$ mho/cm.). The heat developed is therefore 40 watts per cm. length, which is easily removed by water-cooling. For other values of H_c (gauss), r_c (cm.) and σ (mho/cm.) one should use the formulae: current density (amp/cm^2) $= 5H_c/\pi r_c$, field (volt/cm.) $= 5H_c/\pi r_c \sigma$, heating (watt/cm.) $= 25H_c{}^2 \pi\sigma$.

In pulsed operation the full field is required only during a fraction of the time, and the dissipation problem might disappear. The current pulses required to establish the field might then be used (and adjusted in length) to supply normal cathode heating.

§ 4. THE STATIC MAGNETRON

(i) *Cut-off*

We hope to show that the new device is likely to operate, and we wish to find the approximate operating conditions. We therefore modify some of the theories which were developed in connection with the ordinary magnetron (Collins 1948) so that they apply to the new geometry (straight version). We begin with the static case.

A cut-off potential can be derived for the condition when the electric field is static and purely radial; the equation for the axial acceleration is then

$$\frac{d^2z}{dt^2} = \frac{dr}{dt}\frac{eH}{mc} = \frac{eH_c r_c}{mc}\frac{dr/dt}{r},$$

giving, by integration,

$$\frac{dz}{dt} = \frac{eH_c r_c}{mc}\ln\frac{r}{r_c} \qquad \ldots\ldots(2)$$

for zero emission velocity at the cathode. The potential relative to the cathode must therefore exceed a value $V(r)$ given by

$$\frac{eV(r)}{mc^2} = \frac{1}{2}\left(\frac{eH_c r_c}{mc^2}\right)^2 \left(\ln\frac{r}{r_c}\right)^2. \qquad \ldots\ldots(3)$$

This takes the place of Hull's (1921) cut-off formula, into which it transforms on introducing the approximation

$$\ln\frac{r}{r_c} \simeq \frac{1}{2}\left(\frac{r}{r_c} - \frac{r_c}{r}\right), \qquad \ldots\ldots(4)$$

correct to cubes of $\ln(r/r_c)$.

In a (V, H_c) plot one obtains a parabola. Likewise a $(V, \ln r)$ plot for constant H_c yields a parabola (as against a catenary for ordinary magnetrons). In practical units we use

$$mc^2/e = 510\,\text{kv.} = 1{,}700\,\text{gauss.cm.},$$

and for a typical example we choose H_c, r_c as in § 3, and $r = 1{\cdot}36$ cm., so that $\ln(r/r_c) = 1{\cdot}00$. We then obtain $V = 50$ kv. for cut-off.

(ii) *Single Stream Steady State*

When the anode voltage is below cut-off, a self-consistent, zero current steady state can be obtained in which all electrons move axially only $(dr/dt = 0,\ d\theta/dt = 0)$ with velocity dz/dt given by (2), so that the potential follows the $(V, \ln r)$ parabola given by (3) as far as the stream extends, i.e. from the cathode, $r = r_c$, to the electron cloud surface, $r = r_s$. Beyond this there is no charge and the potential varies linearly with $\ln r$. Continuity of the field at $r = r_s$ requires the potential line to be tangential to the parabola there. Thus, writing l for $\ln(r/r_c)$,

$$V = V_s + \left(\frac{dV}{dl}\right)_s (l - l_s)$$

or

$$\frac{eV}{mc^2} = \frac{1}{2}\left(\frac{eH_c r_c}{mc^2}\right)^2 [l_s^2 + 2l_s(l - l_s)] = \frac{1}{2}\left(\frac{eH_c r_c}{mc^2}\right)^2 [l^2 - (l - l_s)^2] \qquad \text{......(5)}$$

beyond the cloud. For given anode voltage less than cut-off, l_s, and hence the cloud radius, can be found by constructing on the (V, l) plot the tangent to the cut-off parabola from the point (V_a, l_a) representing the anode, or by solving (5) for l_s.

Assuming H_c, r_c and $r = r_a$, as in the example above, but an anode voltage of, say, 42 kv., we obtain $l_s = 0{\cdot}60$, $r_s = 0{\cdot}91$ cm.

The confined electron beam has the following further properties:

Electronic density:

$$\rho = \frac{1}{4\pi}\nabla^2 V = \frac{mc^2}{4\pi e}\left(\frac{eH_c r_c}{mc^2}\right)^2 \frac{1}{r^2}. \qquad \text{......(6)}$$

Current density:

$$j = \rho\frac{dz}{dt} = \frac{mc^3}{4\pi e}\left(\frac{eH_c r_c}{mc^2}\right)^3 \frac{\ln(r/r_c)}{r^2}.$$

Beam current:

$$I = \int_{r_c}^{r_s} 2\pi r j\, dr = \frac{mc^3}{4\pi e}\left(\frac{eH_c r_c}{mc^2}\right)^3 \pi\left(\ln\frac{r_s}{r_c}\right)^2. \qquad \text{......(7)}$$

To obtain the beam current in practical units we use

$$mc^3/4\pi e = 1{,}350\,\text{amp.},$$

and we get 130 amp. in the quoted example. In some of the resonance considerations we require also the 'plasma electron frequency', which is $(e\rho/\pi m)^{1/2}$ (see, for instance, Stratton 1941, ch. v, 5.16, equation 27). By substitution from (5) we obtain

$$\nu_{\text{plasma}} = \frac{1}{2\pi}\frac{eH_c r_c}{mcr}, \qquad \text{......(8)}$$

i.e. the 'cyclotron frequency' at radius r and the plasma frequency are identical.

The axial beam described here is the counterpart to Brillouin's (1941) circulating steady state in ordinary magnetrons. Most of the formulae quoted are the same as for Brillouin's state, except for correction factors which differ from unity by quantities of the order $[\ln (r/r_c)]^2$. There is an essential difference in the total beam current, in that length and circumference are interchanged in the two types of magnetron: the beam current, in Brillouin's state, is roughly $(L/2\pi r)$ times that given above, L being the axial length.

§ 5. THE OPERATING MAGNETRON

(i) *Threshold Voltage*

The threshold voltage which the author derived for conventional magnetrons (Manchester Group 1942, Collins 1948, pp. 30, 31, 238, 340, 341) can be obtained more easily in the present case. One assumes the electric fields to be neither purely radial nor static, but of the travelling wave type, so that they appear static (yet still not purely radial) when viewed from a frame of reference travelling with the wave.

In such a frame the equations of motion are the same as if the frame were stationary, except for a force which arises from the fact that all electrons, in addition to their velocity relative to the frame, share the frame velocity w. This force is $ewH(r)/c = ewH_c r_c/cr$, and is directed inwards when the wave travels in the same direction as the main electron flow. It has a potential $e(w/c)H_c r_c \ln (r/r_c)$. We must therefore subtract $(w/c)H_c r_c \ln (r/r_c)$ from the electrostatic potential V and can then write the equations of motion as if the frame were stationary. Particles are emitted with kinetic energy $\frac{1}{2}mw^2$ in the travelling frame, and any change in their kinetic energy must be due to the electrostatic potential, modified as described. In all regions reached by particles we must have, therefore,

$$eV - \frac{w}{c} eH_c r_c \ln \frac{r}{r_c} + \tfrac{1}{2}mw^2 \geqslant 0.$$

The threshold voltage V_T is the lowest anode voltage for which this inequality is satisfied:

$$\frac{eV_T}{mc^2} = \frac{w}{c}\,\frac{eH_c r_c}{mc^2} \ln \frac{r_a}{r_c} - \frac{1}{2}\left(\frac{w}{c}\right)^2 \qquad \text{......(9)}$$

or

$$\frac{V_T}{510\,\text{kv.}} = \frac{\lambda^*}{\lambda}\,\frac{H_c r_c}{1{,}700\,\text{gauss.cm.}} \ln \frac{r_a}{r_c} - \frac{1}{2}\left(\frac{\lambda^*}{\lambda}\right)^2, \qquad \text{......(9')}$$

where λ^* is the wavelength in the guide, λ that in free space, so that $\lambda^*/\lambda = w/c$. In a typical case we might choose $\lambda = 10$ cm., $\lambda^* = 2$ cm., H_c, r_c and r_a as above and obtain $V_T = 35$ kv. At this voltage the steady state surface (see equation (4)) lies at $l = 0{\cdot}45$ or $r = 0{\cdot}784$ cm.

Equations (9) and (9′) represent straight lines on a (V_T, H_c) diagram, tangential to the cut-off parabola. The approximation (4) changes (9) into the threshold formula for conventional magnetrons, provided one remembers that there the guide wavelength is $2\pi r_a$ divided by n, the number of repeats of the wave around the block.

(ii) *Synchronism*

Equation (9) may be rewritten

$$\frac{eV_{\mathrm{T}}}{mc^2}=\frac{1}{2}\left(\frac{eH_c r_c}{mc^2}\right)^2\left[l_{\mathrm{a}}^2-\left(l_{\mathrm{a}}-w\Big/\frac{eH_c r_c}{mc}\right)^2\right],$$

which, on comparison with (5), shows that when $V_{\mathrm{a}}=V_{\mathrm{T}}$, $w=\frac{eH_c r_c}{mc}l_s=$ axial velocity of the surface stream of the steady beam (see equation (2)). In the axial flow magnetron the threshold condition and the condition of synchronism between wave and outer electrons are identical. In the conventional magnetron this is *not* so: under threshold conditions the outer electrons are faster than the wave (see the author's Manchester report 1942).

It is reasonable to expect that, in order to do work on the radio-frequency field, the electrons have to be faster than the wave, i.e. to push the wave along. The threshold formula may therefore underestimate the voltage necessary for oscillation, and we proceed to explore alternative voltage criteria.

(iii) '*Plasma Resonance*'

A resonance phenomenon which was discussed by the author in another Manchester report (Manchester Group 1943) arises from the interaction between electrons and waves which occurs when the electron stream encounters the wave crests at its plasma frequency (see also Collins 1948, p. 260). We assume the electrons to be overtaking the waves so that the velocity of encounter is $(eH_c r_c l/mc)-w$. The wavelength in the guide is λ^* and the condition for plasma resonance is

$$\frac{eH_c r_c l}{mc}-w=\lambda^*\frac{1}{2\pi}\frac{eH_c r_c}{mcr}. \qquad \ldots\ldots(10)$$

With some algebraic manipulation this can be reduced to

$$\frac{2\pi r}{\lambda^*}\exp(-\lambda^*/2\pi r)=\frac{2\pi r_0}{\lambda^*}, \qquad \ldots\ldots(11)$$

where $r_0=$ radius of synchronous layer, $r=$ radius of resonant layer. Given λ^*, λ and $H_c r_c$, one can obtain r_0 from (2) and then r from (11) or from the following table:

Radius of Layer in Plasma Resonance, r, and Radius of Synchronous Layer, r_0
(both in units of $\lambda^*/2\pi$)

$2\pi r_0/\lambda^*$	0	0·5	1·0	1·5	2·0	2·5	3·0	3·5	4·0	4·5	5·0	large
$2\pi r/\lambda^*$	0	1·172	1·764	2·311	2·842	3·365	3·881	4·394	4·904	5·413	5·920	$\frac{2\pi r_0}{\lambda^*}+1$

The new value of r can then be fed into (5) to give the anode voltage at which the electron cloud is wide enough for the surface to be in plasma resonance. In our particular case we have seen that the synchronous radius is 0·784 cm., and as $\lambda^*=2$ cm., we get $\ln(r/r_c)=0{\cdot}75$, which, from formula (5), corresponds to an anode voltage of 47 kv.—very near cut-off and well above threshold.

(iv) *Small Amplitude Theory*

The small amplitude theory (Collins 1948, §6.7, Manchester Group 1944) can be applied to the axial flow magnetron. It has not been followed through in detail, but an outline of the procedure is given in the Appendix. The entire analysis is very similar in the two types of magnetron and the change of geometry results only in minor modifications in some of the perturbation equations. We can therefore predict with confidence that the new type of valve will oscillate and that spontaneous response (exponential growth of amplitudes from the background of thermal noise) will occur when the electrons are 'matched' to the load, somewhere between the conditions of synchronism and 'plasma resonance'.

Exact matching requires knowledge of the Q of the load. To avoid lengthy calculations we choose for the radius of a 'matched' electron cloud in our particular example the value $r_s = 0{\cdot}91$ giving $l_s = 0{\cdot}60$, which is half-way between the synchronous and resonant values of l (0·45 and 0·75). It corresponds to 42 kv. anode voltage (see §4 (ii)).

In the ordinary cavity megnetron, threshold and charge cloud instability due to matching occur at very close levels, and one cannot easily decide which of the two is relevant. Here, the threshold level, being identical with synchronism, is always below the instability level. Thus the crests of the spontaneous charge cloud waves will always be able to penetrate to the anode. It is possible that the success of the threshold condition was only fortuitous, owing to its proximity to the (rather more complicated) instability condition. It is unlikely that oscillation will begin without instability. If the threshold condition is only a necessary but not a sufficient condition we shall be able to disregard it in the new magnetron. On the other hand, there may be some deeper significance in the proximity between threshold and instability in ordinary cavity magnetrons (perhaps in connection with moding problems). In that case the new device would fail.

§6. ELECTRONIC CURRENTS

Theory is, unfortunately, unable to make reliable predictions of the amount of electronic current which the magnetron will pass under operating conditions. The nearest approach to calculating currents in ordinary magnetrons was achieved in the self-consistent field and orbit calculations done by the Manchester team under Hartree's direction and in similar calculations carried out at Leeds under Stoner. These required an immense amount of numerical work in each particular case.

A rough estimate—probably an upper limit—of the current can be obtained from the argument that under oscillatory conditions of large amplitude something like the axial beam current of §4 (ii) will be diverted to the anode in every wavelength λ^*. In our example this would lead to 130 amp. per wavelength, the total for a valve of axial length L being $130\, L/\lambda^*$ amp. The question is how long (in terms of number of wavelengths) the magnetron can be made.

In an ordinary magnetron of similar dimensions we should have obtained, by the same argument, total current = circulating current in Brillouin's state times number of waves around the block $= 130\,(L/2\pi r)n = 130\,(L/2\pi r)\,(2\pi r/\lambda^*) = 130\, L/\lambda^*$, as above.

One restriction on length is absent in the new device: that arising from space limitations of the magnetic field, and we might thus gain a real advantage in the new type of valve.

§7. EFFICIENCIES

Formulae for an ideal efficiency were given by the author (Manchester Group 1942) for conventional magnetrons. Similar formulae apply in the present case: particles which reach the anode at threshold condition ($V_a = V_T$) are stationary with respect to the wave, i.e. travel with velocity w relative to fixed axes. Of the total energy eV_T which they have acquired from the D.C. field they have retained $\frac{1}{2}mw^2$ and surrendered the balance, $eV_T - \frac{1}{2}mw^2$, to the radio-frequency field. At operation appreciably above threshold ($V_a > V_T$) one would guess that the electrons carry away the excess $eV_a - eV_T$, still leaving only $eV_T - \frac{1}{2}mw^2$ for the radio-frequency field. The efficiency is thus

$$\eta \simeq \frac{eV_T - \frac{1}{2}mw^2}{eV_a}.$$

For our example ($V_T = 35$ kv., $V_a = 42$ kv., $w = 0{\cdot}2\,c$) we obtain 58%.

§8. OUTPUT POWER

The input power in our example is 2·7 MW. per cm. length: hence an output of perhaps up to $1\frac{1}{2}$ MW. per cm. might be anticipated, thus if we assume five internal wavelengths along the magnetron ($L = 5\lambda^* = 10$ cm.), we obtain 15 MW. The procedure for calculating outputs for different dimensions, fields and frequencies is obvious. If the ordinary magnetron of similar anode and cathode radii could be made as long as 10 cm. the output would be similar.

§9. CONTINUOUS ELECTRON BEAM IN TOROIDAL GEOMETRY

The reason for proposing a toroidal arrangement rather than a straight arrangement is the necessity of establishing continuity of the electron stream. The electrons drift along equipotentials in crossed fields. If an equipotential is interrupted by an insulator (as it would have to be in the straight device of finite length), the insulator may be destroyed unless elaborate 'dumping' arrangements are made for the electrons. In the toroidal device the leads could be shaped for partial or complete mutual annulment of their magnetic fields in the vicinity of the seals through which they are brought out. The seals could thus be protected from bombardment, and perhaps further by not coating the cathode 'upstream' of the roots of the leads. An alternative to the toroidal arrangement would be the 'race track', i.e. two straight sections joined by semicircular electron- and waveguides.

§10. MODE PROBLEMS

A certain limitation to the length, and therefore to the output, will be set by the condition of mode stability. Separation of the wave velocities, i.e. of λ^*/λ, is of importance in the threshold and synchronism conditions. But in the plasma resonance formula λ^* and λ figure individually, and it is not possible to say that high dispersion of wave velocities only is of importance.

The spectrum of modes in the projected valve has not yet been studied. In the first place one ought to investigate the case of a straight corrugated guide of finite length with a periodicity condition at the ends, in approximation to the corrugated torus. If azimuthal modes in the guide can be ignored, there is hope that the length might be made quite substantial, i.e. many guide wavelengths long, without excessive closeness in the wave velocities of the various modes. There should exist a considerable amount of experience in this field, from studies of the linear accelerator. The principle of the 'rising sun' can, of course, be applied. There is, however, no obvious way of translating the idea of strapping.

§ 11. CONCLUSIONS

Having shown that the new type of magnetron geometry is equivalent to the old type as far as charge cloud instability and small amplitude phenomena are concerned, we may be confident that the device will oscillate. We have seen also that most of the more elementary calculations on magnetron space-charge behaviour can be translated with ease. Conditions of operation can then be derived which are in most respects similar to the usual magnetron conditions. There is one qualitative difference which may turn out to be significant, in that the threshold voltage is identical with that for which the electron cloud surface is only just as fast as the wave, whereas charge-cloud instability theory requires the electrons to be somewhat faster. However, there is no known reason why this should prevent operation at instability conditions.

The power derivable from the new device depends on the length of the cathode which, in turn, depends on the stability against unwanted modes. It is hoped that the length can be increased beyond that in the ordinary magnetron.

ACKNOWLEDGMENT

Acknowledgment is made to the Director of the Atomic Energy Research Establishment for permitting publication of this paper.

REFERENCES

Brillouin, L., 1941, *Phys. Rev.*, **60,** 385.
Collins, G. B., 1948, *Microwave Magnetrons* (New York : McGraw-Hill), § 6.
Hull, A. W., 1921, *Phys. Rev.*, **18,** 31.
Lamb, H., 1945, *Hydrodynamics* (New York : Dover Publications), 6th edition.
Manchester Group, 1942, *C.V.D. Mag.*, 10, 11, 17; 1943, *Ibid.*, 31,; 1944, *Ibid.*, 37.
Stratton, J. A., 1941, *Electromagnetic Theory* (New York : McGraw -Hill).

APPENDIX

SMALL AMPLITUDE THEORY

The instabilities of the Brillouin charge cloud were obtained by the author, using a perturbation method (Collins 1948, § 6.7). Unfortunately, the simple mechanical analogy of a rotating platform which is used in the Manchester Group report (1944) in order to simulate the action of the magnetic field cannot be taken over into the theory of the axial flow magnetron as the magnetic field is no longer uniform. A more complicated analysis is necessary before a velocity potential can be introduced and before the hydrodynamical approach of the above report can be repeated.

The equation of motion is

$$m\frac{d\mathbf{v}}{dt}=e\left(\operatorname{grad} V-\frac{\mathbf{v}}{c}\wedge\operatorname{curl}\mathbf{A}\right), \qquad \ldots\ldots(\text{A}\,1)$$

where **A** is the vector potential of the magnetic field. **A** has only an axial component A_z of value $H_c r_c \ln(r/r_c)$. We apply Eulerian methods to express $m d\mathbf{v}/dt$ in terms of partial derivatives:

$$\begin{aligned} m\frac{d\mathbf{v}}{dt} &= m\frac{\partial\mathbf{v}}{\partial t}+m(\mathbf{v}\,.\operatorname{grad})\,\mathbf{v} \\ &= m\frac{\partial\mathbf{v}}{\partial t}+\operatorname{grad}(\tfrac{1}{2}mv^2)-\mathbf{v}\wedge\operatorname{curl} m\mathbf{v}. \qquad \ldots\ldots(\text{A}\,2)\end{aligned}$$

We introduce the generalized momentum for electrons in a magnetic field,

$$\mathbf{p} = m\mathbf{v} - e\mathbf{A}/c, \qquad \text{......(A 3)}$$

and obtain, by combining (A 1) and (A 2), the following equation for $\mathbf{p}$:

$$\frac{\partial \mathbf{p}}{\partial t} = \mathbf{v} \wedge \operatorname{curl} \mathbf{p} + \operatorname{grad}(eV - \tfrac{1}{2}mv^2). \qquad \text{......(A 4)}$$

In the ordinary magnetron $\mathbf{p}$ is simply the momentum relative to the Larmor frame of reference, where we know $\mathbf{p}$ to be irrotational. We try to prove that $\mathbf{p}$ is irrotational in the axial flow magnetron by studying curl $\mathbf{p}$, which we denote by $\mathbf{q}$. We can find an equation for the change of $\mathbf{q}$ with time, following the electrons:

$$\begin{aligned} \frac{d\mathbf{q}}{dt} &= \frac{\partial \mathbf{q}}{\partial t} + (\mathbf{v}\,.\,\operatorname{grad})\,\mathbf{q} = \operatorname{curl}\left(\frac{\partial \mathbf{p}}{\partial t}\right) + (\mathbf{v}\,.\,\operatorname{grad})\,\mathbf{q} \\ &= \operatorname{curl}(\mathbf{v} \wedge \mathbf{q}) + (\mathbf{v}\,.\,\operatorname{grad})\,\mathbf{q} \quad \text{(from (A 4))} \\ &= (\mathbf{q}\,.\,\operatorname{grad})\,\mathbf{v} - \mathbf{q} \operatorname{div} \mathbf{v}. \end{aligned}$$

This equation shows that the property of zero vorticity, provided it occurs at all, is retained and carried along by the electrons. As no vortices are being emitted from the cathode (the proof is similar to that for ordinary magnetrons), no vortices will be formed and curl $\mathbf{p}$ will vanish everywhere.

The vector $\mathbf{p}$ can therefore be expressed as the gradient of a scalar to be denoted mF. (The quantity F is then equivalent to that in the Manchester Group report (1944), where it appears as the velocity potential in the Larmor Frame.)

By substituting $\mathbf{p} = \operatorname{grad} mF$ in (A 4), and integrating, one obtains the generalized Bernoulli equation (Lamb 1945, Ch. II, Art. 17):

$$\frac{2eV}{m} = v^2 + 2\frac{\partial F}{\partial t}. \qquad \text{.......(A 5)}$$

The steady state axial beam is characterized by $F = 0$ and hence $\mathbf{p} = 0$. We study undulatory perturbations of this state, i.e. perturbations whose z and t variation is given by the factor $\exp\{2\pi i(wt - z)/\lambda^*\}$, so that $\partial/\partial t = 2\pi i w/\lambda^*$ and $\partial/\partial z = -2\pi i/\lambda^*$. We put

$$F = \delta F = f(r) \exp\{2\pi i(wt - z)/\lambda^*\}$$

and derive for the perturbations of velocities, potentials and densities (unperturbed values are given in § 4 (ii)):

$$\begin{aligned} \delta v_r &= v_r = df/dr, \\ \delta v_z &= 2\pi i f/\lambda^*, \\ \delta V &= \frac{iH_c}{c}\left(\frac{2\pi mc^2}{eH_c\lambda} - \frac{2\pi r_c}{\lambda^*}\ln\frac{r}{r_c}\right)f, \\ \delta\rho &= -\frac{1}{4\pi}\left(\frac{1}{r}\frac{d}{dr}\left(r\frac{d}{dr}\right) - \frac{4\pi^2}{\lambda^{*2}}\right)\frac{iH_c}{c}\left(\frac{2\pi mc^2}{eH_c\lambda} - \frac{2\pi r_c}{\lambda^*}\ln\frac{r}{r_c}\right)f, \end{aligned}$$

omitting in each case the exponential factor.

The equation of continuity (first-order perturbations) becomes

$$\frac{1}{r}\frac{\partial}{\partial r}(r\rho_{\rm unp}\delta v_r)+\frac{\partial}{\partial z}\rho_{\rm unp}\delta v_z+\frac{\partial}{\partial z}v_{z,\,{\rm unp}}\delta\rho+\frac{\partial\delta\rho}{\partial t}=0,$$

which, on substitution, yields a second-order differential equation for f:

$$r\frac{d}{dr}\frac{r_{\rm c}^2}{r^2}\frac{df}{dr}-\frac{4\pi r_{\rm c}^2}{\lambda^{*2}}f-\left(\frac{2\pi mc^2}{eH_{\rm c}\lambda}-\frac{2\pi r_{\rm c}}{\lambda^*}l\right)\left(\left(r\frac{d}{dr}\right)^2-\frac{4\pi r^2}{\lambda^{*2}}\right)\left(\frac{2\pi mc^2}{eH_{\rm c}\lambda}-\frac{2\pi r_{\rm c}}{\lambda^*}l\right)f=0.$$

This can be simplified to

$$\frac{d}{dl}g(l)\frac{df}{dl}=h(l)f \qquad \text{......(A 6)}$$

where $g(l)=e^{-2l}-\left(\frac{2\pi mc^2}{eH_{\rm c}\lambda}-\frac{2\pi r_{\rm c}}{\lambda^*}l\right)^2$ and $h(l)=\left(\frac{2\pi r}{\lambda^*}\right)^2 g(l)$.

This equation is of the same form as the perturbation equation for ordinary magnetrons. To change to the latter from (A 6) one must replace λ^* by $2\pi r/n$ and multiply some of the terms in g and h by factors of the type $1+O(l)^2$ or $1\pm 2/n^2$. These are minor modifications which will not change the qualitative features of the equation. Of these, the most important are the zeros of $g(l)$, i.e. the singularities which occur at the plasma resonances (see § 5, (iii)) and at which the general solution becomes logarithmically infinite, as in the ordinary magnetron.

Calculation of the charge-cloud impedance from the perturbation theory will thus give results as in the Manchester Group report (1944): negative resistance beyond the singularity, reactance varying inversely with frequency before the singularity is reached, so that the resistance in the load can be matched to the electrons by assuming an exponential increase of amplitudes (Manchester Group 1944, Collins 1948, § 6.7).

Viscous Flow Transverse to a Circular Cylinder

By C. N. DAVIES
(Member of Scientific Staff, Medical Research Council),
London School of Hygiene and Tropical Medicine, Keppel Street, London

MS. received 12*th September* 1949

ABSTRACT. Expressions for the flow field about a circular cylinder are derived which are valid for small values of the Reynolds' number. These are obtained by Lamb's method from Oseen's equation, and it is shown that the formulae previously given by Lamb involve the neglect of a first order term. Lamb's expression for the drag is correct to the first order in the Reynolds' number.

If the Navier–Stokes equations of hydrodynamics are linearized by neglecting the inertia terms it is impossible to obtain a steady state solution with finite velocity at infinity for the two dimensional flow of incompressible fluid past a circular cylinder. By linearizing according to Oseen's method, however, Lamb (1911) obtained an approximate solution. Later, Bairstow, Cave and Lang (1923) and Faxén (1927) published exact solutions. These, however, are complicated and since the formulation of Oseen's linearized equation involves assumptions which are only acceptable, in general, at low values of the Reynolds' number, R, a simple approximate formula, accurate to the first order in R, is all that is really required.

When Lamb's approximation was examined in connection with the application of his results to the theory of fibrous air filters it was found to be incorrect owing to the unjustifiable neglect of a term of the first order in R. In the present paper Lamb's method is followed and expressions for the field of flow accurate to the first order in R are derived. It is shown that his well-known formula for the drag on a cylinder is correct.

The general dynamical equation for an incompressible fluid in the absence of body forces is

$$\frac{\partial \mathbf{Q}}{\partial t} + (\mathbf{Q}\cdot\nabla)\mathbf{Q} = -\frac{1}{\rho}\nabla p + \nu\nabla^2\mathbf{Q}, \qquad \ldots\ldots(1)$$

where $\mathbf{Q}$ and p, the velocity and pressure in the fluid, are functions of position, ρ is the density and ν is the kinematic viscosity. For steady flow with complete neglect of the inertia term the right-hand side is equal to zero. As an alternative, Oseen replaced $\mathbf{Q}$ by $U\hat{\mathbf{i}} + \mathbf{q}$, where $U\hat{\mathbf{i}}$ represents the velocity of the undisturbed stream and $\mathbf{q}$ the perturbation produced by an obstacle. Now only non-linear terms in $\mathbf{q}$ are neglected, so that for steady flow equation (1) reduces to

$$(U\hat{\mathbf{i}}\cdot\nabla)\mathbf{q} = U\frac{\partial \mathbf{q}}{\partial x} = -\frac{1}{\rho}\nabla p + \nu\nabla^2\mathbf{q}. \qquad \ldots\ldots(2)$$

It can be shown (Lamb 1932) that this leads to a more accurate representation of the flow field at a distance from the obstacle than is obtained if the inertia term $(\mathbf{Q}\cdot\nabla)\mathbf{Q}$ is completely neglected. The effect of the approximation introduced into the fundamental equation can be regarded as the change produced by a small body force, acting upon the fluid, which is a function of position. Complete neglect of the inertia term means that only viscous forces are assumed to act on each element of fluid; in this case the compensating body force tends to zero at the surface of the obstacle so that the approximation is a good one near the surface. Oseen's partial allowance for inertia leads to the result that the body force does not vanish at the surface, but its ratio to the viscous force is of the same order of magnitude as the Reynolds' number R. Hence, if R is small, the result is satisfactory near the obstacle as well as at a distance from it.

Putting $k = U/2\nu$ equation (1) becomes

$$\frac{1}{\rho}\nabla p = \nu\left(\nabla^2 - 2k\frac{\partial}{\partial x}\right)\mathbf{q}. \qquad \ldots\ldots(3)$$

We have also the equation of continuity

$$\nabla\cdot\mathbf{q} = 0. \qquad \ldots\ldots(4)$$

Differentiating (3) gives $\nabla^2 p = 0$ of which a solution is

$$p = \rho U\,\partial\phi/\partial x, \qquad \ldots\ldots(5)$$

provided

$$\nabla^2\phi = 0. \qquad \ldots\ldots(6)$$

The velocity field can be divided into an irrotational component, $\mathbf{q}_1$, and a component $\mathbf{q}_2$ which is associated with the vorticity. Then

$$\mathbf{q} = \mathbf{q}_1 + \mathbf{q}_2, \qquad \ldots\ldots(7)$$

where $\mathbf{q}_1 = -\nabla\phi$. Hence $\nabla\cdot\mathbf{q}_1 = \nabla\cdot\mathbf{q}_2 = 0$; $\nabla^2\mathbf{q}_1 = 0$; $\nabla\times\mathbf{q}_1 = 0$. Now,

$$\frac{1}{\rho}\nabla p = \frac{1}{\rho}\nabla\rho U\frac{\partial\phi}{\partial x} = U\frac{\partial}{\partial x}\nabla\phi = -2k\nu\frac{\partial\mathbf{q}_1}{\partial x}.$$

Therefore

$$\frac{1}{\rho}\nabla p = \nu\left(\nabla^2 - 2k\frac{\partial}{\partial x}\right)\mathbf{q}_1.$$

In order to satisfy (3) it is thus necessary to have

$$\left(\nabla^2 - 2k\frac{\partial}{\partial x}\right)\mathbf{q}_2 = 0, \qquad \ldots\ldots(8)$$

which suggests putting

$$\mathbf{q}_2 = \frac{1}{2k}(\nabla - 2k\hat{\mathbf{i}})\chi.$$

Since $\nabla\cdot\mathbf{q}_2 = 0$, this gives

$$\left(\nabla^2 - 2k\frac{\partial}{\partial x}\right)\chi = 0, \qquad \ldots\ldots(9)$$

and the expression for $\mathbf{q}_2$ is easily shown to satisfy equation (8). Combining this result with (7) gives

$$\mathbf{q} = -\nabla\phi + \left(\frac{1}{2k}\nabla - \hat{\mathbf{i}}\right)\chi, \qquad \ldots\ldots(10)$$

where ϕ is a solution of Laplace's equation (6) and χ is a solution of (9).

For transverse flow past an infinite cylinder of radius a it is therefore necessary to solve the following equations:

$$\left.\begin{aligned} u &= -\frac{\partial\phi}{\partial x} + \frac{1}{2k}\frac{\partial\chi}{\partial x} - \chi, \\ v &= -\frac{\partial\phi}{\partial y} + \frac{1}{2k}\frac{\partial\chi}{\partial y}, \end{aligned}\right\} \qquad \ldots\ldots(11)$$

where

$$\left(\nabla^2 - 2k\frac{\partial}{\partial x}\right)\chi = 0 \qquad \ldots\ldots(9)$$

and

$$\nabla^2\phi = 0. \qquad \ldots\ldots(6)$$

The boundary conditions are

$$u = v = 0 \text{ at } r = \infty; \qquad u = -U, \quad v = 0 \text{ at } r = a; \qquad \ldots\ldots(12)$$

where $x = r\cos\theta$, $y = r\sin\theta$ and the origin of coordinates is taken at the centre of the cylinder.

A solution of (9) which is found to be accurate to the first order is

$$\chi = Ce^{kx}K_0(kr), \qquad \ldots\ldots(13)$$

where $K_0(kr)$ is a modified Bessel function of the second kind. An expansion for (13), valid for small values of kr only, gives

$$\chi \simeq -C(1 + kx)(\gamma + \ln\tfrac{1}{2}kr). \qquad \ldots\ldots(14)$$

The general solution of Laplace's equation in two dimensional polar coordinates is

$$\phi = A_0\ln r + B_0\theta + C_0\theta\ln r + D_0 + \sum_{l=1}^{\infty} r^{\pm l}(A_l\cos l\theta + B_l\sin l\theta); \qquad \ldots\ldots(15)$$

Lamb selects from this the terms giving

$$\phi = A_0 \ln r + A_1 \frac{\partial}{\partial x} \ln r, \qquad \ldots\ldots(16)$$

which makes $\nabla\phi$ tend to zero as r becomes infinite.

Substitution of the values of ϕ and χ from (14) and (16) into (11) gives for the flow field near the cylinder

$$\left.\begin{aligned} u &= -\left(A_0 + \frac{C}{2k}\right)\frac{\partial}{\partial x}\ln r + \left(\frac{Cr^2}{4} - A_1\right)\frac{\partial^2}{\partial x^2}\ln r \\ &\qquad - \frac{C}{2}\left(\tfrac{1}{2} - \gamma - \ln \tfrac{1}{2}kr\right) + Ckx\left(\gamma + \ln \tfrac{1}{2}kr\right), \\ v &= -\left(A_0 + \frac{C}{2k}\right)\frac{\partial}{\partial y}\ln r + \left(\frac{Cr^2}{4} - A_1\right)\frac{\partial^2}{\partial x \partial y}\ln r. \end{aligned}\right\} \qquad \ldots\ldots(17)$$

The first term in each of these expressions is equal to zero. Lamb tacitly neglects the last term in the expression for u, although it is of the first order in kx, and applies the boundary conditions at $r = a$ to obtain

$$A_0 = -\frac{C}{2k}, \qquad A_1 = \frac{Ca^2}{4}, \qquad C = \frac{2U}{\frac{1}{2} - \gamma - \ln \frac{1}{2}ka}. \qquad \ldots\ldots(18)$$

This solution obeys the surface conditions but begins to fail at a small distance giving velocities which tend linearly to infinity as the distance increases, on account of the approximation (14) introduced for χ. If the exact expression is used for χ we obtain from (13)

$$\begin{aligned} \frac{\partial \chi}{\partial x} &= Ce^{kx}\left\{kK_0(kr) + \frac{\partial}{\partial r}K_0(kr)\frac{\partial r}{\partial x}\right\} \\ &= Cke^{kx}\left\{K_0(kr) - K_1(kr)\frac{\partial r}{\partial x}\right\}, \end{aligned}$$

where

$$K_1(kr) = -\frac{\pi}{2}H_1^{(1)}(ikr) = -\frac{\pi}{2}H_1^{(2)}(-ikr).$$

Hence

$$\left.\begin{aligned} \frac{1}{2k}\frac{\partial \chi}{\partial x} - \chi &= -\frac{C}{2}e^{kx}\left\{K_0(kr) + \frac{x}{r}K_1(kr)\right\}, \\ \frac{1}{2k}\frac{\partial \chi}{\partial y} &= -\frac{C}{2}e^{kx}\frac{y}{r}K_1(kr). \end{aligned}\right\} \qquad \ldots\ldots(19)$$

The calculation of u and v using these equations, together with the value of ϕ given by (16) and the constants (18), leads to a velocity field which is correct at infinity but which does not have the right values on the surface of the cylinder, owing to the neglect of the term $Ckx(\gamma + \ln \frac{1}{2}kr)$ in equation (17). To obtain an accurate result it is necessary to take more terms in the solution of $\nabla^2\phi = 0$.

It is clear that expansion of the exponential in (19) gives terms in x^n in the equation for u and $x^n y$ in the equation for v; $\partial\phi/\partial x$ and $\partial\phi/\partial y$ must contain corresponding terms, so that the constants can be determined from the conditions at $r = a$. The terms in θ and $\sin l\theta$ in the general solution (15) for ϕ are unwanted.

The pressure distribution about the cylinder is obtained by differentiating (15) and using equation (5). It will be seen that terms in (15) containing θ and $\sin l\theta$ lead to odd functions in the pressure equation, so that the pressure distribution would be asymmetrical; this is the type of solution which would be required for a rotating cylinder with which we are not at present concerned. Clearly, also, only negative values of l will be of interest; it was found necessary, after some trials, to go as far as $l=-4$ so as to be sure of the error involved by neglecting higher terms. Equation (16) is therefore replaced by the following expression:

$$\phi = A_0 \ln r + A_1 \frac{\cos\theta}{r} + A_2 \frac{\cos 2\theta}{r^2} + A_3 \frac{\cos 3\theta}{r^3} + A_4 \frac{\cos 4\theta}{r^4}.$$

Differentiation and suitable arrangement of the terms then leads to

$$\left.\begin{aligned} \frac{\partial\phi}{\partial x} &= \left(\frac{A_1}{r^2} - \frac{3A_3}{r^4}\right) + \left(\frac{A_0}{r^2} + \frac{6A_2}{r^4} - \frac{20A_4}{r^6}\right)x + \left(-\frac{2A_1}{r^4} + \frac{24A_3}{r^6}\right)x^2 \\ &\quad + \left(-\frac{8A_2}{r^6} + \frac{80A_4}{r^8}\right)x^3 - \frac{24A_3}{r^8}x^4 - \frac{64A_4}{r^{10}}x^5, \\ \frac{\partial\phi}{\partial y} &= \left(\frac{A_0}{r^2} + \frac{2A_2}{r^4} - \frac{4A_4}{r^6}\right)y + \left(-\frac{2A_1}{r^4} + \frac{12A_3}{r^6}\right)xy \\ &\quad + \left(-\frac{8A_2}{r^6} + \frac{48A_4}{r^8}\right)\Big(x^2y - \frac{24A_3}{r^8}x^3y - \frac{64A_4}{r^{10}}x^4y. \end{aligned}\right\} \qquad \ldots\ldots(20)$$

Meanwhile, expanding the exponentials in (19) as far as x^3 gives

$$\left.\begin{aligned} \frac{1}{2k}\frac{\partial\chi}{\partial x} - \chi &= -\frac{C}{2}\left\{K_0 + \left(kK_0 + \frac{K_1}{r}\right)x + \left(\tfrac{1}{2}k^2K_0 + \frac{kK_1}{r}\right)x^2 + \left(\tfrac{1}{6}k^3K_0 + \frac{k^2K_1}{2r}\right)x^3\right\} \\ \frac{1}{2k}\frac{\partial\chi}{\partial y} &= -\frac{C}{2}\left\{\frac{K_1}{r}y + \frac{kK_1}{r}xy + \frac{k^2K_1}{2r}x^2y\right\} \end{aligned}\right\},$$

where K_0 and K_1 are used as abbreviations for the modified second kind Bessel functions of kr. Combining these results and dropping the coefficients of terms of order above x^3,

$$\left.\begin{aligned} u &= \left(-\frac{A_1}{r^2} + \frac{3A_3}{r^4} - \frac{CK_0}{2}\right) + \left(-\frac{CkK_0}{2} - \frac{CK_1}{2r} - \frac{A_0}{r^2} - \frac{6A_2}{r^4} + \frac{20A_4}{r^6}\right)x \\ &\quad + \left(-\frac{Ck^2K_0}{4} - \frac{CkK_1}{2r} + \frac{2A_1}{r^4} - \frac{24A_3}{r^6}\right)x^2 \\ &\quad + \left(-\frac{Ck^3K_0}{12} - \frac{Ck^2K_1}{4r} + \frac{8A_2}{r^6} - \frac{80A_4}{r^8}\right)x^3, \\ v &= \left(-\frac{CK_1}{2r} - \frac{A_0}{r^2} - \frac{2A_2}{r^4} + \frac{4A_4}{r^6}\right)y + \left(-\frac{CkK_1}{2r} + \frac{2A_1}{r^4} - \frac{12A_3}{r^6}\right)xy \\ &\quad + \left(-\frac{Ck^2K_1}{4r} + \frac{8A_2}{r^6} - \frac{48A_4}{r^8}\right)x^2y. \end{aligned}\right\} \qquad ,\ldots\ldots(21)$$

Inserting the boundary conditions at $r=a$ and now using K_0 and K_1 as abbreviations for the functions of ka we find

$$\left.\begin{aligned}
A_0 &= -\frac{Ca}{2}\left(K_1-\frac{ka}{4}K_0+\frac{k^2a^2}{16}K_1-\frac{k^3a^3}{32}K_0\right),\\
A_1 &= \frac{Ca^2}{4}\left(kaK_1-\frac{k^2a^2}{2}K_0\right),\\
A_2 &= \frac{Ca^3}{32}k^2a^2\left(K_1-\frac{ka}{2}K_0\right),\\
A_3 &= -\frac{Ca^4}{48}k^2a^2K_0,\\
A_4 &= \frac{Ca^5}{32}ka\left(K_0+\frac{ka}{4}K_1-\frac{k^2a^2}{8}K_0\right) \text{ (from the } x \text{ and } y \text{ terms)},\\
C &= \frac{2U}{K_0+\dfrac{ka}{2}\left(K_1-\dfrac{ka}{4}K_0\right)}.
\end{aligned}\right\} \quad \ldots\ldots(22)$$

It is impossible from the coefficients of equation (21) to find a unique value of A_4. Further expansion of the expression for ϕ would be necessary to fix A_4, while higher order terms would appear in the other constants. The coefficients of x^3 and x^2y are out of balance by a quantity of order of magnitude ka.

Since

$$K_0(ka) = -(\gamma+\ln\tfrac{1}{2}ka)\left(1+\frac{k^2a^2}{4}\right)+\frac{k^2a^2}{4}+O(k^4a^4),$$

$$K_1(ka) = -\frac{1}{k}\frac{d}{da}K_0(ka) = \frac{1}{ka}+\frac{ka}{2}(\gamma+\ln\tfrac{1}{2}ka-\tfrac{1}{2})+O(k^3a^3),$$

we can clear the constants of Bessel functions and obtain

$$\left.\begin{aligned}
A_0 &= -\frac{Ca}{2}\left\{\frac{1}{ka}+\frac{3ka}{4}(\gamma+\ln\tfrac{1}{2}ka-\tfrac{1}{4})+O(k^3a^3)\right\},\\
A_1 &= \frac{Ca^2}{4}\left\{1+\frac{k^2a^2}{4}(\gamma+\ln\tfrac{1}{2}ka-\tfrac{1}{2})+O(k^4a^4)\right\},\\
A_2 &= \frac{Ca^3}{32}ka+O(k^3a^3),\\
A_3 &= \frac{Ca^4}{48}k^2a^2(\gamma+\ln\tfrac{1}{2}ka)+O(k^4a^4),\\
A_4 &= -\frac{Ca^5}{32}ka(\gamma+\ln\tfrac{1}{2}ka-\tfrac{1}{4})+O(k^3a^3),\\
C &= \frac{-2U}{(\gamma+\ln\tfrac{1}{2}ka-\tfrac{1}{2})-\dfrac{k^2a^2}{8}(\gamma+\ln\tfrac{1}{2}ka+1)}+O(k^3a^3).
\end{aligned}\right\} \quad \ldots\ldots(23)$$

The Reynolds' number R is equal to $2Ua/\nu=4ka$. In view of the fundamental limitation of Oseen's approximation, there is no point in calculating the constants with allowance for terms above k^2a^2. Tables of K_0 and K_1 are given by G. N. Watson (1922) and it is probably easier to use these for computation than it is to use the expansions.

It will be noticed that A_0, A_2 and A_4 do not reduce to Lamb's values ($-C/2k$, 0 and 0) when only first powers of ka are retained, although A_1, A_3 and C do so.

Substitution of the values of the constants given by (22) into equation (20), while dropping terms in k^3a^3 and the coefficients of x^4 and x^3y, gives as the solution of the problem, after using (11) and (19):

$$\left.\begin{aligned}
\frac{U}{u}\bigg\{K_0+\frac{ka}{2}\bigg(K_1-\frac{ka}{4}K_0\bigg)\bigg\} &= -\frac{a^2}{2r^2}\bigg(kaK_1(ka)-\frac{k^2a^2}{2}[K_0(ka)]\bigg(1-\frac{a^2}{2r^2}\bigg)\bigg\} \\
&\quad+\frac{ax}{r^2}\bigg\{K_1(ka)-\frac{ka}{4}[K_0(ka)]\bigg(1-5\frac{a^4}{r^4}\bigg)+\frac{k^2a^2}{16}[K_1(ka)]\bigg(1-6\frac{a^2}{r^2}+5\frac{a^4}{r^4}\bigg)\bigg\} \\
&\quad+\frac{a^2x^2}{r^4}\bigg\{kaK_1(ka)-\frac{k^2a^2}{2}[K_0(ka)]\bigg(1-2\frac{a^2}{r^2}\bigg)\bigg\} \\
&\quad+\frac{a^3x^3}{r^6}\cdot\frac{k^2a^2}{2}K_1(ka)-e^{kx}\bigg\{K_0(kr)+\frac{x}{r}K_1(kr)\bigg\}, \\[1ex]
\frac{v}{U}\bigg\{K_0+\frac{ka}{2}\bigg(K_1-\frac{ka}{4}K_0\bigg)\bigg\} &= \frac{ay}{r^2}\bigg\{K_1(ka)-\frac{ka}{4}[K_0(ka)]\bigg(1-\frac{a^4}{r^4}\bigg) \\
&\quad+\frac{k^2a^2}{16}[K_1(ka)]\bigg(1-2\frac{a^2}{r^2}+\frac{a^4}{r^4}\bigg)\bigg\} \\
&\quad+\frac{a^2xy}{r^4}\bigg\{kaK_1(ka)-\frac{k^2a^2}{2}[K_0(ka)]\bigg(1-\frac{a^2}{r^2}\bigg)\bigg\} \\
&\quad+\frac{a^3x^2y}{r^6}\cdot\frac{k^2a^2}{2}K_1(ka)-e^{kx}\frac{y}{r}K_1(kr).
\end{aligned}\right\} \quad \ldots\ldots(24)$$

These formulae fit the boundary conditions closely. Very near the surface of the cylinder there will be some error in the field which is of the same order as that introduced by Oseen's treatment of the dynamical equations and is negligible at small Reynolds' numbers. The expressions can be written in terms of R, neglecting R^2, as follows:

$$\left.\begin{aligned}
\frac{u}{U}\bigg\{K_0\bigg(\frac{R}{4}\bigg)+\tfrac{1}{2}\bigg\} &= -\frac{a^2}{2r^2}+\frac{ax}{r^2}\bigg\{K_1\bigg(\frac{R}{4}\bigg)-\frac{R}{16}\bigg[K_0\bigg(\frac{R}{4}\bigg)\bigg]\bigg(1-5\frac{a^4}{r^4}\bigg) \\
&\quad+\frac{R}{64}\bigg(1-6\frac{a^2}{r^2}+5\frac{a^4}{r^4}\bigg)\bigg\}+\frac{a^2x^2}{r^4}+\frac{a^3x^3}{r^6}\cdot\frac{R}{8} \\
&\quad-\exp\bigg(\frac{R}{4}\frac{x}{a}\bigg)\bigg\{K_0\bigg(\frac{R}{4}\frac{r}{a}\bigg)+\frac{x}{r}K_1\bigg(\frac{R}{4}\frac{r}{a}\bigg)\bigg\}, \\
\frac{v}{U}\bigg\{K_0\bigg(\frac{R}{4}\bigg)+\tfrac{1}{2}\bigg\} &= \frac{ay}{r^2}\bigg\{K_1\bigg(\frac{R}{4}\bigg)-\frac{R}{16}\bigg[K_0\bigg(\frac{R}{4}\bigg)\bigg]\bigg(1-\frac{a^4}{r^4}\bigg) \\
&\quad+\frac{R}{64}\bigg(1-2\frac{a^2}{r^2}+\frac{a^4}{r^4}\bigg)\bigg\}+\frac{a^2xy}{r^4}+\frac{a^3x^2y}{r^6}\cdot\frac{R}{8} \\
&\quad-\exp\bigg(\frac{R}{4}\frac{x}{a}\bigg)\frac{y}{r}K_1\bigg(\frac{R}{4}\frac{r}{a}\bigg).
\end{aligned}\right\} \quad \ldots\ldots(25)$$

Velocities computed from equation (25) agree very closely with those from the more complicated expressions when the Reynolds' number is below 0·2. At $R=0{\cdot}4$ both formulae give a reverse flow near the rear stagnation point due to formation of trailing vortices. The upper limit for the validity of (25) is probably about $R=0{\cdot}2$. There may be some advantage in using (24) to calculate the field at a distance for higher Reynolds' numbers.

In order to find the drag on the cylinder, W, Filon's (1927) theorem may be used. This shows that

$$W=\rho UE, \qquad \ldots\ldots(26)$$

where E is the outflow of fluid over an imaginary closed surface surrounding the cylinder at a great distance.

Let q_n be the normal outward velocity resolute at a point on a concentric cylindrical surface of radius r, where r is large. Then the net flow of fluid across unit length of this cylinder is

$$\int_0^{2\pi} q_n r\, d\theta, \qquad \ldots\ldots(27)$$

which must be equal to zero. In evaluating the integral a positive term, E, denoting the outflow will be balanced by a negative term which gives the inflow along the wake.

If we take equation (24) and neglect terms in $1/r$ while putting

$$G=K_0+\frac{ka}{2}\left(K_1-\frac{ka}{4}K_0\right); \qquad H=K_1-\frac{ka}{4}K_0+\frac{k^2a^2}{16}K_1,$$

these being functions of ka only, we find

$$\left.\begin{aligned}\frac{ru}{U}G&=aH\cos\theta-re^{kx}\{K_0(kr)+\cos\theta\, K_1(kr)\},\\ \frac{rv}{U}G&=aH\sin\theta-re^{kx}\sin\theta\, K_1(kr).\end{aligned}\right\}$$

Hence

$$q_n=r(u\cos\theta+v\sin\theta)=\frac{U}{G}\{aH-re^{kx}[\cos\theta\, K_0(kr)+K_1(kr)]\}.$$

When r is large

$$K_0(kr)=\left(\frac{\pi}{2kr}\right)^{\frac{1}{2}}e^{-kr},$$

$$K_1(kr)=[K_0(kr)]\left(1+\frac{1}{2kr}\right)\simeq K_0(kr),$$

so that

$$q_n r=\frac{2\nu}{G}\left\{kaH-\left(\frac{\pi}{2}kr\right)^{\frac{1}{2}}\exp\{-kr(1-\cos\theta)\}(1+\cos\theta)\right\}. \qquad \ldots\ldots(28)$$

When integrated over all values of θ the first term of this equation is the outflow, E, and the second term the inflow. We notice, first, that the part of the second term inside the scroll brackets is independent of the radius a. If powers of ka higher than the first are neglected we have $kaH=1$, but if higher powers are included kaH is a function of a. It is therefore impossible to balance the outflow and inflow unless ka is small. It was not apparent from previous reasoning that an approximation of this nature had been introduced at a distance from the cylinder. If a more general solution to equation (9) had been taken in place of (13), involving higher order Bessel functions, additional constants would have been included which were functions of a, so that the outflow and inflow terms would presumably have balanced with larger values of ka.

Next it will be observed that along the x axis, behind the cylinder where $\theta = 0$, the inflow term tends to infinity. When θ is sufficiently large, however, between 0 and $\pi/2$, the inflow vanishes as r increases. Thus the inflow region of the wake decreases in width as we go downstream but the inflow velocity rises.

The outflow term gives, using (27),

$$E = 4\pi\nu kaH/G. \qquad \ldots\ldots(29)$$

From (26), therefore,

$$W = 4\pi\eta UkaH/G.$$

Neglecting k^2a8^2 etc., we obtain

$$W = \frac{4\pi\eta U}{K_0(ka) + \frac{1}{2}} = \frac{4\pi\eta U}{\frac{1}{2} - \gamma - \ln\frac{1}{2}ka} = \frac{4\pi\eta U}{2{\cdot}0022 - \ln R} \qquad \ldots\ldots(30)$$

in agreement with Lamb.

In order to evaluate the inflow term it is necessary to consider the integral

$$\int_{-\pi}^{\pi} \{\exp(kr\cos\theta)\}(1 + \cos\theta)\,d\theta = \int_{-\pi}^{\pi} \exp(kr\cos\theta)\,d\theta + \int_{-\pi}^{\pi} \{\exp(kr\cos\theta)\}\cos\theta\,d\theta.$$

Since

$$I_0(x) = \frac{1}{2\pi}\int_{-\pi}^{\pi} \exp(x\cos\theta)\,d\theta$$

and

$$I_1(x) = \frac{d}{dx}I_0(x) = \frac{1}{2\pi}\int_{-\pi}^{\pi} \{\exp(x\cos\theta)\}\cos\theta\,d\theta,$$

the integral is equal to $2\pi\{I_0(kr) + I_1(kr)\}$.

For large values of kr the asymptotic expansions of the Bessel functions show that

$$I_0(kr) = I_1(kr) = e^{kr}/(2\pi kr)^{\frac{1}{2}},$$

hence the integral is equal to $2e^{kr}(2\pi/kr)^{\frac{1}{2}}$ and the inflow, from equation (28), is $4\pi\nu/G$, which is equal to the outflow if k^2a^2 and higher terms are negligible.

ACKNOWLEDGMENT

It gives the author very great pleasure to express his thanks to Mr. A. C. Stevenson for his patient and friendly instruction in hydrodynamics and for the trouble he has taken in reading and criticizing this paper.

REFERENCES

Bairstow, L., Cave, B. M., and Lang, E. D., 1923, *Phil. Trans.* A, **223,** 383.

Faxén, H., 1927, *Nova Acta Soc. Reg. Upsal.* Vol. 1, Ext. Ord.

Filon, L. N. G., 1927, *Proc. Roy. Soc.* A, **113,** 7.

Lamb, H., 1911, *Phil. Mag.*, **21,** 112; 1932, *Hydrodynamics*, 6th Edition (Cambridge: University Press), p. 613.

Watson, G. N., 1922, *Theory of Bessel Functions* (Cambridge : University Press).

On the Fluctuating Concentration of X-Ray Products in Water Dispersions

By F. H. KRENZ*
National Research Council, Chalk River, Ontario, Canada

Communicated by N. Feather; MS. received 28th December 1949

ABSTRACT. It has been found that the partial pressure of decomposition gases over water irradiated with x-rays fluctuates more or less regularly with the irradiation time. The experiments suggest that the fluctuations are caused by impurities in the water, and that this phenomenon is possibly related to the periodic rise and fall of electrophoretic mobility observed in the case of certain colloids when these are subjected to x-irradiation.

In 1937 Crowther and Liebmann announced the discovery of a peculiar effect of x-rays on the electrophoretic mobility of colloidal graphite in water (Crowther and Liebmann 1937). The effect was described as a periodic fluctuation of the electrophoretic mobility of the graphite with the dose of x-rays given to the sol at constant intensity. Liebmann and Jones (see Crowther 1938) showed that the effect could be produced as well in aqueous dispersions of gold. Gray, Read and Liebmann (1941) later showed that the effect could be produced in graphite sols by γ-rays and neutrons.

In the course of investigating the effects of ionizing radiations on water and aqueous systems a phenomenon has been observed in this laboratory which may throw some light on the Crowther effect. It was found that when certain samples of water in a closed, evacuated system were subjected to an intense beam of x-rays the pressure of decomposition gases over the samples rose and fell regularly with time.

The source of radiation in these experiments was a Machlett AEG-50-T x-ray tube operating at full power. The integrated dose rate over the whole sample was determined to be approximately 300 r/sec. The samples consisted of 1 to 3 ml. of water purified by distillation from potassium permanganate and vacuum distilled into a water-jacketed Pyrex cell which admitted x-rays through a thin (0·5 mm.) Pyrex window. The water through the jacket was supplied from a constant temperature bath operating at 15° c.

The pressure was measured with a McLeod gauge after the water vapour was condensed in a cold trap cooled with liquid nitrogen during pressure measurements. The trap and gauge were isolated from the cell during measurements by a stopcock, and the trap was always warmed to room temperature before the stopcock was opened. The measuring technique did not contribute to pressure fluctuations. It was demonstrated in later experiments with a palladium valve that the changes in pressure observed when water was irradiated were due entirely to the evolution of hydrogen or its disappearance.

When the residual pressure of oxygen over the samples was reduced by prolonged pumping to approximately 10^{-4} mm. of mercury (10^{-3} mm. was the limit of the gauge) they could be irradiated for periods up to an hour with a barely detectable increase in pressure (Figure 1, curve A). At residual pressures of 1–5 microns, however, decomposition of the water commenced almost immediately upon irradiation. Figure 1, curve B, shows fluctuations in pressure detected with a McLeod gauge during the irradiation of a sample. It was suspected that contamination of the water by mercury might be contributing to this phenomenon, and the McLeod gauge was replaced by a Pirani gauge calibrated for hydrogen. When this was done, and the system baked out *in vacuo* for several hours before the water was distilled into the cell, curve C of Figure 1 was obtained.

---

* Now at the Department of Natural Philosophy, The University, Edinburgh.

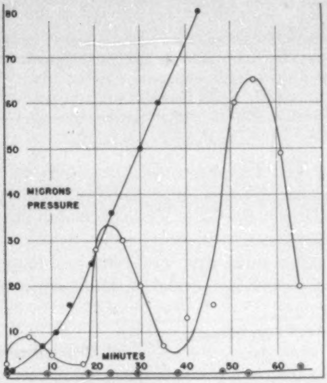

Figure 1. Irradiation of water.

○ A : Mercury-contaminated (McLeod gauge), pressure $O_2 \simeq 10^{-4}$ mm
○ B : Mercury-contaminated (McLeod gauge), pressure $O_2 = 2\text{–}3\ \mu$.
● C : Mercury-free (Pirani gauge).

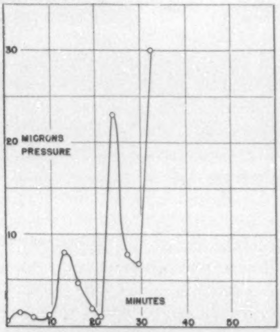

Figure 2. Irradiation of graphite sol.
Temperature of water jacket 15·00 ± 0·10° c.

Figure 2 shows fluctuations in pressure measured with the Pirani gauge over a sample of graphite sol prepared by Crowther's technique (Crowther, Liebmann and Lane 1937). In this case the dose rate was reduced to approximately 100 r/sec. The pressure changes were found to be due entirely to hydrogen.

When the samples of water were purposely contaminated by exposure to mercury vapour and irradiated, pressure fluctuations like those of Figure 1, curve B, could be detected with the Pirani gauge. It was also found that the pressure continued to fluctuate when the x-rays were turned off (Figure 3).

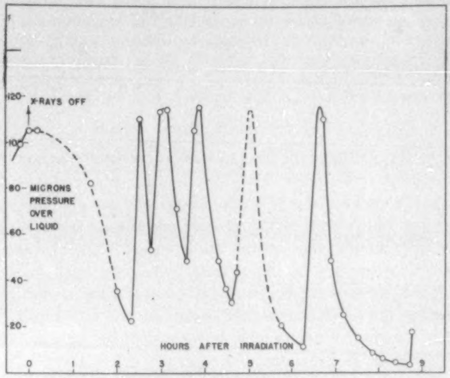

Figure 3. Post-irradiation phenomenon : water (mercury-contaminated). Temperature of water jacket 15·15 ± 0·10° c.

These fluctuations were maintained at least up to 24 hours after irradiation. The pressure changes were found to be entirely due to hydrogen. No such after-effect was observed in the case of colloidal graphite.

REFERENCES

Crowther, J. A., 1938, *Nature, Lond.*, **142,** 569.
Crowther, J. A., and Liebmann, H., 1937, *Nature, Lond.*, **140,** 28.
Crowther, J. A., Liebmann, H., and Lane, T. B., 1937, *Phil. Mag.*, **24,** 654.
Gray, L. H., Read, J., and Liebmann, H., 1941, *Brit. J. Radiol.*, **14,** 102.

On the Retarding Field Current in Diodes

By R. FÜRTH* and D. K. C. MacDONALD†

MS. received 26th October 1949

ABSTRACT. In a previous paper the authors have shown how the space charge distribution in plane and cylindrical diodes under retarding field conditions can be calculated by well-known methods of statistical thermodynamics, and have derived expressions for the upper limit of current for which this condition holds. In the present paper certain inaccuracies in the previous treatment are rectified, the argument is completed, and certain erroneous views, expressed in a recent paper by D. A. Bell, are criticized.

In a paper on the spontaneous fluctuations of electricity in thermionic valves under retarding field conditions (MacDonald and Fürth 1947) we have shown that the distribution of space-charge density and the upper limit I_c of the current for which true retarding field conditions hold can be obtained in a comparatively simple way by the application of well-known methods of statistical thermodynamics. In the present paper we wish to rectify certain inaccuracies in the previous treatment and to complete the argument, and finally once again to stress the significance of the results for the determination of cathode temperatures in thermionic valves in view of certain erroneous views expressed in a recent paper by D. A. Beil (1949).

In the case of a plane-parallel diode the maximum ρ_m of the space-charge density, which under the above-mentioned limiting condition must coincide with the cold electrode, is equal to

$$\rho_m = \frac{\pi \boldsymbol{k} T}{8 \boldsymbol{e} d^2}, \qquad \ldots\ldots(1)$$

where $\boldsymbol{e}$ is the magnitude of the electronic charge and d the inter-electrode distance. The current I is connected with the saturation current J by

$$I = J \exp\left[\frac{\boldsymbol{e}(V+v_a)}{\boldsymbol{k}T}\right], \qquad \ldots\ldots(2)$$

where V is the (negative) anode potential and v_a a possible potential barrier at the surface of the cold electrode. The saturation current satisfies the classical Richardson relation

$$J = \rho_0 a(\boldsymbol{k}T/2\pi \boldsymbol{m})^{1/2}, \qquad \ldots\ldots(3)$$

in which ρ_0 is the electronic density at the hot-electrode surface and $\boldsymbol{m}$ the electronic mass. Finally, one has for thermodynamic equilibrium within the space charge

$$\rho_m = \rho_0 \exp[\boldsymbol{e}V/\boldsymbol{k}T]. \qquad \ldots\ldots(4)$$

From (1), (2), (3) and (4) one obtains the expression for the limiting current I_c

$$I_c = \frac{\sqrt{\pi}}{8\sqrt{2}} \frac{\boldsymbol{k}^{3/2}}{\boldsymbol{e}\sqrt{\boldsymbol{m}}} \frac{T^{3/2}a}{d^2} \exp[\boldsymbol{e}v_a/\boldsymbol{k}T], \qquad \ldots\ldots(5)$$

which is identical with equation (31) of our first paper, and which differs only by an insignificant numerical factor from the expression obtained on the basis of Langmuir's kinetic theory.

---

* Birkbeck College, University of London.
† Clarendon Laboratory, University of Oxford.

In the case of a cylindrical diode equation (1) is to be replaced by

$$\rho_{\mathrm{m}} = \frac{1+B^2}{(2\pi \boldsymbol{e}/\boldsymbol{k}T) r_{\mathrm{a}}^{2}}, \qquad \ldots\ldots(6)$$

where r_{a} is the radius of the anode-cylinder and B is the root of the transcendental equation

$$\tan\left[B \log (r_{\mathrm{a}}/r_{\mathrm{c}})\right] = -B, \qquad \ldots\ldots(7)$$

r_{c} being the radius of the cathode cylinder.

Instead of the relation (2) we have now to use an expression obtained by Schottky (1914) from elementary dynamical considerations:

$$I = \frac{2}{\sqrt{\pi}} J \left\{ e^{-A} \int_{0}^{\sqrt{(A/\eta)}} \exp\left[(\eta-1)x^2\right] dx + \int_{\sqrt{(A/\eta)}}^{\infty} \exp(-x^2)\, dx \right\}, \qquad \ldots\ldots(8)$$

with

$$\eta = 1-(r_{\mathrm{c}}/r_{\mathrm{a}})^2 \qquad \ldots\ldots(9)$$

and

$$A = -\boldsymbol{e}V/\boldsymbol{k}T. \qquad \ldots\ldots(10)$$

The expression (8) has to be multiplied by the factor $\exp(\boldsymbol{e}v_{\mathrm{a}}/\boldsymbol{k}T)$ in the case of the existence of a potential barrier v_{a}.

For $\eta \ll 1$, (8) becomes

$$I = \frac{r_{\mathrm{a}}}{r_{\mathrm{c}}} J e^{-A}, \qquad \ldots\ldots(8a)$$

and for $\eta \simeq 1$ and $A \gg 1$ it can be expanded in the form

$$I = \frac{2}{\sqrt{\pi}} J e^{-A} \sqrt{A} \left[1 + \frac{1}{2A} - \frac{1}{4A^2} + \ldots\right]. \qquad \ldots\ldots(8b)$$

In any case I always contains the Boltzmann factor $\exp(-A) = \exp(\boldsymbol{e}V/\boldsymbol{k}T)$, in agreement with general results of statistical thermodynamics, whereas a factor of the form $\exp(-A/2)$, as suggested by Bell (1949), is clearly in contradiction to statistical thermodynamics.

The limiting current is obtained from (6) and (8) in connection with (3) and (4), which remain in force. Thus we obtain for a cylinder of length l

$$I_{\mathrm{c}} = \frac{\sqrt{2}(1+B^2)}{\pi} \frac{\boldsymbol{k}^{3/2}}{\boldsymbol{e}\sqrt{\boldsymbol{m}}} \frac{T^{3/2} l r_{\mathrm{c}}}{r_{\mathrm{a}}^{2}} \left\{ \int_{0}^{\sqrt{(A/\eta)}} \exp\left[(\eta-1)x^2\right] dx + e^{A} \int_{\sqrt{(A/\eta)}}^{\infty} \exp(-x^2)\, dx \right\} \times \exp\left(\frac{\boldsymbol{e}v_{\mathrm{a}}}{\boldsymbol{k}T}\right), \qquad \ldots\ldots(11)$$

which has to replace equation (36) of our first paper.

The statistical equilibrium of the space charge, which is the basic assumption of our treatment, is, strictly speaking, incompatible with the flow of a steady current. Consequently the formula (4) and the expressions (1) and (6) are not strictly valid (especially in the neighbourhood of the minimum), but the relations which are obtained by eliminating ρ_{m} from (1) and (4) or (6) respectively are still very nearly correct. This accounts for the fact that the resulting expressions for I_{c} coincide essentially with those obtainable from detailed kinetic treatment. It also indicates why it would in fact be wrong to attempt to evaluate I_{c} directly as the 'emission' current from the surface $\rho = \rho_{\mathrm{m}}$ from formula (3) by replacing ρ_0 by ρ_{m} and identifying a with the area of that surface. This procedure happens to give the right result in the plane-parallel case because of the non-diverging character of the current flow, but would give a wrong result in the cylindrical case, in particular yielding a finite value for I_{c} for $r_{\mathrm{c}} \to 0$.

When r_a/r_c is of the order of magnitude unity it follows from (7) that

$$B \sim \frac{\pi}{2\log(r_a/r_c)} \gg 1 \qquad \ldots\ldots (12)$$

and, further, $\eta \ll 1$. Thus (11) becomes

$$I_c = \frac{\pi^{3/2}}{4\sqrt{2}} \frac{\boldsymbol{k}^{3/2}}{\boldsymbol{e}\sqrt{\boldsymbol{m}}} \frac{T^{3/2}l}{r_a \log^2(r_a/r_c)} \exp\left[\frac{\boldsymbol{e}v_a}{\boldsymbol{k}T}\right] \qquad \left(\frac{r_a}{r_c} \sim 1\right). \qquad \ldots\ldots (13)$$

This differs from our previous expression (37) by a factor r_a/r_c, and is now, apart from the exponential factor involving v_a, identical with the corresponding formula of Möller and Detels (1926) obtained from kinetic theory under the condition $B \gg 1$.

When on the other hand r_a/r_c is large compared with unity, one has from (7)

$$B \sim \frac{\pi}{\log(r_a/r_c)}, \qquad \ldots\ldots (14)$$

and this is evidently not large compared with unity. Hence the application of formula (13) to this case by Möller and Detels is unjustified. From (4), (6) and (10) follows

$$A = \log(\rho_0/\rho_m) = \log\left[\frac{2\pi\boldsymbol{e}\rho_0 r_a^{\,2}}{\boldsymbol{k}T(1+B^2)}\right], \qquad \ldots\ldots (15)$$

which under ordinary conditions is a large quantity. Hence one can use (8*b*), so that (11) becomes

$$I_c = \frac{\sqrt{2}}{\pi}(1+B^2)\frac{\boldsymbol{k}^{3/2}}{\boldsymbol{e}\sqrt{\boldsymbol{m}}}\frac{T^{3/2}lr_c}{r_a^{\,2}}\sqrt{A}\left[1+\frac{1}{2A}-\frac{1}{4A^2}+\ldots\right]\exp\left(\frac{\boldsymbol{e}v_a}{\boldsymbol{k}T}\right)$$
$$\left(\frac{r_a}{r_c} \gg 1\right). \qquad \ldots\ldots (16)$$

For a finite fixed value of r_a, the radius of the anode cylinder, under this condition r_c is very small, i.e. the cathode becomes a thin filament, and the expression (16) tends towards zero unless ρ_0 is concomitantly made very large, so that the quantity $r_c\sqrt{(\log \rho_0)}$ remains finite. For a finite fixed value of r_c, on the other hand, r_a becomes very large, and as A only increases logarithmically with r_a whilst the denominator is proportional to $r_a^{\,2}$, we again obtain a vanishingly small limiting current.

It thus follows that, unless one wishes to resort to extremely small currents, one must maintain $r_a/r_c \sim 1$ in experimental investigations of the retarding field region, in particular directed towards the determination of cathode temperatures. If, however, experiments are conducted *above* the limiting current, a spurious (and *too large*) apparent cathode temperature will ensue from slope measurements of the characteristic. This holds specifically for the experiments quoted by Bell. Also, as pointed out in our previous paper, the method of logarithmic plotting can easily mask a slow 'power' variation of one of the variables involved.

In view of all these considerations the method of plotting the product IR_a (where R_a is the differential resistance of the valve) against I for currents below I_c, as explained in §5 of our first paper, which does not suffer from the abovementioned sources of error, appears to be the most adequate method for such investigation.

REFERENCES

BELL, D. A., 1949, *Proc. Phys. Soc.* B, **62**, 334.

MACDONALD, D. K. C., and FÜRTH, R., 1947, *Proc. Phys. Soc.*, **59**, 375.

MÖLLER, H. G., and DETELS, F., 1926, *Jb. drahtl. Telegr. Teleph.*, **27**, 74.

SCHOTTKY, W., 1914, *Ann. Phys., Lpz.*, **44**, 1011.

CONTENTS FOR SECTION A

PAGE

Dr. E. **Marsden**. Rutherford Memorial Lecture (1948) 305
Mr. R. W. **Cahn**. A New Theory of Recrystallization Nuclei 323
Dr. E. E. **Salpeter**. Nuclear Induction Signals for Long Relaxation Times . 337
Dr. C. B. **van Wyk**. γ-Decay and Mesons of Spin Zero 350
Mr. C. **Balakrishnan** and Dr. J. D. **Craggs**. On the Velocity of Discharge Propagation in Externally Quenched Geiger Counters 358
Prof. C. A. **Coulson** and Mr. N. H. **March**. Momenta in Atoms using the Thomas–Fermi Method 367
Prof. L. F. **Bates** and Mr. F. E. **Neale**. A Quantitative Study of the Domain Structure of Single Crystals of Silicon–Iron by the Powder Pattern Technique. 374
Dr. J. C. **Willmott**. The Infra-red Spectrum of Magnesium Oxide . . 389
Letters to the Editor:
  Mr. F. K. **Goward**, Mr. V. L. **Telegdi** and Mr. J. J. **Wilkins**. The Photo-disintegration of Carbon into Three Alpha-particles 402
  Mr. D. **Bijl**. Paramagnetic Resonance Absorption in Titanium Caesium Alum at Low Temperatures 405
  Dr. B. **Bleaney**. Anisotropy in Titanium Alum 407
  Dr. B. **Bleaney** and Mr. D. J. E. **Ingram**. Paramagnetic Resonance in Copper Fluosilicate 408
  Mr. A. **Abragam** and Prof. M. H. L. **Pryce**. Theoretical Interpretation of Copper Fluosilicate Spectrum 409
  Dr. J. K. **Mackenzie** and Prof. N. F. **Mott**. A Note on the Theory of Melting 411
  Mr. R. K. **Laird** and Dr. R. F. **Barrow**. An Ultra-violet Band-system of CS_2^+ 412
Reviews of Books 413
Contents for Section B 415
Abstracts for Section B 416

ABSTRACTS FOR SECTION A

Rutherford Memorial Lecture (1948), by E. **Marsden**.

A New Theory of Recrystallization Nuclei, by R. W. **Cahn**.

ABSTRACT. After a review of the numerous experimental observations in this field which need to be explained, a new theory is presented of nucleus formation when a cold-worked metal is annealed. The nuclei are held to be formed in the most distorted parts of the lattice, in the 'local curvatures' postulated by Burgers. At these places the lattice locally regains its perfection by the recently discovered process of diffusion of dislocations, or 'polygonization', and the perfect nucleus so created is then able to consume the less perfect crystal in its vicinity. Experimental evidence for this picture is presented. Each potential nucleus is held to have a definite incubation period (as distinct from the fixed probability of becoming active which was the basis of previous theories). By means of certain assumptions as to the distribution of curvatures and the dependence of incubation time on curvature, a quantitative theory is developed, which is found to be capable of accounting for all the experimental data on nucleation rates. The paper concludes by comparing critically the new theory with older ones.

Nuclear Induction Signals for Long Relaxation Times, by E. E. SALPETER.

ABSTRACT. Equations of motion, previously derived by Bloch (1946), for the nuclear magnetic moment in a nuclear induction experiment are applied to the steady state reached when the strong magnetic field H_z is swept sinusoidally about its resonance value. Different approximations for the shapes and sizes of nuclear induction signals are derived for various limiting cases, depending (*a*) whether the passage of H_z is ' adiabatic ' or ' extremely non-adiabatic ' (very weak radio-frequency field) and (*b*) whether the relaxation times are shorter or longer than the period of the sweep of H_z. It is found that quite large signals may be induced by even a very weak radio-frequency field if the relaxation times are very long.

γ-Decay and Mesons of Spin Zero, by C. B. VAN WYK.

ABSTRACT. On the assumption that τ-mesons are scalar particles and have an appreciable interaction with nucleons, the lifetime of a τ-meson at rest decaying into two photons and a pseudoscalar π-meson, is calculated by means of standard perturbation theory. The lifetime obtained is $G \times 10^{-12}$ sec. where G is the reciprocal of the product of the dimensionless meson–nucleon coupling parameters. This result is roughly what can be expected from observations and, taken together with the results of a previous paper, seems to indicate that the heavy mesons have spin zero.

On the Velocity of Discharge Propagation in Externally Quenched Geiger Counters, by C. BALAKRISHNAN and J. D. CRAGGS.

ABSTRACT. A new method for measuring the propagation velocity of the discharge along a Geiger non-proportional counter is described. The results obtained with cylinder grade argon, hydrogen and neon are summarized graphically, and a brief discussion of propagation mechanisms is given.

Momenta in Atoms using the Thomas-Fermi Method, by C. A. COULSON AND N. H. MARCH.

ABSTRACT. The Thomas–Fermi statistical theory of the free atom is used to calculate the momentum distribution and the shape of the Compton profile for X-ray scattering, the results being expressed in dimensionless form applicable to all atoms. The mean momentum, which varies as $Z^{2/3}$, where Z is the atomic number, agrees well with more accurate wave-mechanical calculations. Numerical results are also reported for argon and krypton using the Dirac modification of the original theory, in which exchange effects are taken into account and the atom has a finite radius. Agreement with experiment is not noticeably better with these refinements.

A Quantitative Study of the Domain Structure of Single Crystals of Silicon–Iron by the Powder Pattern Technique, by L. F. BATES AND F. E. NEALE.

ABSTRACT. A quantitative study of the domain structure of single crystals of silicon–iron has been made by the powder pattern method, special examination being made of the patterns formed on a strip specimen whose surface was approximately a (100) plane with a [011] direction parallel to the long edge of the strip. For Mode III magnetization, which occurs when a field acts inside the specimen parallel to the [011] direction, the line deposits formed at right angles thereto were on the average spaced in good accord with Néel's theory in the case of wide strips, but in less good accord for narrow strips. Qualitative results of other measurements on strip and disc specimens are reported and interpreted.

The Infra-red Spectrum of Magnesium Oxide, by J. C. WILLMOTT.

ABSTRACT. An investigation of the infra-red spectrum of magnesium oxide has been carried out in the range up to $25{\cdot}5\,\mu$, both in reflection and transmission. The eigen-frequency is found to be at $17{\cdot}5 \pm 0{\cdot}3\,\mu$ and four subsidiary maxima have been found in transmission. The results of Barnes, Brattain and Seitz in the range up to $15{\cdot}6\,\mu$ have not been confirmed and no detailed fine structure has been found. The reflection spectrum of magnesium oxide has been fully investigated up to $25{\cdot}5\,\mu$, and a broad reflection maximum has been found extending from $17\,\mu$ to $21\,\mu$, with subsidiary maxima at $14{\cdot}02\,\mu$ and $23{\cdot}8\,\mu$.

From the data obtained curves have been drawn to show the behaviour of the two optical constants n and k in the range from $7\,\mu$ to $25\,\mu$.